Actin dynamics control ploidy-dependent size scaling in *Schizosaccharomyces pombe*

Ichiro Yamashita

Center for Gene Science, Hiroshima University, Kagamiyama 1-4-2, Higashihiroshima 739-8527, Japan.

Abstract

It has long been known that eukaryotic cells with more DNA content are larger in cell size. However, no molecular mechanisms for this universal rule have been given. Here I identify cell division genes that dose-dependently control cell growth or cell extension rate (CER) of diploid cells of the fission yeast *Schizosaccharomyces pombe*. Genetic analysis revealed a negative role of Cdc2, a conserved master regulator of eukaryotic cell cycle. Surprisingly, half dosage of *cdc25*$^{+}$ or *nim1*$^{+}$ (*cdc25Δ*/+ or *nim1Δ*/+), both activator for Cdc2, decreased CER. I discovered that these genes constitute three overlapping regulatory mechanisms for Cdc2: positive and negative feedback loops and a feedforward network. In the negative feedback loop, Cdc2-activating Cdc25 is required for nuclear accumulation of GFP-Wee1 that inhibits Cdc2. Actin monomers are associated with nuclear localization of GFP-Wee1 and accelerate CER, while actin polymers are related to nuclear accumulation of Cdc25-GFP. In the positive feedback loop, actin monomers are relevant to inhibition of Nim1 and subsequent activation of Cdc2 independently of Wee1, resulting in decrease in CER. Nim1 also plays a key role in the feedforward network for supplying sufficient amount of nuclear GFP-Wee1 and closely cooperates with Cdc25 in order to adjust CER to ploidy. Remarkably, doubling cell division genes in haploids reproduced CER of diploids. These findings establish that yeast cells control CER dependently upon dosage of cell division genes during G2 period in the cell division cycle, and provide a solid foundation for understanding the cell-size scaling with DNA content in other eukaryotes.

KEYWORDS

actin, *cdc25*, *nim1*, ploidy, scaling, *wee1*

1 | INTRODUCTION

The general association between DNA content and cell size has long been recognized in unicellular eukaryotes, plants, and animals (Cavalier-Smith, 2005; Gregory, 2005; Kondorosi, Roudier, & Gendreau, 2000). Polyploid cells with multiple copies of chromosome sets occur frequently in the development and differentiation of plants and animals, and large polyploid cells are crucial to morphology, metabolism, and tissue-specific function (Hyun, Jean, & Robert, 2009; Orr-Weaver, 2015). However, no mechanisms explaining this universal rule for cell size determination have been demonstrated. Here I used the fission yeast and explored the possibility for the involvement of cell division genes that control cyclin-dependent protein kinase, Cdc2 (Wood & Nurse, 2015): *cdc13*$^{+}$ (cyclin) (Booher & Beach, 1988), *wee1*$^{+}$ (an inhibitory protein kinase) (Russell & Nurse, 1987a), *cdc25*$^{+}$ (an activating protein phosphatase with antagonistic action to Wee1) (Russell & Nurse, 1986), *nim1*$^{+}$/*cdr1*$^{+}$ kinase (inducer of mitosis by inhibiting Wee1) (Feilotter, Nurse, & Young, 1991; Russell & Nurse, 1987b), and its upstream inhibitory effectors, *pom1*$^{+}$ (Bähler & Pringle, 1998) and *nif1*$^{+}$ (Wu & Russell, 1997). I also examined whether *act1*$^{+}$ (actin) (Ishiguro & Kobayashi, 1996) is involved in cell-size control because actin cables are thought to serve as tracks for secretory vesicle transport to the tip (Bendezú & Martin, 2011; Hammer & Sellers, 2012; Kovar, Sirotkin, & Lord, 2011), and in addition, actin dynamics control nuclear transport (Vartiainen, Guettler, Larijani, et al., 2007).

Cdc2 is a conserved key regulator for entry into mitosis and its activity is thought to be critical to cell-size determination (Kellogg, 2003). Loss of Wee1 activity induces premature activation of Cdc2 and therefor causes cells to enter mitosis before sufficient growth has occurred, producing two abnormally small daughter cells. Similarly, mutants with lower Cdc2 activity (such as *cdc2*$^{-}$, *cdc13*$^{-}$, and *cdc25*$^{-}$) undergo delayed entry into mitosis, producing abnormally large cells. However, these genetic analyses overlook the possibility that Cdc2 controls growth rate during G2 period. Throughout this work, I measured growth rate as a major determinant of cell-size scaling with ploidy because diploid cells grow faster than haploid cells during the same doubling time in fission yeast (Sveiczer, Novak, & Mitchison, 1996) as well as in budding yeast (Adams & Hansche, 1974). By using diploid and tetraploid cultivars of ryegrass, Sugiyama demonstrated that polyploidy increases leaf size mainly by increasing the cell elongation rate without significant differences in cell division parameters (Sugiyama, 2005). Zhou et al. also reported that tetraploid crucian carp cells grow bigger than diploid cells without affecting proliferation (or cell division) (Zhou, Wang, Jiang, et al., 2016). Collectively, these results

may lead to a generalization that polyploid cells scale their size or volume by controlling growth rate during G2.

The aim of my investigation was to search for mechanisms that control Cdc2 during G2 and for mechanisms that turn on a switch from G2 to mitosis. This work revealed unprecedentedly that Cdc25 and Nim1 are required for lowering Cdc2 activity which enhance growth rate of diploid cells. I also found that actin dynamics associated with modulation of Cdc2 activity control nuclear content of Cdc25 and Wee1, forming negative feedback loops for Cdc2. Surprisingly, I observed that actin monomers are associated with both nuclear accumulation of Wee1-GFP and inhibition of Nim1, resulting in opposite effects, promotion and inhibition of cell extension, respectively. The latter novel pathway in which Nim1 is involved in negative control of Cdc2 independently of Wee1 may constitute a key module in a positive feedback loop for Cdc2. This pathway works in cooperation with Cdc25 to keep lower Cdc2 activity in diploids, thus increases CER. Furthermore, during the course of this work, I observed that mutant cells with higher Cdc2 activity such as *wee1Δ*/+ show prolonged cycle time concomitantly with reduced content of nuclear Cdc25-GFP. Forced expression of Cdc25 in the nuclei of *wee1Δ*/+ cells by using Cdc25-NLS-GFP (Cdc25-GFP tagged with a nuclear localization signal, NLS) allowed to restore normal cycling time and at the same time accelerated CER. This result verifies my proposal that Cdc25 has a positive role for cell extension and is consistent with the previous conclusion that Cdc25 is a key molecule in the auto-regulatory loop for acute activation of Cdc2 at the G2/M boundary (Lu, Domingo-Sananes, Huzarska, et al., 2012). Collectively, the present study establishes systems level control of Cdc2 as a critical regulator of growth rate and finally cell-size scaling with ploidy, origin of which is copy number of cell division genes.

2 | MATERIALS AND METHODS

2.1 | Strains

The *S. pombe* strains used in the experiment are listed in Table S1. The strains bearing mutant alleles (*cdc2-L7*, *cdc2-3w*, *cdc25-22*, *cdc13-117*, and *wee1-50*) or deletions (*cdc25Δ::ura4*$^+$, *wee1Δ::ura4*$^+$, and *nim1Δ::LEU2*) were gifts from P. Russell and P. Nurse (Gould & Nurse, 1989; Russell & Nurse, 1986; Russell & Nurse, 1987a; Russell & Nurse, 1987b). A strain bearing *pom1Δ::ura4*$^+$ was from J. Bähler and J. R. Pringle (Bähler & Pringle, 1998). A strain bearing *cps8-188* and a plasmid carrying *act1*$^+$ were from J. Ishiguro (Ishiguro & Kobayashi, 1996). Strains bearing *cdc25Δ::ura4*$^+$*::cdc25-GFP::leu1*$^+$ and *cdc25Δ::ura4*$^+$*::cdc25-NLS-GFP::leu1*$^+$ were from P. G. Young (Chua,

Lingner, Frazer, et al., 2002). Strains bearing *wee1Δ::ura4*$^+$ and each of *lys1*$^+$*::GFP-wee1* or *lys1*$^+$*::GFP-NESx2-wee1* were from H. Masuda (Masuda, Fong, Ohtsuki, et al., 2011). Strains bearing deletions of *act1Δ::ura4*$^+$ (Ishiguro & Kobayashi, 1996), *cdc13Δ::ura4*$^+$ (Booher & Beach, 1988), and *nif1Δ::ura4*$^+$ (Wu & Russell, 1997) were constructed as described previously by the one-step gene disruption method (Rothstein, 1983). Strains bearing two copies of *act1*$^+$ (2x*act1*$^+$*::ura4*$^+$), *cdc13*$^+$ (2x*cdc13*$^+$*::ura4*$^+$), *cdc25*$^+$ (2x*cdc25*$^+$*::ura4*$^+$), *nim1*$^+$ (2x*nim1*$^+$*::ura4*$^+$), and *pom1*$^+$ (2x*pom1*$^+$*::ura4*$^+$) were constructed by insertion into native loci of pBR322-based plasmids carrying *ura4*$^+$ and the respective genes (6.5-kb *Eco*RI-*Hin*dIII fragment of *act1*$^+$, 4.6-kb *Pvu*II-*Bam*HI fragment of *cdc13*$^+$, 5.2-kb *Sph*I-*Pvu*II fragment of *cdc25*$^+$, 3.3-kb *Bam*HI-*Eco*RI fragment of *nim1*$^+$, and 6.5-kb *Nhe*I-*Sph*I fragment of *pom1*$^+$) after linearization by digestion within coding regions with *Bam*HI, *Xho*I, *Bam*HI, *Xho*I, and *Bgl*II, respectively. Plasmids carrying *cdc13*$^+$, *cdc25*$^+$, *nif1*$^+$, *nim1*$^+$, and *pom1*$^+$ and an *adf1-1* strain were provided by the National Bio-Resource Project (NBRP), Japan.

Standard procedures were used for cell culture and genetic manipulations (Sabatinos & Forsburg, 2010). Diploid cells were constructed by isolation of prototrophic cells after crossing haploid cells with opposite mating type (h$^+$ or h$^-$), each bearing *ade6-M210* or *ade6-M216*. Diploid cells were also selected after cultivation of haploid cells on YES plates containing phloxin-B. Diploid cells homozygous for mating type (h$^{+/+}$ and h$^{-/-}$) were isolated by manipulator after repeated (usually 2 or 3 times) cultivation of h$^{+/-}$ diploid on EMM2 plates at 28℃ for 2 days. Diploid cells heterozygous for two or three deletions (marked with *ura4*$^+$) were selected after tetrad dissection of asci from tetraploid cells made by mating between h$^{+/+}$ and h$^{-/-}$ diploids, each heterozygous for one or two deletions. Diploids heterozygous for two or three deletions were verified by tetrad analysis after crossing with tester diploids bearing *ura4-D18*/*ura4-D18*, in which Ura$^+$ segregants appear in a manner of PD : NPD : T = 1 : 1: 4 from the cross with the diploid heterozygous for two deletions or in a manner of (2 Ura$^+$: 2 Ura$^-$) : (3 Ura$^+$: 1 Ura$^-$) : (4 Ura$^+$: 0 Ura$^-$) = 1 : 16: 19 from the cross with the diploid heterozygous for three deletions. Haploids bearing two or three loci of two copies of genes (marked with *ura4*$^+$) were also verified by tetrad analysis after crossing with tester haploids bearing *ura4-D18*, in which Ura$^+$ segregants appear as above. Haploids bearing four or five loci of two copies of genes were verified by tetrad analysis after back-crossing with haploids bearing three or four loci of two copies of genes, respectively, in which tetrads were segregated as 2 (longer cells) : 2 (shorter cells).

2.2 | Measurement of CER

Cells were grown exponentially in EMM2 for 24 h to a maximum density of 5 x 10^6 cells/ml before the initiation of all experiments. Temperature-sensitive cells were cultured at 28℃, and other cells were grown at 28℃ or 36.5℃ as indicated. Before measurement of CER, more than three strains with the same genotype were measured for length of long axes of more than 100 cells with septum. Strains having the closest match to average cell length of genotype were chosen for measurement of CER. Aliquot of culture was collected by centrifugation for 30 sec, resuspended and spread on thin EMM2 agar plates. A block (15 x 15 mm) was cut and set upside down on a glass-base dish (diameter, 35 mm; code 3970-035, Iwaki, Japan). The dish was sealed by parafilm and set on a thermo plate (MATS-55RAF20, Tokai Hit, Japan) on inverted microscope (Nikon Eclipse TE2000-U). The dish was fastened with cellotape on the thermo plate, and finally covered by a plastic petri dish (diameter, 85 mm) for temperature control. The temperature on the agar was checked with a contact thermistor in trial experiments, and kept at 28℃ or 36.5℃ as indicated. Room temperature was controlled by air conditioner more than 10℃ lower than the temperature of the agar. Cells were visualized under x40 magnification, and photographed every 30 min for 6 to 10 h depending on doubling time of strains. Images were acquired with a digital CCD camera (C4742-95-12ERG, Hamamatsu Photonics) and processed using HCImage Live U11158-01 software (Hamamatsu Photonics). Long axes of cells were measured during the first and the second divisions. The average cell-length values for 50 to 70 individual cells were plotted against time axis, and CER was calculated in every 30 min. CER of temperature-sensitive cells was determined after 30-min preincubation of agar film at 36.5℃ as follows: for *cdc25-22*, *cdc2-L7*, or *cdc13-117* cells, average cell length of individual cells in the same field was calculated. A minor population of cells that divided within 3 h after the temperature shift was omitted. The average cell length was plotted against incubation time, from which CER was calculated; and for *act1-ts* or *adf1-1* cells, cell length of individual cells was measured until cell lysis and plotted against incubation time, and maximum growth rate of individual cells was used as estimate of growth rate against initial cell length at the temperature shift.

Cell length and CER are presented by average with standard deviation (SD). Statistical significance was tested by student's two-sided *t*-test. *P* values are presented as follows: *, <0.05; **, <0.001; ***, <0.0001; and n.s., not significant.

2.3 | Fluorescence microscopy

Cells were grown exponentially at 28℃. In most experiments, exponential cells grown at 28℃ were shifted to 36.5℃ for further incubation as indicated. Cells were visualized under x40 or x100 oil magnification using the same microscopy set as above with a GFP filter. Number of cells with nuclear localization (not uniform distribution in both nucleus and cytoplasm) of GFP signal was scored. Nuclear localization for each genotype was estimated as an average of more than three independent strains with SD. Total content and intensity of GFP signal in the nuclei were measured by manually surrounding the nuclei and processing using the same software as above. Values are presented by average (arbitrary unit) with SD. Statistical significance was as described above.

3 | RESULTS AND DISCUSSION

3.1 | Diploid cells grow faster than haploid cells

The previous study reported, by measuring cell length of individual cells at birth and septation from time-lapse films, that diploid cells grow faster than haploid cells during the same cycle time (Sveiczer, Novak, & Mitchison, 1996). I began my inquiry by measuring CER of haploid and diploid cells throughout the cell cycle. For this purpose, cells were pre-cultured exponentially in EMM2 at 28℃, spread on EMM2 agar film, and incubated at the same temperature. Cell growth was monitored by taking photos of cells on the agar film every 30 min between one division and the next (Figure 1a) and by measuring long axis of *S. pombe* cells, because they grow only by tip extension. CER was calculated in every 30 min from average cell length of 65 cells (Figure 1b). This analysis clearly indicated that diploid cells grow faster than haploid cells at about 1.5-fold rate until arrest of extension near the septation stage in the cell division cycle.

3.2 | Cell division genes control cell growth

To explore whether cell division genes are involved in growth control, temperature-sensitive mutations that affect Cdc2 activity were examined. For this purpose, cells were pre-cultured exponentially at a permissive temperature (28℃), spread on EMM2 agar film, and incubated at a restrictive temperature (36.5℃). Mutations that abolish Cdc2 activity such as *cdc25-22*, *cdc2-L7*, and *cdc13-117* caused longer cells than wild-type (Figures 2a-d) and increased CER in both haploid and diploid ($p<0.0001$, maximum CER compared between wild and mutant) (Figure 2e). On the contrary, *wee1-50* giving higher Cdc2 activity decreased CER of both haploid and diploid ($p<0.0001$) (Figures 2a, e). These results indicate that Cdc2 activity controls CER negatively. In addition, when

compared between mutant haploid and diploid, I found a remarkable acceleration of CER immediately after the temperature shift exclusively in *cdc25-22*/*cdc25-22* diploid, which may be suggestive of a special role of Cdc25 in diploid (Figure 2f).

3.3 | Haplo-insufficient roles of cell division genes

If cell division genes were involved in ploidy-dependent growth control, deletion of one of two copies of them in diploid would affect CER. To explore this idea, heterozygotes (*cdc25Δ*/+, *wee1Δ*/+, or *act1Δ*/+) were examined for growth kinetics and CER. All heterozygotes grew more slowly than parental diploid, indicating haplo-insufficient positive roles of $cdc25^{+}$, $wee1^{+}$, and $act1^{+}$ (Figure 3). The *cdc25Δ*/+ cells extended cycle time and were finally longer at septation stage than wild-type cells. The *wee1Δ*/+ cells showed an equivalent CER to haploid control, but grew for a longer time as well as the *wee1Δ*/*wee1Δ* cells used as a reference. The *act1Δ*/+ cells, in which actin polymers were considerably reduced (Figure S1), slowed down CER appreciably later in the cycle and delayed cell separation after septation.

To investigate genetic epistatic relationship, heterozygotes with combinations of deletion were also examined (Figure 3). The double heterozygotes harboring *wee1Δ*/+ (*wee1Δ*/+ *cdc25Δ*/+ or *wee1Δ*/+ *act1Δ*/+) showed clear reduction in CER compared with the *cdc25Δ*/+ or *act1Δ*/+ single heterozygote, respectively. Conversely, compared with the *wee1Δ*/+ single heterozygote, the double heterozygotes showed no reduction or indeed slight elevation of CER, respectively. This result indicates that *wee1Δ*/+ is epistatic to *cdc25Δ*/+ or *act1Δ*/+ and suggests that positive roles of Cdc25 and Act1 work under the presence of sufficient amount of Wee1. Next, to investigate relationship between *cdc25Δ*/+ and *act1Δ*/+, the *cdc25Δ*/+ *act1Δ*/+ double heterozygote was examined. The double heterozygote showed similar CER compared with the *cdc25Δ*/+ or *act1Δ*/+ single heterozygote, suggesting a functional link between positive roles of Cdc25 and Act1 (actin). I also examined the triple heterozygote (*wee1Δ*/+ *cdc25Δ*/+ *act1Δ*/+), which elevated CER compared with the *wee1Δ*/+ *cdc25Δ*/+ or *wee1Δ*/+ *act1Δ*/+ double heterozygotes, confirming negative roles of Act1 and Cdc25. Together, I conclude that Cdc25 has two opposite roles; it executes a positive role through actin and Wee1, while, if actin or Wee1 were insufficient in quantity, it appears to behave negatively by activating Cdc2. Similarly, actin is also likely to serve a dual role as a positive and a negative regulator dependently on the amount of Wee1.

3.4 | Cdc2 and actin dynamics control nuclear localization of GFP-Wee1

Since the genetic analysis predicted that Cdc25 and Act1 stimulate CER under the presence of sufficient amount of Wee1, together with my observation that longer cells have more contents of nuclear GFP-Wee1 (Figure S2) and Cdc25-GFP (Figure S3), I supposed that Cdc2 activity and actin dynamics would control Wee1 activity, the inhibitory kinase against Cdc2. For this purpose, I examined whether several mutations affecting Cdc2 activity or actin dynamics as follows could affect intracellular behavior of GFP-Wee1: *cdc2-3w* (giving higher Cdc2 activity), *cdc2-L7*, *cdc25-22*, *cdc13-117* (severe reduction of Cdc2 activity), and two counteracting temperature-sensitive mutations affecting actin dynamics: *cps8-188* (Ishiguro & Kobayashi, 1996), wild type of which encodes actin itself, makes the mutant actin filament collapse to a significant extent at restrictive temperature (hereafter called *act1-ts*); and *adf1-1* (Nakano & Mabuchi, 2006), wild type of which encodes actin-depolymerizing factor/cofilin that promotes dissociation of monomers from the filament, disrupts actin dynamics and makes mutant cells depleted of monomers.

I observed elevated nuclear content of GFP-Wee1 in both haploid and diploid *cdc2-3w* cells (1n *cdc2-3w* or 2n *cdc2-3w*/*cdc2-3w*, respectively) (Figure 4a, b) and, in contrast, reduced nuclear localization of GFP-Wee1 in *cdc2-L7*, *cdc25-22*, and *cdc13-117* cells, regardless of ploidy (Figure 4a). Furthermore, heterozygotes for either *cdc25Δ* or *cdc13Δ* also showed reduced nuclear localization (Figures 4a, c). These results suggest that Cdc2 activity controls nuclear localization of GFP-Wee1 in both haploid and diploid, and that two copies of $cdc25^+$ or $cdc13^+$ are required to keep GFP-Wee1 in the nuclei of diploid cells. Next, I observed that an increased dosage of $act1^+$ (2x$act1^+$ in haploid, which increased actin polymers substantially [Figure S1] or 3x$act1^+$ in diploid) (not shown) and *act1-ts* (Figure 4d) elevated nuclear content of GFP-Wee1, suggesting that increased amounts of actin monomers account for nuclear accumulation of GFP-Wee1. In favor with this result, the *adf1-1/adf1-1* diploid cells decreased nuclear content of GFP-Wee1 (Figure 4d), which was suppressed by *act1-ts/act1-ts* (Figure 4a). I also found that *act1Δ*/+ heterozygote showed reduced nuclear content of GFP-Wee1 (Figures 4c), indicating that one copy of $act1^+$ in diploid is not enough to accumulate GFP-Wee1 in the nucleus. Furthermore, the 3x$act1^+$ and *act1-ts*/*act1-ts* suppressed the reduced nuclear content of GFP-Wee1 in the *cdc25Δ*/+ or *cdc13Δ*/+ heterozygote and the *cdc13-117*/*cdc13-117* diploid, respectively (Figure 4a). Conversely, the *adf1-1*/*adf1-1* suppressed the increased nuclear accumulation of GFP-Wee1 in the *cdc2-3w*/*cdc2-3w* cells (Figure 4a). Together, these results reveal a specific role of actin monomer (or short actin oligomer) in nuclear accumulation of GFP-Wee1 in diploid and suggest that Cdc2

controls nuclear localization of GFP-Wee1 through modulation of actin dynamics. However, actin dynamics play no or limited role in haploid because no apparent effect was found in the *adf1-1* haploid (Figure 4a).

3.5 | Positive roles of Cdc25 and actin depend upon nuclear content of GFP-Wee1

If Cdc25 and actin would control CER through nuclear localization of Wee1, previous manipulation of Wee1 content would likely affect their regulatory activity. To test this idea, I constructed a series of diploid strains harboring different amount of GFP-Wee1 in the nuclei: *GFP-wee1*/*GFP-wee1* (control), *GFP-wee1*/*lys1* (half a dose) , 3x*nim1*$^{+}$ *GFP-wee1*/*lys1* (half a dose with reduced Wee1 activity by excess Nim1) , and *GFP-NESx2-wee1*/*GFP-NESx2-wee1*, a version of GFP-Wee1 tagged with two copies of *n*uclear *e*xport *s*ignal (Masuda, Fong, Ohtsuki, et al., 2011), which was mostly localized around the nuclear periphery with some in the nucleus and the cytoplasm regardless of temperature, ploidy, mutations or deletions of cell division genes, or 3x*act1*$^{+}$ (Figure 4b and data not shown).

Using these backgrounds, I examined growth kinetics and CER of wild-type and *act1Δ*/+ or *cdc25Δ*/+ heterozygotes (Figure 5a). I observed that *act1Δ*/+ decreased CER in *GFP-wee1*/*GFP-wee1* background while did not in *GFP-wee1*/*lys1*, 3x*nim1*$^{+}$ *GFP-wee1*/*lys1*, or *GFP-NESx2-wee1*/*GFP-NESx2-wee1* background, confirming that the positive role of *act1*$^{+}$ depends on nuclear content of Wee1. Contrary to expectations, I observed that *cdc25Δ*/+ increased CER in *GFP-wee1*/*GFP-wee1* background, suggesting that Cdc25 executes a weak positive activity in *GFP-wee1* background relative to wild-type, therefore, acts more negatively. In support of this assumption, cells harboring *GFP-wee1* are longer at septation than wild-type (28.9 μm±3.6 for 2n *GFP-wee1*/*GFP-wee1* cells *vs* 22.7 μm±2.2 for 2n wild-type at 28℃ in EMM2) and considered to have lower Cdc2 activity. The *cdc25Δ*/+ did not affect CER in the cells with half dosage of GFP-wee1 (*GFP-wee1*/*lys1*), while it again increased CER in the cells with more reduced Wee1 activity (3x*nim1*$^{+}$ *GFP-wee1*/*lys1*) and with the nuclearly excluded version of GFP-Wee1 (*GFP-NESx2-wee1*). These results suggest that no effect of *cdc25Δ*/+ on CER of the *GFP-wee1*/*lys1* cells may account for summation of positive and negative effects of Cdc25, and that Cdc25 acts positively depending upon nuclear content of Wee1.

I also examined the effect of *cdc2-3w/cdc2-3w* that increases Cdc2 activity, resulting in elevated nuclear content of GFP-Wee1 but not GFP-NESx2-Wee1 (Figure 4b). I expected that the *cdc2-3w* mutation would reduce CER of cells harboring *GFP-wee1* or *GFP-NESx2-wee1*, while the former cells may increase CER just as much as they have increased nuclear content of GFP-Wee1. As expected, I observed that the *cdc2-3w*

mutation reduced CER more severely in the *GFP-NESx2-wee1* background than in the *GFP-wee1* one (Figure 5b). This result confirms a negative feedback loop in which Cdc2 activity increases nuclear content of Wee1, resulting in feedback inhibition of Cdc2 and increase in CER.

3.6 | Cell-size scaling in cells harboring Cdc25-GFP

To further explore the positive role of Cdc25, I constructed haploid and diploid cells harboring *cdc25-GFP* and series of heterozygotes (single for *cdc25Δ*, *cdc13Δ*, *act1Δ*, and *wee1Δ*, and their double or triple combinations), and examined growth kinetics and CER. Surprisingly, single heterozygotes (*cdc25Δ*/+, *cdc13Δ*/+, *act1Δ*/+, or *wee1Δ*/+) showed severe reduction in CER (Figures 6a, b) compared with the wild-type background (Figure 3). I assume that Cdc25-GFP activates Cdc2 more strongly and expresses a stronger positive activity because cells harboring *cdc25-GFP* are shorter in cell length at septation than wild-type (19.5 μm±1.8 for 2n cdc25-*GFP*/cdc25-*GFP* cells *vs* 22.7 μm±2.2 for 2n wild-type at 28℃ in EMM2). Although CER was reduced more intensely, genetic relationship between these genes were preserved because these genes served as positive regulators dependently on Wee1 dosage (*wee1Δ*/+ or +/+), and could also act negatively. The most surprising was the triple heterozygote harboring *cdc25-GFP*/*Δ*, *act1Δ*/+, and *wee1Δ*/+ showing almost the same growth kinetics as haploid. This result strongly supports my proposal that a regulatory circuit comprising cell division genes is central to ploidy-dependent size scaling.

Using *cdc25-GFP* background, I further examined the dependency of positive role of Cdc25-GFP upon Wee1 dosage. The *cdc25-GFP*/*cdc25-22* reduced CER intensely compared with *cdc25-GFP*/*cdc25-GFP*, however, increased CER in the absence of Wee1 (*wee1-50*/*wee1-50*) (Figure 6c), confirming Wee1-dependent positive role of Cdc25-GFP. I also examined the effect of *cdc25-GFP*/*cdc25-22* under the condition where increased dosage of $act1^{+}$ (4x$act1^{+}$) retains Wee1 in the nuclei. The *cdc25-GFP*/*cdc25-22* did not reduce CER, whereas, as expected, *wee1-50*/*wee1-50* reduced CER because of the most downstream hierarchy of Wee1 (Figure 6d). Collectively, these results indicate that positive role of Cdc25 does not work in the absence of Wee1 or in the presence of excess Wee1, and again support the conclusion that Cdc25 activates Cdc2, which induces nuclear accumulation of Wee1, inhibition of Cdc2, then acceleration of CER.

3.7 | Cdc2 and actin dynamics control nuclear localization of Cdc25-GFP

Next I searched for possible relation of nuclear localization of Cdc25-GFP to Cdc2 activity and actin dynamics, because Cdc2 is known to be involved in actin dynamics:

actin filaments develop well or poorly in cells with lower or higher Cdc2 activity, respectively (Kamasaki, Arai, Osumi, et al., 2005; Kovar, Sirotkin, & Lord, 2011; Verde, Mata, & Nurse, 1995; Verde, Wiley, & Nurse, 1998) (Figure S1), and because nuclear content of Cdc25-GFP increases with cell size (Figure S3). I first examined whether mutational modulation of Cdc2 activity could affect nuclear localization of Cdc25-GFP by using mutant cells with higher (*wee1-50*) or severely reduced (*cdc13-117*) Cdc2 activity. I observed, after the shift to restrictive temperature (36.5℃), exclusion from the nuclei and uniform cellular distribution of Cdc25-GFP in *wee1-50* haploid and *wee1-50*/*wee1-50* diploid, respectively (Figure 7a, b). I found constant nuclear localization of Cdc25-NLS-GFP (a version of Cdc25-GFP fused with a *n*uclear *l*ocalization *s*ignal) in both *wee1-50* haploid and *wee1-50*/*wee1-50* diploid cells (Figure 7a), suggesting a specific role in nuclear localization. Conversely, *cdc13-117* cells accumulated nuclear Cdc25-GFP more abundantly irrespective of ploidy (Figure 7a, b). I also examined the effect of *wee1* Δ/+, resulting in clear reduction of nuclear content of Cdc25-GFP but constant nuclear localization of Cdc25-NLS-GFP (Figure 7a, c). These results indicate that nuclear localization of Cdc25-GFP is associated with Cdc2 activity and suggest a possible relation to actin dynamics: polymer but not monomer form of actin is favorable to nuclear localization of Cdc25-GFP.

Next I searched for control of nuclear localization of Cdc25-GFP through actin dynamics. To test this, I first used latrunculin A, a chemical reagent that destabilizes actin filament (Rupeš, Webb, Mak, et al., 2001). I found uniform cellular distribution of Cdc25-GFP but constant nuclear localization of Cdc25-NLS-GFP (not shown), suggesting a specific role of actin dynamics in nuclear localization of Cdc25-GFP. I next used two counteracting temperature-sensitive mutations for actin dynamics, *act1-ts* and *adf1-1*. I observed that both *act1-ts* and *adf1-1* mutations greatly decreased nuclear accumulation of Cdc25-GFP irrespective of ploidy, but did not affect nuclear localization of Cdc25-NLS-GFP (Figure 7a, d). The *adf1-1* mutation was also effective in both *cdc13-117* haploid and *cdc13-117/cdc13-117* diploid (Figure 7a), in which otherwise Cdc25-GFP accumulates in the nuclei more abundantly than in wild-type cells (Figure 7b), revealing an active role of actin filament in the nuclear localization of Cdc25-GFP. However, I observed that *act1-ts* decreased nuclear localization of Cdc25-GFP in *cdc13-117/cdc13-117* diploid but did not in *cdc13-117* haploid (Figure 7a), suggesting more active roles of actin in diploid than in haploid. This result is reminiscent of the observation that the *cdc25-22*/*cdc25-22* diploid cells elevated CER most drastically after the temperature shift compared with other mutant cells with reduced Cdc2 activity including haploid *cdc25-22* cells (Figure 2f), and is consistent with speculation that Cdc25 activates Cdc2 more

strongly in diploid than in haploid. I also examined the effect of *act1Δ*/+, resulting in only a slight reduction of nuclear content of Cdc25-GFP (Figure 7a). The *act1Δ*/+ did not worsen or ameliorate the effect of *wee1Δ*/+ (Figure 7a).

To examine whether Cdc2 and actin cooperatively control nuclear localization of Cdc25-GFP, I constructed double mutants bearing *wee1-50* and *act1-ts* or *adf1-1*. I found synthetic decrease of nuclear content of Cdc25-GFP in diploid homozygous for *wee1-50* and *adf1-1* (but not *act1-ts*) at permissive temperature (Figure 7a), suggesting a functional link between Cdc2 and actin dynamics.

3.8 | Positive roles of Cdc25 both in CER and division timing

I postulated that the reduced nuclear content of Cdc25-GFP accounts for both the decrease in CER and longer cycle time in the heterozygote harboring *wee1Δ*/+. To test this, I constructed *wee1Δ*/+ diploids harboring *cdc25-NLS-GFP*/*cdc25-NLS-GFP* for forced expression of Cdc25 in the nucleus as well as haploid and diploid controls (1n *cdc25-NLS-GFP* and 2n *cdc25-NLS-GFP*/*cdc25-NLS-GFP*, respectively). I observed that both controls show ploidy-dependent growth kinetics and CER as the *cdc25-GFP* background (Figure 8). However, the *wee1Δ*/+ diploids harboring *cdc25-NLS-GFP*/*cdc25-NLS-GFP* elevated CER sharply compared with the *wee1Δ*/+ diploids harboring *cdc25-GFP*/*cdc25-GFP* and simultaneously recovered the delayed cycle time (Figure 8). These results again confirm my proposal that Cdc25 acts as a positive regulator for cell extension during G2, and are consistent with the previous conclusion that Cdc25 as a key molecule constitutes the auto-regulatory loop for acute activation of Cdc2 at the G2/M boundary (Lu, Domingo-Sananes, Huzarska, et al., 2012).

3.9 | Feedforward network

Because Wee1 plays a critical role in ploidy-dependent growth control, I asked whether Nim1, known as an inhibitory kinase against Wee1, would control CER dose-dependently. I also examined dose-dependent abilities of Pom1 and Nif1, both acting as negative regulators of Nim1. I assumed that *nim1Δ*/+ heterozygote would activate Wee1 then increase CER whereas *pom1Δ*/+ and *nif1Δ*/+ heterozygotes would activate Nim1 and slow down CER. I observed that both heterozygotes (*Δ*/+) and homozygotes (*Δ*/*Δ*) for each of *pom1Δ* or *nif1Δ* decreased CER (Figures 9a), indicating haplo-insufficient positive roles of these genes. Unexpectedly, I observed that *nim1Δ*/+ heterozygote also decreased CER to an equivalent level to the haploid control (Figure 9a), indicating a positive role of Nim1. This was confirmed by the observation that double heterozygote *nim1Δ*/+ *pom1Δ*/+, in which Nim1 activity is higher than in the *nim1Δ*/+ heterozygote, grew faster than the

nim1Δ/+ heterozygote (Figure 9b). The *nim1Δ*/+ cells vastly extended cycle time and were finally longer at septation than wild-type cells. As expected, *nim1Δ*/*nim1Δ* homozygote grew faster than wild-type diploid (Figure 9a), indicating a negative role of Nim1. The *nim1Δ*/*nim1Δ* homozygote also extended cycle time. Together, these results revealed a feedforward network comprised of Nim1, Pom1, and Nif1 acting as a dosage-dependent positive or negative regulator for CER.

3.10 | Feedforward network controls nuclear localization of GFP-Wee1

Since genetic analysis uncovered positive or negative activity of the feedforward pathway for CER, I supposed that the *nim1Δ*/+ could increase Cdc2 activity indirectly through removal of Wee1 from the nuclei as observed in the *cdc25Δ*/+ heterozygote (Figure 4c). To investigate this, I examined whether the *nim1Δ*/+ could affect nuclear localization of GFP-Wee1. I observed reduced nuclear localization of GFP-Wee1 (Figures 10a, b). The *pom1Δ*/+ suppressed the defect of *nim1Δ*/+ in nuclear localization (Figure 10a) as observed in CER (Figure 9b). These results suggest that a partial decrease in Nim1 activity indirectly leads to reduction in nuclear content of Wee1 and concomitant increase in Cdc2 activity.

I also examined the effect of the *nim1Δ*/*nim1Δ* on nuclear content of GFP-Wee1. I observed increased content of nuclear GFP-Wee1 (Figure 10b) despite the expectation that low Cdc2 activity caused by *nim1Δ*/*nim1Δ* removes GFP-Wee1 from the nuclei. To further investigate the activity of Nim1, I examined the effect of increased dosage of *nim1*$^+$ (4x*nim1*$^+$). I observed severe reduction of nuclear localization of GFP-Wee1 at 36.5℃ but no apparent effect at 28℃ (Figures 10a). The different results may occur by lower sensitivity of GFP-Wee1 to 4x*nim1*$^+$ at 28℃ than at 36℃, which coincides with both observations that diploid cells bearing *GFP-wee1* become shorter in length at septation after the temperature shift from 28℃ to 36℃ (approximately 10% reduction for 4h) and that nuclear content of GFP-Wee1 is concordantly lower at 36.5℃ than at 28℃ (Figure 4d, 10c). Together, these results suggest that phosphorylated forms of Wee1 by Nim1 kinase tend to remove from the nuclei.

Next, I examined the effects of *pom1Δ* and an increased dosage of *pom1*$^+$ on nuclear localization of GFP-Wee1. I observed that GFP-Wee1 was excluded from the nuclei particularly at 36.5℃ in both the *pom1Δ*/+ heterozygote and *pom1Δ*/*pom1Δ* homozygote (Figure 10a, c). As expected, in the *nim1Δ*/*nim1Δ* background, the *pom1Δ*/+ did not affect the *nim1Δ*-induced nuclear accumulation of GFP-Wee1 (Figure 10a). The increased dosage of *pom1*+ (4x*pom1*$^+$) also reduced nuclear GFP-Wee1 content (Figure 10a) possibly through partial inhibition of Nim1 as observed in the *nim1Δ*/+ heterozygote.

I also examined the effect of *nif1Δ* on nuclear localization of GFP-Wee1. I observed relatively uniform distribution of GFP-Wee1 in both the *nif1Δ*/+ heterozygote and *nif1Δ*/*nif1Δ* homozygote (Figure 10a, c), suggesting a reduction in nuclear localization. I also observed an unexpected effect that the *nif1Δ*/*nif1Δ* was so effective as to reduce the nuclear content of GFP-Wee1 in the *nim1Δ*/*nim1Δ* background (Figure 10a), suggesting a Nim1-independent role.

I asked whether the feedforward network would control nuclear localization of GFP-Wee1 in haploid cells. I observed no clear effect in haploid of *pom1Δ*, *nim1Δ*, or *nif1Δ* (Figure 10a), indicating no or limited role of Pom1, Nim1, and Nif1 in haploid.

Since actin dynamics modulate nuclear content of GFP-Wee1 in response to Cdc2 activity, I asked whether the control of nuclear GFP-Wee1 content by the feedforward network would be associated with actin dynamics. To explore this, I examined the effects of *act1-ts* or 3x*act1*$^{+}$ on the reduced nuclear content of GFP-Wee1 in cells harboring *pom1Δ*/+, *nim1Δ*/+, *nif1Δ*/+, *nif1Δ*/*nif1Δ*, 4x*pom1*$^{+}$, or 4x*nim1*$^{+}$, and the effect of *adf1-1* on the increased nuclear content of GFP-Wee1 in the *nim1Δ*/*nim1Δ* cells (Figure 10a). I observed clear suppression by *act1-ts*, 3x*act1*$^{+}$, and *adf1-1* (Figures 10a). These results indicate that actin dynamics control nuclear content of GFP-Wee1 in concert with the feedforward network.

3.11 | Feedforward network controls CER both in Wee1-dependent and -independent pathways

Since the feedforward pathway controls CER in association with alteration of nuclear GFP-Wee1 content, I asked whether modulation of Wee1 dosage would affect CER of *nim1Δ*/+ or *pom1Δ*/+ cells. For this purpose, I constructed two types of strains, each harboring *wee1Δ*/+ for half dosage of *wee1*$^{+}$ or 3x*act1*$^{+}$ for increased content of nuclear Wee1, both harboring *nim1Δ*/+ or *pom1Δ*/+. I observed that *nim1Δ*/+ did not decrease CER in *wee1Δ*/+ cells (Figure 9c). Likewise, *pom1Δ*/+ did not decrease CER in *wee1Δ*/+ cells (Figure 9d). These results are consistent with a proposal that Nim1 and Pom1 play a positive role while maintaining nuclear content of Wee1. I also observed that *pom1Δ*/+ elevated CER in *wee1Δ*/+ cells with the *cdc25-GFP* background (Figure 9e), inspiring me with a possible presence of a Wee1-independent positive route in which Nim1 inhibits Cdc2 and stimulate CER. Furthermore, I observed that the 3x*act1*$^{+}$-induced preservation of nuclear Wee1 cancelled the defect in CER of *nim1Δ*/+ and *pom1Δ*/+ cells (Figure 9f), suggesting that the defects are mainly caused by the removal of Wee1 from the nuclei. As expected, *nim1Δ*/*nim1Δ* elevated CER significantly (Figure 9f), which may occur through activation of Wee1 by relief from the Nim1 inhibitory kinase.

To investigate whether Pom1 and Nif1 control CER through inhibition of Nim1, I examined genetic hierarchy between *nim1Δ* and *pom1Δ* or *nif1Δ*. The *pom1Δ*/+ did not affect CER of the *nim1Δ*/*nim1Δ* homozygote, as expected, while the *pom1Δ*/*pom1Δ* clearly decreased CER in the *nim1Δ*/*nim1Δ* homozygote (Figure 9g). The latter result may occur by monopolar extension specific to *pom1Δ*/*pom1Δ* (Bhatia, Hachet, Hersch, et al., 2014). Next, I observed that the *nif1Δ*/*nif1Δ* decreased CER in the *nim1Δ*/*nim1Δ* homozygote (Figure 9h), suggesting a *nim1*$^{+}$-independent positive role of Nif1. This is consistent with my observation that Nif1 is required for increased accumulation of nuclear GFP-Wee1 in the *nim1Δ*/*nim1Δ* homozygote (Figure 10a).

To verify the presence of Wee1-independent positive route for CER, I constructed strains harboring *wee1Δ*/*wee1Δ* in combination with *nif1Δ*/*nif1Δ* and/or *nim1Δ*/*nim1Δ*. I observed that *wee1Δ*/*wee1Δ* homozygotes bearing *nif1Δ*/*nif1Δ*, *nim1Δ*/*nim1Δ*, or *nif1Δ*/*nif1Δ nim1Δ*/*nim1Δ* grew more slowly and were smaller in cell length at division than the *wee1Δ*/*wee1Δ* homozygote (Figure 9i), revealing *wee1*$^{+}$-independent role of Nim1 and Nif1. Furthermore, I gave a clear evidence for the positive role of Nim1 in the absence of both *cdc25*$^{+}$ and *wee1*$^{+}$ (Figure 9j). The *nim1Δ*/*nim1Δ* cells bearing both *cdc25-22/cdc25-22* and *wee1*Δ/*wee1Δ* grew more slowly with shorter cell length at septation than the control cells harboring *cdc25-22/cdc25-22* and *wee1*Δ/*wee1Δ*. Collectively, these results revealed that Nim1 increases CER independently of both Wee1 and Cdc25 possibly playing an inhibitory role against Cdc2. In the present study, Nif1 controls CER in a more complicated manner such that it increases CER through inhibition of Nim1 in the authentic pathway, retention of nuclear Wee1 antagonistically against Nim1, and Nim1- and Wee1-independent pathway.

3.12 | A close cooperation between Cdc25 and Nim1

Since Cdc25 activates CER by accumulating Wee1 in the nuclei, I asked whether Nim1 would support Cdc25 by keeping Cdc2 activity low through retention of nuclear Wee1 or through inhibition of Cdc2 in the Wee1-independent pathway. For this purpose, I constructed double heterozygotes harboring *cdc25Δ*/+ and *nim1Δ*/+, and examined growth kinetics and CER. I observed that *cdc25Δ*/+ did not decrease CER in the *nim1Δ*/+ heterozygote, while *nim1Δ*/+ decreased CER in the *cdc25Δ*/+ heterozygote (Figure 11a). These results indicate that Nim1 acts downstream of Cdc25 and suggest that Cdc25 serves as a positive regulator in cooperation with Nim1 or that Nim1 increases CER independently of Cdc25 possibly through the novel pathway in which Nim1 inhibits Cdc2.

I also asked how Pom1 regulates CER through nuclear localization of Wee1 together with the negative feedback circuit involving Cdc25. To explore this, I combined *pom1Δ*/+

with *cdc25Δ*/+ and examined the effect of their combination on CER. I observed that *pom1Δ*/+ did not decrease CER of the *cdc25Δ*/+ heterozygote (Figure 11b). The reverse showed the same effect: *cdc25Δ*/+ did not decrease, in fact, increased CER of the *pom1Δ*/+ heterozygote (Figure 11b). These results revealed interdependency between *pom1*$^{+}$ and *cdc25*$^{+}$, and suggest that Pom1 and Cdc25 increases CER when cells have enough Wee1 in the nuclei. Furthermore, I again observed, using *cdc25-GFP* background, the interdependency between *pom1Δ*/+ and *cdc25Δ*/+, in addition, between *pom1Δ*/+ and *cdc13Δ*/+ (Figure 11c), confirming that Cdc2 activity is controlled coordinately both through the negative feedback loop and the Pom1-Nim1 route in order to adjust CER to dosage of cell division genes or ploidy.

3.13 | Actin monomers control CER both in positive and negative manners

The present study suggests that Cdc2 controls CER positively through nuclear localization of Wee1 possibly with the aid of actin monomer. I wondered how actin monomers and polymers (or actin cables) work for cell extension at the same time since actin cables and exocytic machineries play parallel roles for polarized growth in fission yeast (Bendezú & Martin, 2011; Hammer & Sellers, 2012). To clarify this, I first examined the effects of *act1-ts*. Cells pre-grown exponentially at 28℃ were shifted to 36.5℃, and inspected for cell growth. I observed three growth patterns regardless of ploidy (Figures 12a, b for haploid; Figures 12d, e for diploid): smaller cells at the temperature shift did not grow for about 2 h and thereafter initiated extension (late induction) or a minor fraction of cells did not grow at all during the experiment (no growth), while longer cells grew immediately (early induction) at moderate CER (Figure 12h). These results are consistent with the previous report that actin cables are not essential for polarized growth (Bendezú & Martin, 2011) and suggest a specific role of actin filament in the initiation of growth during early G2 phase, or alternatively, that actin monomers inhibit cell extension.

I also examined the effect of *act1-ts* in cells with higher or lower Cdc2 activity (induced by *wee1-50* or *cdc25-22*, respectively), because the modulation of Cdc2 activity is effective for gathering early or late G2 cells and for change in actin dynamics: higher or lower Cdc2 activity is expected to strengthen or weaken the effect of *act1-ts*, respectively. As expected, *wee1-50*/*wee1-50* greatly increased population with no growth in *act1-ts*/*act1-ts* diploid (Figures 12f, g), and conversely, *cdc25-22*/*cdc25-22* attenuated the defective growth in *act1-ts*/*act1-ts* or *act1-ts*/*act1-ts wee1-50*/*wee1-50* diploid (Figure 12g). Haploid *act1-ts* cells responded weakly to the modulation of Cdc2 activity (Figures 12c, g). In these experiments, cells with early induction grew at moderate CER

irrespective of ploidy (Figure 12h). These results further underline a critical role of actin dynamics in the initiation of growth during early G2 phase.

To clarify the ambiguous implication for the role of actin dynamics, either positive role of polymers or negative of monomers, I used the diploid strain harboring triple mutation (*act1-ts*/*act1-ts, cdc25-22*/*cdc25-22*, and *wee1-50*/*wee1-50*) as a control. Half of the population arrested growth after the shift to 36.5℃. However, *pom1Δ*/+ completely abolished the negative effect of *act1-ts*/*act1-ts*, which was returned by addition of *nim1Δ*/*nim1Δ* (Figure 12i). This should be considered as that reactivation of Nim1 (caused by *pom1Δ*/+) specifically cancelled the negative effect of actin monomers on Nim1 rather than that it recovered the activity of actin cables in *act1-ts*/*act1-ts* cells. Collectively, I propose that actin monomer inhibits Nim1 directly or indirectly through activation of Pom1, forming a novel positive feedback loop, in which Cdc2 stimulates actin monomer formation, resulting in inhibition of Nim1 and simultaneous activation of Cdc2 in the absence of both Cdc25 and Wee1.

Next, I asked whether the positive feedback loop would explain the negative effect of *act1Δ*/+ in *wee1Δ*/+ cells (Figure 3), because the half dosage of $act1^{+}$ is expected to decrease actin monomers, resulting in activation of Nim1, inhibition of Cdc2, and elevation of CER, and because *act1Δ*/+ showed no effect on nuclear content of Cdc25-GFP in *wee1Δ*/+ cells (Figure 7a). For this purpose, I examined the effect of *act1Δ*/+ in double heterozygote harboring *wee1Δ*/+ and *nim1Δ*/+ in the hope that the half $nim1^{+}$ dosage would reduce active Nim1. As expected, I observed that the *act1Δ*/+ did not elevate but decreased CER of the *wee1Δ*/+ *nim1Δ*/+ heterozygote (Figure 12j). The decrease in CER can be explained by reduction of the positive pathway in which actin monomers stimulate CER by increasing nuclear content of Wee1. Together, these results confirm the active role of the positive feedback loop.

On the other hand, to verify the positive role of actin monomers, I used the *GFP-NESx2-wee1* background because different kinds of treatment that disrupt normal actin dynamics such as increased dosage of $act1^{+}$, *act1-ts*, and *adf1-1* did not apparently affect the nuclear exclusion of GFP-NESx2-Wee1 (not shown). As controls, I examined the effects of *act1-ts*, *adf1-1*, and their combination *act1-ts adf1-1* on CER of diploid cells harboring *GFP-wee1*/*GFP-wee1*. For this purpose, cells grown exponentially at 28℃ were shifted to 36.5℃ and further incubated before cell lysis, during which CER of individual cells was estimated and plotted against initial cell length at the temperature shift. I observed that the cells harboring *act1-ts*/*act1-ts GFP-wee1*/*GFP-wee1* initiated growth immediately without showing late induction found in the *act1-ts*/*act1-ts* cells of normal $wee1^{+}$ background and extended cell length at moderately decreased CER (Figure

13). This may occur because *act1-ts*-induced monomers do not effectively increase Cdc2 activity in the *GFP-wee1*/*GFP-wee1* cells with lower Cdc2 activity than the normal *wee1*$^+$ diploid. Alternatively, increased amount of actin monomers would be expected to activate the positive pathway concomitantly with activation of the negative route. However, the *adf1-1*/*adf1-1* cells showed a considerable decrease in CER (Figure 13). This result is expected if supposed that substantial decrease in actin monomers by the *adf1-1* mutation would abolish positive activity of actin monomers more extensively rather than that it would induce Nim1 activation, subsequent inhibition of Cdc2, and elevation of CER. If the above speculation would be correct, cells harboring both *adf1-1*/*adf1-1* and *act1-ts*/*act1-ts* would increase monomer forms of actin and activate the positive pathway more strongly. As expected, the double heterozygote showed elevated CER compared with the *adf1-1*/*adf1-1* cells (Figure 13).

Since actin monomers have no effect on nuclear content of GFP-NESx2-Wee1, I expected that, in the *GFP-NESx2-wee1* background, *act1-ts*-induced increase in actin monomers could not activate positive route but activate negative route normally, then would greatly decrease CER. As expected, I observed that CER was heavily decreased by *act1-ts*/*act1-ts* in diploid cells bearing *GFP-NESx2-wee1*/*GFP-NESx2-wee1* (Figure 13). However, *adf1-1*/*adf1-1* reduced CER of *GFP-NESx2-wee1*/*GFP-NESx2-wee1* cells at the same level as did in the *GFP-wee1*/*GFP-wee1* cells (Figure 13), consistent with the notion that only Nim1 activates CER in both cells. On the contrary, I found that *act1-ts*/*act1-ts* did not suppress *adf1-1*/*adf1-1* in diploids bearing *GFP-NESx2-wee1*/*GFP-NESx2-wee1* (Figure 13), confirming a significant positive role of actin monomers in association with nuclear localization of Wee1. Collectively, I propose that actin monomer acts positively on CER through nuclear localization of Wee1.

3.14 | Doubling cell division genes in haploid reproduces diploid growth

Since I identified key genes to ploidy-dependent control of cell size by deleting one copy of them from diploid, I next explored whether these genes could replicate this control in haploid, by constructing haploid cells bearing two copies of each genes or their combinations. I observed that two copies of *wee1*$^+$ (*GFP-wee1* and *wee1*$^+$) elevated CER effectively as compared with wild-type haploid or a reference haploid bearing *GFP-wee1* (1n *GFP-wee1 wee1* Δ) (Figure 14a). However, two copies of *pom1*$^+$ (2x*pom1*$^+$) or *act1*$^+$ (2x*act1*$^+$) did not affect or slightly decreased CER, respectively. As expected, two copies of *cdc25*$^+$ (2x*cdc25*$^+$) or *cdc13*$^+$ (2x*cdc13*$^+$) decreased CER. Next, I examined combinatorial effects of 2x*act1*$^+$ and 2x*pom1*$^+$ in the haploid bearing two copies of *wee1*$^+$ (*GFP-wee1* and *wee1*$^+$). Surprisingly, I found that haploid cells bearing both 2x*act1*$^+$ and

2x*pom1*$^+$ at a time in addition to two copies of *wee1*$^+$ (*GFP-wee1* and *wee1*$^+$) showed an elevated CER equivalent to control diploid (2n *GFP-wee1*/*lys1 wee1Δ*/+) (Figure 14b), while either 2x*act1*$^+$ or 2x*pom1*$^+$ did not affect CER. These results suggest that 2x*act1*$^+$ stimulates CER under the condition where 2x*pom1*$^+$ activates Wee1 by inhibiting the authentic activity of Nim1 as inhibitory kinase against Wee1. To explore this assumption, I performed the same experiment using haploids bearing *GFP-NESx2-wee1* and *wee1*$^+$ in the hope that reduced content of nuclear Wee1 would depress the combinatorial effect. As expected, I observed no effect of 2x*act1*$^+$ in combination with 2x*pom1*$^+$ (Figure 14c). Together, these results indicate the importance of cooperation among *wee1*$^+$, *act1*$^+$, and *pom1*$^+$ in haploid. However, haploid cells bearing the triple combination showed slower initial growth, delayed cytokinesis, and longer doubling time, implying artifacts of doubling cell division genes in haploid.

Next I investigated the effect of quintuple combination of two copies of genes (*GFP-wee1* plus *wee1*$^+$, 2x*act1*$^+$, 2x*pom1*$^+$, 2x*cdc25*$^+$, and 2x*cdc13*$^+$). I observed that haploid cells with the quintuple combination showed an equivalent CER to the control diploid (2n *GFP-wee1*/*lys1 wee1Δ*/+), albeit earlier slowdown of CER and following shorter cell length at septation (Figure 14d). Any quadruple combination without each of 2x*act1*$^+$, 2x*pom1*$^+$, 2x*cdc25*$^+$, or 2x*cdc13*$^+$ showed lower CER, confirming the dose-dependent positive roles of these genes. I also performed the same experiment using haploids bearing *GFP-NESx2-wee1* plus *wee1*$^+$ to verify the significance of nuclear content of Wee1 in the combinatorial elevation of CER (Figure 14e). I observed that haploid cells bearing *GFP-NESx2-wee1* plus *wee1*$^+$, 2x*act1*$^+$, 2x*pom1*$^+$, 2x*cdc25*$^+$, and 2x*cdc13*$^+$ showed a greatly decreased CER compared with a control diploid (2n *GFP-NESx2-wee1*/*lys1 wee1Δ*/+). I also observed no effects on CER by subtraction of 1x*act1*$^+$ or 1x*pom1*$^+$. These results confirm that the combinatorial effect exerts its ability under sufficient amount of nuclear Wee1. On the other hand, I observed increase in CER by subtraction of either 1x*cdc25*$^+$ or 1x*cdc13*$^+$, indicating that they play negatively against CER under the Wee1-deficient condition where they cannot act well positively. These results are consistent with the observation showing Wee1-dependent positive functions of Cdc25 and Cdc13 (Figure 6).

Since the genetic analyses revealed that nuclear content of Wee1 is important for the combinatorial elevation of CER, I next explored whether doubling of genes and their combinations could affect nuclear content of GFP-wee1. I observed that 2x*act1*$^+$ increased nuclear GFP-Wee1 content (Figure 14f, upper panel). While 2x*pom1*$^+$ alone slightly decreased nuclear content, it increased one in combination with 2x*act1*$^+$. These results are consistent with the combinatorial elevation of CER by 2x*act1*$^+$ and 2x*pom1*$^+$ (Figure 14b), suggesting that lowering Cdc2 activity by the increased nuclear content of

GFP-wee1 caused the increase in CER. Next, I also examined whether 2x*cdc25*$^+$ and 2x*cdc13*$^+$ exerted a positive role for CER by accumulating GFP-Wee1 in the nuclei. I found a clear reduction in nuclear localization of GFP-Wee1 by subtracting 1x*cdc25*$^+$ or 1x*cdc13*$^+$ from the quintuple combination (Figure 14f, bottom panel), confirming the dose-dependent roles of these genes in nuclear accumulation of GFP-Wee1 (Figure 4a).

Next, I asked whether two copies of *nim1*$^+$ (2x*nim1*$^+$) could act positively for CER in haploid. For this purpose, I constructed haploids bearing all combinations of 2x*nim1*$^+$, 2x*pom1*$^+$, two copies of *wee1*$^+$ (*GFP-wee1* plus *wee1*$^+$ or *GFP-NESx2-wee1* plus *wee1*$^+$), 2x*act1*$^+$, 2x*cdc25*$^+$, and 2x*cdc13*$^+$, and examined growth kinetics and CER. I observed that 2x*nim1*$^+$ exclusively increased CER of haploid cells bearing two copies of *wee1*$^+$ (*GFP-wee1* plus *wee1*$^+$), 2x*act1*$^+$, 2x*cdc25*$^+$, and 2x*cdc13*$^+$ (Figure 15), and decreased CER of haploid cells with all other combinations (not shown) as shown partly (Figure 15): replacement of *GFP-wee1* with *GFP-NESx2-wee1*, or subtraction of each of 1x*act1*$^+$, 1x*cdc25*$^+$, or 1x*cdc13*$^+$. The positive effect of 2x*nim1*$^+$ was lost by addition of 2x*pom1*$^+$ (Figure 15), indicating a specific activity of Nim1. Collectively, these results suggest that positive role of Nim1 was manifested in haploid with sufficient amount of nuclear Wee1 that could resist the inhibitory activity of Nim1. I also observed that 2x*nim1*$^+$ shortened cycle time of the haploid cells bearing two copies of *wee1*$^+$ (*GFP-wee1* plus *wee1*$^+$), 2x*act1*$^+$, 2x*cdc25*$^+$, and 2x*cdc13*$^+$, which was returned to a former condition by further addition of 2x*pom1*$^+$. This result is consistent with the prolonged cycle time caused by *nim1Δ*/+ (Figure 9a), indicating a dosage-dependent specific role of Nim1 for ending cell division cycle possibly through inhibition of Cdc2.

3.15 | A model for cell-size scaling

This study uncovers a mechanism contributing to cell-size scaling with ploidy, and establishes unambiguously that limited numbers of specific genes but not total mass of DNA determine cell size. I found that systems level control of Cdc2 activity is crucial for cell size determination and that copy number of cell division genes controlling Cdc2 activity is origin of ploidy information (Figure 16). In this model, Cdc2 activity level determines CER during the G2 growth phase: higher or lower Cdc2 inhibits or accelerates CER, respectively. Scaling device consists of three mechanisms, positive and negative feedback loops and a feedforward network. In the negative feedback circuit, Cdc25 activates Cdc2 activity in order to accumulate enough Wee1 in the nucleus backward to inhibit Cdc2. Cdc2 controls nuclear content of Cdc25 and Wee1 through affecting actin dynamics. Actin monomers and polymers are associated with nuclear localization of Wee1 and Cdc25, respectively. In the positive feedback loop, actin dynamics also play a

critical role as a gatekeeper to switch ON/OFF the loop. Actin monomers inhibit Nim1 (or indirectly through activation of Pom1) in order to activate Cdc2, while skewed transition toward actin polymers activates Nim1 resulting in inhibition of Cdc2. This positive loop acts to maintain lower Cdc2 activity in cooperation with Cdc25 in order to increase CER in diploid. Nif1, Nim1, and Pom1 constitute the feedforward network and control Wee1 activity not only through the authentic way (Marshall, Young, Swaffer, et al., 2012; Wood & Nurse, 2015; Zhu & Wu, 2014) but also nuclear localization of Wee1. The role of Nim1 is bidirectional dependently on dosage or activity of itself. Half dosage of Nim1 is not sufficient to keep enough Cdc2 activity to accumulate nuclear Wee1 resulting in exclusion of Wee1 from the nuclei in the same way as Cdc25, while loss of Nim1 increases nuclear content of Wee1. I propose that the bidirectional control serves to narrow threshold of Nim1 for nuclear accumulation of Wee1. If supposed that Nim1 activity becomes increased with cell cycle progression during G2 in response to increase in actin polymers (or decrease in actin monomers), nuclear accumulation of Wee1 would be suppressed by Nim1 at early G2 followed by acceleration at a later stage. Nif1 also acts to inhibit Cdc2 independently of Nim1 and Wee1. Collectively, I propose that Cdc2 activity becomes decreased progressively mainly in response to increasing nuclear content of Wee1 during G2 period in diploid cells. Cdc25 and Nim1 are key regulators for nuclear accumulation of Wee1, with the former accumulating in the nuclei and the latter increased in activity during G2 progression. On the other hand, in haploid, nuclear localization of Wee1 is free from actin dynamics and the feedforward network. Therefore, coordinated actions of the positive and negative feedback mechanisms and the feedforward network are central to ploidy-dependent control of nuclear localization of Wee1 and finally cell-size scaling with ploidy. Recently, Cao et al. reported that a synthetic gene circuit generates robust scaling of ring formation with colony size in bacteria, which is mediated by integral feedback and incoherent feedforward control (Cao, Ryser, Payne, et al., 2016). Thus, this type of regulatory network may be underscored as a common mechanism for biological scaling.

Here I identified a genetic architecture for control of cell-size scaling with ploidy, however, molecular details remain unsolved. Regardless of the exact mechanism, my findings have important implications for understanding a longstanding and universal issue 'DNA content-cell size rule' in other eukaryotes including plants and animals, in which polyploidy may control tissue-specific cell size and function (Orr-Weaver, 2015; Pandit, Westendorp, & de Bruin, 2013). Finally, my results may advance agricultural application to breeding of crops and gardening plants and lay the groundwork for therapy of diseases in which polyploid cells are involved.

ACKNOWLEDGEMENTS

I thank P. Russell, P. Nurse, J. Bähler, J. R. Pringle, J. Ishiguro, P. G. Young, H. Masuda, K. Kitamura, K. Kume, D. Hirata and the National Bio-Resource Project (NBRP) Japan for reagents and T. Toda, M. Mizunuma and K. Kume for discussions.

CONFLICT OF INTEREST

The author declares that he has no conflict of interest.

ORCID

Ichiro Yamashita https://orcid.org/0000-0001-6016-5438

REFERENCES

Adams, J., & Hansche, P. E. (1974). Population studies in microorganism I. evolution of diploidy in *Sacchromyces cerevisiae*. *Genetics, 76,* 327-338.

Bähler, J., & Pringle, J. R. (1998). Pom1p, a fission yeast protein kinase that provides positional information for both polarized growth and cytokinesis. *Genes and Development, 12,* 1356-1370.

Bendezú, F. O., & Martin, S. G. (2011). Actin cables and the exocyst form two independent morphogenesis pathways in the fission yeast. *Molecular Biology of the Cell, 22,* 44-53.

Bhatia, P., Hachet, O, Hersch, M, Rincon, S., Berthelot-Grosjean, M., Dalessi, S., Basterra, L., Bergmann, S., Paoletti, A., & Martin, S. G. (2014). Distinct levels in Pom1 gradients limit Cdr2 activity and localization to time and position division. *Cell Cycle, 13,* 538-552.

Booher, R., & Beach, D. (1988). Involvement of *cdc13*$^{+}$ in mitotic control in *Schizosaccharomyces pombe*: possible interaction of the gene product with microtubules. *EMBO Journal, 7,* 2321-2327.

Cao, Y., Ryser, M. D., Payne, S., Li, B., Rao, C. V., & You, L. (2016). Collective space-sensing coordinates pattern scaling in engineered bacteria. *Cell, 165,* 620-630.

Cavalier-Smith, T. (2005). Economy, speed and size matter: evolutionary forces driving nuclear genome miniaturization and expansion. *Annals of Botany*, *95*, 147-175.

Chua, G., Lingner, C., Frazer, C., & Young, P. G. (2002). The *sal3*$^{+}$ gene encodes an importin-β implicated in the nuclear import of Cdc25 in *Schizosaccharomyces pombe*. *Genetics*, *162*, 689–703.

Feilotter, H., Nurse, P., & Young, P. G. (1991). Genetic and molecular analysis of *cdr1*/*nim1* in *Schizosaccharomyces pombe*. *Genetics*, *127*, 309-318.

Gould, K. L., & Nurse, P. (1989). Tyrosine phosphorylation of the fission yeast *cdc2*$^{+}$ protein kinase regulates entry into mitosis. *Nature*, *342*, 39-45.

Gregory, T. R. (2005). The C-value enigma in plants and animals: a review of parallels and an appeal for partnership. *Annals of Botany*, *95*, 133-146.

Hammer, J. A. 3rd, & Sellers, J. R. (2012). Walking to work: roles for class V myosins as cargo transporters. *Nature Reviews Molecular Cell Biology*, *13*, 13-26.

Hyun, O. L., Jean, M. D., & Robert, J. D. (2009). Endoreplication: polyploidy with purpose. *Genes and Development*, *23*, 2461-2477.

Ishiguro, J., & Kobayashi, W. (1996). An actin point-mutation neighboring the 'hydrophobic plug' causes defects in the maintenance of cell polarity and septum organization in the fission yeast *Schizosaccharomyces pombe*. *FEBS Letters*, *392*, 237-241.

Kamasaki, T., Arai, R., Osumi, M., & Mabuchi, I. (2005). Directionality of F-actin cables changes during the fission yeast cell cycle. *Nature Cell Biology*, *7*, 916-917.

Kellogg, D. R. (2003). Wee1-dependent mechanisms required for coordination of cell growth and cell division. *Journal of Cell Science*, *116*, 4883-4890.

Kondorosi, E., Roudier, F., & Gendreau, E. (2000). Plant cell-size control: growing by ploidy? *Current Opinion in Plant Biology*, *3*, 488–492.

Kovar, D. R., Sirotkin, V., & Lord, M. (2011). Three's company: the fission yeast actin cytoskeleton. *Trends in Cell Biology*, *21*, 177-187.

Lu, L. X., Domingo-Sananes, M. R., Huzarska, M., Novak, B, & Gould, K. L. (2012). Multisite phosphoregulation of Cdc25 activity refines the mitotic entrance and exit switches. *Proceedings of the National Academy of Sciences USA*, *109*, 9899–9904.

Marshall, W. F., Young, K. D., Swaffer, M., Wood, E., Nurse, P., Kimura, A., Frankel, J., Wallingford, J., Walbot, V., Qu, X., & Roeder, A. H. K. (2012). What determines cell size? *BMC Biology*, *10*, 101.

Masuda, H., Fong, C. S., Ohtsuki, C., Haraguchi, T., & Hiraoka, Y. (2011). Spatiotemporal regulations of Wee1 at the G2/M transition. *Molecular Biology of the Cell*, *22*, 555-569.

Nakano, K., & Mabuchi, I. (2006). Actin-depolymerizing protein Adf1 is required for formation and maintenance of the contractile ring during cytokinesis in fission yeast. *Molecular Biology of the Cell*, *17*, 1933-1945.

Orr-Weaver, T. L. (2015). When bigger is better: the role of polyploidy in organogenesis. *Trends in Genetics*, *31*, 307-315.

Pandit, S. K., Westendorp, B., & de Bruin, A. (2013). Physiological significance of polyploidization in mammalian cells. *Trends in Cell Biology*, *23*, 556-566.

Rothstein, R. J. (1983). One-step gene disruption in yeast. *Methods in Enzymology*, *101*, 202-211.

Rupeš, I., Webb, B. A., Mak, A., & Young, P. G. (2001). G2/M arrest caused by actin disruption is a manifestation of the cell size checkpoint in fission yeast. *Molecular Biology of the Cell*, *12*, 3892–3903.

Russell, P., & Nurse, P. (1986). *cdc25*$^{+}$ functions as an inducer in the mitotic control of fission yeast. *Cell*, *45*, 145-153.

Russell, P., & Nurse, P. (1987a). Negative regulation of mitosis by *wee1*$^{+}$, a gene encoding a protein kinase homolog. *Cell*, *49*, 559-567.

Russell, P., & Nurse, P. (1987b). The mitotic Inducer *nim1*$^{+}$ functions in a regulatory network of protein kinase homologs controlling the initiation of mitosis. *Cell, 49*, 569-576.

Sabatinos, S. A., & Forsburg, S. L. (2010). Molecular genetics of *Schizosaccharomyces pombe*. *Methods in Enzymology, 470*, 759-795.

Sugiyama, S. (2005). Polyploidy and cellular mechanisms changing leaf size: comparison of diploid and autotetraploid populations in two species of *Lolium*. *Annals of Botany, 96*, 931–938.

Sveiczer, A., Novak, B., & Mitchison, J. M. (1996). The size control of fission yeast revisited. *Journal of Cell Science, 109*, 2947-2957.

Vartiainen, M. K., Guettler, S., Larijani, B., & Treisman, R. (2007). Nuclear actin regulates dynamic subcellular localization and activity of the SRF cofactor MAL. *Science, 316*, 1749-1752.

Verde, F., Mata, J., & Nurse, P. (1995). Fission yeast cell morphogenesis: identification of new genes and analysis of their role during the cell cycle. *Journal of Cell Biology, 131*, 1529-1538.

Verde, F., Wiley, D. J., & Nurse, P. (1998). Fission yeast *orb6*, a ser/thr protein kinase related to mammalian rho kinase and myotonic dystrophy kinase, is required for maintenance of cell polarity and coordinates cell morphogenesis with the cell cycle. *Proceedings of the National Academy of Sciences USA, 95*, 7526–7531.

Wood, E., & Nurse, P. (2015). Sizing up to divide: mitotic cell-size control in fission yeast. *Annual Review of Cell and Developmental Biology, 31*, 11–29.

Wu, L., & Russell, P. (1997). Nif1, a novel mitotic inhibitor in *Schizosaccharomyces pombe*. *EMBO Journal, 16*, 1342-1350.

Zhou, Y., Wang, M., Jiang, M., Peng, L., Wan, C., Liu, J., Liu, W., Zhao, R., Zhao, X., Hu, W., Liu, S, & Xiao, Y. (2016). Autotetraploid cell Line induced by SP600125 from crucian carp and its developmental potentiality. *Scientific Reports*, *6*, 21814.

Zhu, Y.-H. & Wu, J.-Q. (2014). Cell-size control: complicated. *Cell Cycle*, *13*, 693–694.

FIGURE 1 CER of haploid and diploid cells. (a) Time-lapse images of wild-type haploid (1n) and diploid (2n) cells at 28℃. Photographs were taken every 30 min. Arrowheads indicate the same growing cells with cell length in μm. (b) Growth kinetics (*top*) and CER (*bottom*), starting from one division to the next.

FIGURE 2 Cdc2 controls CER negatively. (a-d) Growth kinetics at 36.5℃. Wild-type, *wee1-50* (a), *cdc25-22* (b), *cdc2-L7* (c), and *cdc13-117* (d). (e) CER. (f) Relative CER. Data in (e) were redrawn by setting the 0.5-h CER value to zero.

FIGURE 3 Haplo-insufficient positive and negative roles for CER. Growth kinetics (*left*) and maximum CER (*right*) during incubation at 28℃ of heterozygotes (*cdc25Δ*/+, *wee1Δ*/+, or *act1Δ*/+), those bearing combinations of deletion, and the homozygote bearing *wee1Δ*/*wee1Δ* used as a reference. Data for wild-type cells are the same as shown in Figure 1. Statistical significance (*p* value) against the strain marked by bar or one in parenthesis is presented.

FIGURE 4 Cdc2 and actin dynamics control nuclear localization of GFP-Wee1. (a) Nuclear localization of GFP-Wee1 at 28℃ and after the shift to 36.5℃ for 20 and 30 min for haploid and diploid, respectively. (b-d) Fluorescence images of live cells. (b) Wild-type and *cdc2-3w* cells bearing *GFP-wee1* or *GFP-NESx2-wee1*. Intensity of nuclear GFP-Wee1 is also presented. (c) Wild-type, *cdc25Δ*/+, and *act1Δ*/+ cells. (d) Wild-type, *act1-ts*/*act1-ts*, and *adf1-1*/*adf1-1* cells. Bar, 10 μm.

FIGURE 5 Positive roles of Cdc25 and Act1 depend upon nuclear content of GFP-Wee1. (a) Growth kinetics and maximum CER at 36.5℃ of diploid cells bearing series of genotypes for Wee1 and their heterozygotes (*act1Δ*/+ or *cdc25Δ*/+). Haploid cells were used as a reference. (b) Growth kinetics and maximum CER at 28℃ of the diploid cells indicated.

FIGURE 6 Cell-size scaling in cells harboring *cdc25-GFP*. Growth kinetics and maximum CER at 28℃ (a, b) and 36.5℃ (c, d). (a) Haploid (*cdc25-GFP*) and diploid (*cdc25-GFP*/*cdc25-GFP*) controls, heterozygotes (*cdc25-GFP*/*Δ*, *wee1Δ*/+, or *act1Δ*/+), and those bearing combinations of deletion. (b) Heterozygote (*cdc13Δ*/+) and its combinatorial heterozygotes. Data for haploid and diploid controls and the *wee1Δ*/+ heterozygote are the same as shown in (a). (c) The haploid and diploid controls, heterozygote (*cdc25-GFP*/*cdc25-22*), its combination with *wee1-50*/*wee1-50*, and a

wee1-50/*wee1-50* control. (d) Control diploid bearing 4x*act1*$^{+}$, its heterozygote (*cdc25-GFP*/*cdc25-22*) and homozygote (*wee1-50*/*wee1-50*).

FIGURE 7 Cdc2 and actin dynamics control nuclear localization of Cdc25-GFP. (a) Nuclear localization of Cdc25-GFP or Cdc25-NLS-GFP at 28℃ and after the shift to 36.5℃ for 1 or 2 h. (b-d) Fluorescence images of live cells. (b) Wild-type, *wee1-50*/*wee1-50*, or *cdc13-117/cdc13-117* cells. (c) Wild-type or *wee1Δ*/+ cells. (d) *act1-ts*/*act1-ts* or *adf1-1*/*adf1-1* cells. Bar, 10 μm.

FIGURE 8 Cell-size scaling in cells harboring *cdc25-NLS-GFP*. Growth kinetics and maximum CER at 28℃ in haploid (*cdc25-NLS-GFP*), diploid (*cdc25-NLS-GFP*/*cdc25-NLS-GFP*), and its heterozygote (*wee1Δ*/+). Data for their counterparts bearing *cdc25-GFP* are the same as shown in Figure 6.

FIGURE 9 Feedforward network controls CER. Growth kinetics and maximum CER at 28℃ (a-i) or 36.5℃ (j). (a) Heterozygotes or homozygotes for *nim1Δ*, *pom1Δ*, or *nif1Δ*. (b) *nim1Δ*/+ heterozygote or its combination (*nim1Δ*/+ *pom1Δ*/+). (c, d) *wee1Δ*/+ heterozygote or its combinations, *wee1Δ*/+ *nim1Δ*/+ (c) or *wee1Δ*/+ *pom1Δ*/+ (d). (e) Cells with *cdc25-GFP* background. *pom1Δ*/+ or *wee1Δ*/+ heterozygote or their combination (*wee1Δ*/+ *pom1Δ*/+). (f) Diploid cells bearing 3x*act1*$^{+}$ or its combinations with *nim1Δ*/+, *nim1Δ*/*nim1Δ*, or *pom1Δ*/+. (g, h) *nim1Δ*/*nim1Δ* homozygote or its combinations with *pom1Δ*/+ or *pom1Δ*/*pom1Δ* (g) or *nif1Δ*/*nif1Δ* (h). (i) *wee1Δ*/*wee1Δ* homozygote or its combinations with *nif1Δ*/*nif1Δ*, *nim1Δ*/*nim1Δ*, or *nif1Δ*/*nif1Δ nim1Δ*/*nim1Δ*. (j) Diploid cells bearing *cdc25-22*/*cdc25-22 wee1Δ*/*wee1Δ* or its combination with *nim1Δ*/*nim1Δ*. CER of individual cells were also plotted against cell length at septation. Data for wild-type cells (a, f, i), *wee1Δ*/+ or *wee1Δ*/*wee1Δ* cells (c, d, i), or cells bearing *cdc25-GFP*/*cdc25-GFP* or *wee1Δ*/+ (e) are the same as shown in Figure 1, 3, or 6, respectively.

FIGURE 10 Feedforward network controls nuclear localization of GFP-Wee1. (a) Nuclear localization of GFP-Wee1 at 28℃ and after the shift to 36.5℃ for 20 and 30 min for haploid and diploid, respectively. (b, c) Fluorescence images of live cells. (b) Wild-type, *nim1Δ*/+, and *nim1Δ*/*nim1Δ* cells. Intensity of nuclear GFP-Wee1 is also presented. (c) Wild-type, *pom1Δ*/+, and *nif1Δ*/+ cells. Bar, 10 μm.

FIGURE 11 A close cooperation between the negative feedback loop and the Nim1-Pom1 route. Growth kinetics and maximum CER at 28℃ in wild-type (a, b) or *cdc25-GFP* (c) background. (a) *cdc25Δ*/+ *nim1Δ*/+, (b) *cdc25Δ*/+ *pom1Δ*/+, (c) *cdc25-GFP*/*Δ pom1Δ*/+ or *cdc13Δ*/+ *pom1Δ*/+. Data for other cells are the same as shown in Figures 1, 3, 6, and 9.

FIGURE 12 Actin monomers inhibit CER through Nim1-Pom1. Growth kinetics of typical haploid cells (1n *act1-ts*) (a) and diploid cells (2n *act1-ts*/*act1-ts*) (d) after the shift to 36.5℃, showing early or late induction of extension. (b, c, e, and f) CER of individual cells plotted against initial cell length at the temperature shift. Haploid *act1-ts* (b) or *act1-ts wee1-50* (c), and diploid *act1-ts*/*act1-ts* (e) or *act1-ts*/*act1-ts wee1-50*/*wee1-50* (f). (g) Proportion of cells showing early or late induction, or no growth. (h) Average CER of individual cells showing early induction. (i) Diploid cells bearing *act1-ts*/*act1-ts cdc25-22*/*cdc25-22 wee1-50*/*wee1-50*, or its combinations with *pom1Δ*/+ or *pom1Δ*/+ *nim1Δ*/*nim1Δ*. (j) Growth kinetics and maximum CER at 28℃ of diploid cells bearing *wee1Δ*/+ *nim1Δ*/+ *act1Δ*/+. Data for other cells are the same as shown in Figures 3 and 9.

FIGURE 13 Actin monomers stimulate CER through nuclear accumulation of GFP-Wee1. CER of individual cells harboring *GFP-wee1*/*GFP-wee1* or *GFP-NESx2-wee1*/*GFP-NESx2-wee1*, and their combinations with *act1-ts*/*act1-ts*, *adf1-1*/*adf1-1*, or *adf1-1*/*adf1-1 act1-ts*/*act1-ts* after the shift to 36.5℃, plotted against initial cell length at the temperature shift. Average values with SD are also presented.

FIGURE 14 Doubling cell division genes in haploid reproduces diploid growth. (a-e) Growth kinetics and maximum CER at 36.5℃. (a) Haploids bearing two copies of *cdc13*$^+$, *cdc25*$^+$, *pom1*$^+$, *act1*$^+$, or *wee1*$^+$ (*GFP-wee1* and *wee1*$^+$), and controls (wild and *GFP-wee1 wee1Δ*). (b) Haploid bearing two copies of *wee1*$^+$ (*GFP-wee1* and *wee1*$^+$) (the same in [a]) and its combinations with 2x*pom1*$^+$, 2x*act1*$^+$, or 2x*pom1*$^+$ 2x*act1*$^+$. Diploid control (2n *GFP-wee1*/*lys1 wee1Δ*/+) also shown. (c) Haploid bearing *GFP-NESx2-wee1* and *wee1*$^+$ and its combinations with 2x*pom1*$^+$, 2x*act1*$^+$, or 2x*pom1*$^+$ 2x*act1*$^+$. (d) Haploid bearing quintuple combination of two copies of genes (*GFP-wee1* plus *wee1*$^+$, 2x*act1*$^+$, 2x*pom1*$^+$, 2x*cdc25*$^+$, and 2x*cdc13*$^+$) and haploids bearing quadruple combination without each of 2x*act1*$^+$, 2x*pom1*$^+$, 2x*cdc25*$^+$, or 2x*cdc13*$^+$. Diploid control (2n *GFP-wee1*/*lys1 wee1Δ*/+) (the same in [b]). (e) Haploid bearing quintuple combination of two copies of genes (*GFP-NESx2-wee1* plus *wee1*$^+$, 2x*act1*$^+$, 2x*pom1*$^+$, 2x*cdc25*$^+$, and 2x*cdc13*$^+$) and haploids bearing quadruple combination without each of 2x*act1*$^+$, 2x*pom1*$^+$, 2x*cdc25*$^+$, or

2x*cdc13*$^{+}$. Diploid control (2n *GFP-NESx2-wee1*/*lys1 wee1Δ*/+) also shown. (f) Intensity of nuclear GFP-Wee1 (*top*) and nuclear localization of GFP-Wee1 (*bottom*) after the shift to 36.5℃ for 60 and 20 min, respectively.

FIGURE 15 Positive role of Nim1 in haploid. Growth kinetics and maximum CER at 36.5℃. Series of haploids bearing quadruple or triple combination of *GFP-wee1* (or *GFP-NESx2-wee1*) plus *wee1*$^{+}$, 2x*act1*$^{+}$, 2x*cdc25*$^{+}$, and 2x*cdc13*$^{+}$ indicated and their combinations with two copies of *nim1*$^{+}$ (2x*nim1*$^{+}$) or with 2x*nim1*$^{+}$ plus 2x*pom1*$^{+}$.

FIGURE 16 A model for how fission yeast cells scale their size with ploidy. (*Left*) Genetic framework for control of CER in diploid. (*Right*) Proposed fluctuation of protein activity or content together with CER during G2 progression in diploid cells. See text for details.

FIGURE S1 Fluorescence images of actin. Cells pre-grown exponentially at 28℃ in EMM2 (or supplemented with requirements) were incubated at 36.5℃ for 4 h before staining with rhodamine-phalloidin as described previously (Rupeš, Webb, Mak, et al., 2001). Bar, 10 μm.

FIGURE S2 Fluorescence images of GFP-Wee1 in haploid and diploid cells. Cells were cultured exponentially at 28℃ in EMM2. Contents of GFP-Wee1 (in arbitrary unit) in the nuclei of individual cells were plotted against cell length. Bar, 10 μm.

FIGURE S3 Fluorescence images of Cdc25-GFP in haploid and diploid cells. Cells were cultured exponentially at 28℃ in EMM2. Contents of Cdc25-GFP (in arbitrary unit) in the nuclei of individual cells were plotted against cell length. Bar, 10 μm.

TABLE S1 The *S. pombe* strains used.

Experiment	Strain	Genotype
Figure 1	2802	h^- wild
	2829	$h^{+/-}$ *ade6-M210/ade6-M216*
Figure 2	2802	h^- wild
	2829	$h^{+/-}$ *ade6-M210/ade6-M216*
	3967	h^- *wee1-50*
	4031	$h^{+/-}$ *wee1-50/wee1-50 leu1-32/+ ade6-M210/ade6-M216*
	3823	h^- *cdc25-22*
	3691	$h^{+/-}$ *cdc25-22/cdc25-22 ade6-M210/ade6-M216*
	3779	h^- *cdc2-L7*
	3800	$h^{+/-}$ *cdc2-L7/cdc2-L7 ade6-M210/ade6-M216*
	4017	h^- *cdc13-117*
	4035	$h^{+/-}$ *cdc13-117/cdc13-117 ade6-M210/ade6-M216*
Figure 3	2802	h^- wild
	2829	$h^{+/-}$ *ade6-M210/ade6-M216*
	5646	$h^{-/-}$ *cdc25Δ::ura4*$^+$*/+ leu1-32/+ ura4-D18/ura4-D18 ade6-M210/ade6-M216*
	4684	$h^{+/-}$ *wee1Δ::ura4*$^+$*/+ leu1-32/+ ura4-D18/ura4-D18 ade6-M210/ade6-M216*
	5649	$h^{-/-}$ *act1Δ::ura4*$^+$*/+ leu1-32/+ ura4-D18/ura4-D18 ade6-M210/ade6-M216*
	5667	$h^{+/+}$ *cdc25Δ::ura4*$^+$*/+ wee1Δ::ura4*$^+$*/+ leu1-32/+ ura4-D18/ura4-D18 ade6-M210/ade6-M216*
	5670	$h^{-/-}$ *act1Δ::ura4*$^+$*/+ cdc25Δ::ura4*$^+$*/+ leu1-32/+ ura4-D18/ura4-D18 ade6-M210/ade6-M216*
	5669	$h^{-/-}$ *act1Δ::ura4*$^+$*/+ wee1Δ::ura4*$^+$*/+ leu1-32/+ ura4-D18/ura4-D18 ade6-M210/ade6-M216*
	6021	$h^{-/-}$ *cdc25Δ::ura4*$^+$*/+ wee1Δ::ura4*$^+$*/+ act1Δ::ura4*$^+$*/+ leu1-32/+* (or +/+) *ura4-D18/ura4-D18 ade6-M210/ade6-M216*
	4688	$h^{+/-}$ *wee1Δ::ura4*$^+$*/wee1Δ::ura4*$^+$ *leu1-32/+ ura4-D18/ura4-D18 ade6-M210/ade6-M216*
Figure 4	3174	h^+ *lys1*$^+$*::GFP-wee1 wee1Δ::ura4*$^+$ *ura4-D18*
	3234	h^- *cdc2-3w lys1*$^+$*::GFP-wee1 wee1Δ::ura4*$^+$ *ura4-D18*

Figure 4	3707	h^{-} *cdc2-L7 lys1^{+}::GFP-wee1 wee1Δ::ura4^{+} ura4-D18* (or *-294*)
	3891	h^{+} *cdc25-22 lys1^{+}::GFP-wee1 wee1Δ::ura4^{+} ura4-D18 ade6-M210*
	4042	h^{+} *cdc13-117 lys1^{+}::GFP-wee1 wee1Δ::ura4^{+} ura4-D18*
	4181	h^{+} *2xact1^{+}::ura4^{+} lys1^{+}::GFP-wee1 wee1Δ::ura4-3233 ura4-D18*
	5701	h^{+} *cdc13-117 2xact1^{+}::ura4^{+} lys1^{+}::GFP-wee1 wee1Δ::ura4-3233 ura4-D18 ade6-M210*
	1371	h^{-} *act1-ts lys1^{+}::GFP-wee1 wee1Δ::ura4^{+} leu1-32 ura4-D18*
	5685	h^{-} *act1-ts cdc13-117 lys1^{+}::GFP-wee1 wee1Δ::ura4^{+} leu1-32 ura4-D18 ade6-M210*
	4699	h^{-} *adf1-1 lys1^{+}::GFP-wee1 wee1Δ::ura4^{+} ura4-D18*
	5301	h^{-} *adf1-1 cdc2-3w lys1^{+}::GFP-wee1 wee1Δ::ura4^{+} ura4-D18*
	3180	h$^{+/-}$ *lys1^{+}::GFP-wee1/lys1^{+}::GFP-wee1 wee1Δ::ura4^{+}/wee1Δ::ura4^{+} leu1-32/+ ura4-D18/ura4-D18 ade6-M210/ade6-M216*
	3256	h$^{+/-}$ *cdc2-3w/cdc2-3w lys1^{+}::GFP-wee1/lys1^{+}::GFP-wee1 wee1Δ::ura4^{+}/wee1Δ::ura4^{+} ura4-D18/ura4-D18 ade6-M210/ade6-M216*
	3728	h$^{+/-}$ *cdc2-L7/cdc2-L7 lys1^{+}::GFP-wee1/lys1^{+}::GFP-wee1 wee1Δ::ura4^{+}/wee1Δ::ura4^{+} ura4-D18* (or *-294*)*/ura4-D18* (or *-294*) *ade6-M210/ade6-M216*
	3892	h$^{+/-}$ *cdc25-22/cdc25-22 lys1^{+}::GFP-wee1/lys1^{+}::GFP-wee1 wee1Δ::ura4^{+}/wee1Δ::ura4^{+} leu1-32/+ ura4-D18/ura4-D18 ade6-M210/ade6-M216*
	4060	h$^{+/-}$ *cdc13-117/cdc13-117 lys1^{+}::GFP-wee1/lys1^{+}::GFP-wee1 wee1Δ::ura4^{+}/wee1Δ::ura4^{+} ura4-D18/ura4-D18 ade6-M210/ade6-M216*

Figure 4	3452	h$^{-/-}$ *cdc25Δ::ura4^{+}/+ lys1^{+}::GFP-wee1/lys1^{+}::GFP-wee1 wee1Δ::ura4-3233/wee1Δ::ura4-3233 leu1-32/+ ura4-D18/ura4-D18 ade6-M210/ade6-M216*
	3927	h$^{-/-}$ *cdc13Δ::ura4^{+}/+ lys1^{+}::GFP-wee1/lys1^{+}::GFP-wee1 wee1Δ::ura4-3233/wee1Δ::ura4-3233 leu1-32/+ ura4-D18/ura4-D18 ade6-M210/ade6-M216*
	3322	h$^{+/-}$ *act1Δ::ura4^{+}/+ lys1^{+}::GFP-wee1/lys1^{+}::GFP-wee1 wee1Δ::ura4-3233/wee1Δ::ura4-3233 leu1-32/+ ura4-D18/ura4-D18 ade6-M210/ade6-M216*
	4813	h$^{+/-}$ 2x*act1^{+}::ura4^{+}*/+ (3x*act1^{+}*) *lys1^{+}::GFP-wee1/lys1^{+}::GFP-wee1 wee1Δ::ura4-3233/wee1Δ::ura4-3233 ura4-D18/ura4-D18 ade6-M210/ade6-M216*
	5731	h$^{+/-}$ *cdc13-117/cdc13-117* 2x*act1^{+}::ura4^{+}*/+ (3x*act1^{+}*) *lys1^{+}::GFP-wee1/lys1^{+}::GFP-wee1 wee1Δ::ura4-3233/wee1Δ::ura4-3233 ura4-D18/ura4-D18 ade6-M210/ade6-M216*
	4951	h$^{+/-}$ *cdc25Δ::ura4^{+}/+* 2x*act1^{+}::ura4^{+}*/+ (3x*act1^{+}*) *lys1^{+}::GFP-wee1/lys1^{+}::GFP-wee1 wee1Δ::ura4-3233/wee1Δ::ura4-3233 ura4-D18/ura4-D18 ade6-M210/ade6-M216*
	4953	h$^{-/-}$ *cdc13Δ::ura4^{+}/+* 2x*act1^{+}::ura4^{+}*/+ (3x*act1^{+}*) *lys1^{+}::GFP-wee1/lys1^{+}::GFP-wee1 wee1Δ::ura4-3233/wee1Δ::ura4-3233 ura4-D18/ura4-D18 ade6-M210/ade6-M216*
	3636	h$^{+/-}$ *act1-ts/act1-ts lys1^{+}::GFP-wee1/lys1^{+}::GFP-wee1 wee1Δ::ura4^{+}/wee1Δ::ura4-3233 leu1-32/+ ura4-D18/ura4-D18 ade6-M210/ade6-M216*
	5691	h$^{+/-}$ *act1-ts/act1-ts cdc13-117/cdc13-117 lys1^{+}::GFP-wee1/lys1^{+}::GFP-wee1 wee1Δ::ura4^{+}/wee1Δ::ura4^{+} leu1-32/leu1-32 ura4-D18/ura4-D18 ade6-M210/ade6-M216*
	4734	h$^{+/-}$ *adf1-1/adf1-1 lys1^{+}::GFP-wee1/lys1^{+}::GFP-wee1 wee1Δ::ura4^{+}/wee1Δ::ura4^{+} ura4-D18/ura4-D18 ade6-M210/ade6-M216*

Figure 4	4854	h$^{+/-}$ *act1-ts/act1-ts adf1-1/adf1-1 lys1^{+}::GFP-wee1/lys1^{+}::GFP-wee1 wee1Δ::ura4^{+}/wee1Δ::ura4^{+} ura4-D18/ura4-D18 ade6-M210/ade6-M216*
	5320	h$^{+/-}$ *adf1-1/adf1-1 cdc2-3w/cdc2-3w lys1^{+}::GFP-wee1/lys1^{+}::GFP-wee1 wee1Δ::ura4^{+}/wee1Δ::ura4^{+} ura4-D18/ura4-D18 ade6-M210/ade6-M216*
	3212	h$^{+/-}$ *lys1^{+}::GFP-NESx2-wee1/lys1^{+}::GFP-NESx2-wee1 wee1Δ::ura4^{+}/wee1Δ::ura4^{+} leu1-32/+ ura4-D18/ura4-D18 ade6-M210/ade6-M216*
	3260	h$^{+/-}$ *cdc2-3w/cdc2-3w lys1^{+}::GFP-NESx2-wee1/lys1^{+}::GFP-NESx2-wee1 wee1Δ::ura4^{+}/wee1Δ::ura4^{+} ura4-D18/ura4-D18 ade6-M210/ade6-M216*
Figure 5	3174	h^{+} *lys1^{+}::GFP-wee1 wee1Δ::ura4^{+} ura4-D18*
	3180	h$^{+/-}$ *lys1^{+}::GFP-wee1/lys1^{+}::GFP-wee1 wee1Δ::ura4^{+}/wee1Δ::ura4^{+} leu1-32/+ ura4-D18/ura4-D18 ade6-M210/ade6-M216*
	3322	h$^{+/-}$ *act1Δ::ura4^{+}/+ lys1^{+}::GFP-wee1/lys1^{+}::GFP-wee1 wee1Δ::ura4-3233/wee1Δ::ura4-3233 leu1-32/+ ura4-D18/ura4-D18 ade6-M210/ade6-M216*
	3452	h$^{-/-}$ *cdc25Δ::ura4^{+}/+ lys1^{+}::GFP-wee1/lys1^{+}::GFP-wee1 wee1Δ::ura4-3233/wee1Δ::ura4-3233 leu1-32/+ ura4-D18/ura4-D18 ade6-M210/ade6-M216*
	3416	h$^{+/-}$ *lys1^{+}::GFP-wee1/lys1-131 wee1Δ::ura4-3233/wee1Δ::ura4-3233 ura4-D18/+ ade6-M210/ade6-M216*
	3453	h$^{+/-}$ *act1Δ::ura4^{+}/+ lys1^{+}::GFP-wee1/lys1-131 wee1Δ::ura4-3233/wee1Δ::ura4-3233 ura4-D18/ura4-D18 ade6-M210/ade6-M216*
	5794	h$^{-/-}$ *cdc25Δ::ura4^{+}/+ lys1^{+}::GFP-wee1/lys1-131 wee1Δ::ura4-3233/wee1Δ::ura4-3233 leu1-32/+* (or +/+) *ura4-D18/ura4-D18 ade6-M210/ade6-M216*

Figure 5	5854	h$^{+/+}$ 2x*nim1^{+}::ura4^{+}*/+ (3x*nim1^{+}*) *lys1^{+}::GFP-wee1/lys1-131 wee1Δ::ura4-3233/wee1Δ::ura4-3233 ura4-D18/ura4-D18 ade6-M210/ade6-M216*
	5904	h$^{+/+}$ *act1Δ::ura4^{+}*/+ 2x*nim1^{+}::ura4^{+}*/+ (3x*nim1^{+}*) *lys1^{+}::GFP-wee1/lys1-131 wee1Δ::ura4-3233/wee1Δ::ura4-3233 ura4-D18/ura4-D18 ade6-M210/ade6-M216*
	5902	h$^{+/+}$ *cdc25Δ::ura4^{+}*/+ 2x*nim1^{+}::ura4^{+}*/+ (3x*nim1^{+}*) *lys1^{+}::GFP-wee1/lys1-131 wee1Δ::ura4-3233/wee1Δ::ura4-3233 leu1-32*/+ (or +/+) *ura4-D18/ura4-D18 ade6-M210/ade6-M216*
	3206	h^{-} *lys1^{+}::GFP-NESx2-wee1 wee1Δ::ura4^{+} ura4-D18*
	3212	h$^{+/-}$ *lys1^{+}::GFP-NESx2-wee1/lys1^{+}::GFP-NESx2-wee1 wee1Δ::ura4^{+}/wee1Δ::ura4^{+} leu1-32*/+ *ura4-D18/ura4-D18 ade6-M210/ade6-M216*
	3325	h$^{+/+}$ *act1Δ::ura4^{+}*/+ *lys1^{+}::GFP-NESx2-wee1/lys1^{+}::GFP-NESx2-wee1 wee1Δ::ura4-3233/wee1Δ::ura4-3233 leu1-32*/+ *ura4-D18/ura4-D18 ade6-M210/ade6-M216*
	3540	h$^{+/+}$ *cdc25Δ::ura4^{+}*/+ *lys1^{+}::GFP-NESx2-wee1/lys1^{+}::GFP-NESx2-wee1 wee1Δ::ura4-3233/wee1Δ::ura4-3233 leu1-32*/+ *ura4-D18/ura4-D18 ade6-M210/ade6-M216*
	3256	h$^{+/-}$ *cdc2-3w/cdc2-3w lys1^{+}::GFP-wee1/lys1^{+}::GFP-wee1 wee1Δ::ura4^{+}/wee1Δ::ura4^{+} ura4-D18/ura4-D18 ade6-M210/ade6-M216*
	3260	h$^{+/-}$ *cdc2-3w/cdc2-3w lys1^{+}::GFP-NESx2-wee1/lys1^{+}::GFP-NESx2-wee1 wee1Δ::ura4^{+}/wee1Δ::ura4^{+} ura4-D18/ura4-D18 ade6-M210/ade6-M216*
Figure 6	1461	h^{-} *cdc25Δ::ura4^{+}::cdc25-GFP::leu1^{+} leu1-32 ura4-D18*
	3614	h$^{-/-}$ *cdc25Δ::ura4^{+}::cdc25-GFP::leu1^{+}/ cdc25Δ::ura4^{+}::cdc25-GFP::leu1^{+} leu1-32/leu1-32 ura4-D18/ura4-D18 ade6-M210/ade6-M216*

Figure 6	3884	h$^{-/-}$ *cdc25Δ::ura4^{+}/cdc25Δ::ura4-2012::cdc25-GFP::leu1^{+} leu1-32/leu1-32 ura4-D18/ura4-D18 ade6-M210/ade6-M216*
	3592	h$^{-/-}$ *wee1Δ::ura4^{+}/+ cdc25Δ::ura4-2012::cdc25-GFP::leu1^{+}/ cdc25Δ::ura4-2012::cdc25-GFP::leu1^{+} leu1-32/leu1-32 ura4-D18/ura4-D18 ade6-M210/ade6-M216*
	2141	h$^{-/-}$ *act1Δ::ura4^{+}/+ cdc25Δ::ura4-2012::cdc25-GFP::leu1^{+}/ cdc25Δ::ura4-2012::cdc25-GFP::leu1^{+} leu1-32/leu1-32 ura4-D18/ura4-D18 ade6-M210/ade6-M216*
	3962	h$^{-/-}$ *wee1Δ::ura4^{+}/+ cdc25Δ::ura4^{+}/cdc25Δ::ura4-2012::cdc25-GFP::leu1^{+} leu1-32/leu1-32 ura4-D18/ura4-D18 ade6-M210/ade6-M216*
	3983	h$^{-/-}$ *act1Δ::ura4^{+}/+ cdc25Δ::ura4^{+}/cdc25Δ::ura4-2012::cdc25-GFP::leu1^{+} leu1-32/leu1-32 ura4-D18/ura4-D18 ade6-M210/ade6-M216*
	3705	h$^{-/-}$ *wee1Δ::ura4^{+}/+ act1Δ::ura4^{+}/+ cdc25Δ::ura4-2012::cdc25-GFP::leu1^{+}/ cdc25Δ::ura4-2012::cdc25-GFP::leu1^{+} leu1-32/leu1-32 ura4-D18/ura4-D18 ade6-M210/ade6-M216*
	4072	h$^{+/+}$ *act1Δ::ura4^{+}/+ wee1Δ::ura4^{+}/+ cdc25Δ::ura4^{+}/cdc25Δ::ura4-2012::cdc25-GFP::leu1^{+} leu1-32/leu1-32 ura4-D18/ura4-D18 ade6-M210/ade6-M216*
	3733	h$^{-/-}$ *cdc13Δ::ura4^{+}/+ cdc25Δ::ura4-2012::cdc25-GFP::leu1^{+}/ cdc25Δ::ura4-2012::cdc25-GFP::leu1^{+} leu1-32/leu1-32 ura4-D18/ura4-D18 ade6-M210/ade6-M216*
	3960	h$^{-/-}$ *cdc13Δ::ura4^{+}/+ cdc25Δ::ura4^{+}/cdc25Δ::ura4-2012::cdc25-GFP::leu1^{+} leu1-32/leu1-32 ura4-D18/ura4-D18 ade6-M210/ade6-M216*

Figure 6	3984	h$^{-/-}$ *cdc13Δ::ura4*$^{+}$/+ *wee1Δ::ura4*$^{+}$/+ *cdc25Δ::ura4-2012::cdc25-GFP::leu1*$^{+}$/ *cdc25Δ::ura4-2012::cdc25-GFP::leu1*$^{+}$ *leu1-32/leu1-32 ura4-D18/ura4-D18 ade6-M210/ade6-M216*
	4165	h$^{+/+}$ *cdc13Δ::ura4*$^{+}$/+ *act1Δ::ura4*$^{+}$/+ *cdc25Δ::ura4*$^{+}$/*cdc25Δ::ura4-2012::cdc25-GFP::leu1*$^{+}$ *leu1-32/leu1-32 ura4-D18/ura4-D18 ade6-M210/ade6-M216*
	3011	h$^{+/-}$ *cdc25-22/cdc25Δ::ura4*$^{+}$*::cdc25-GFP::leu1*$^{+}$ *leu1-32/leu1-32 ura4-D18/ura4-D18 ade6-M210/ade6-M216*
	2789	h$^{+/-}$ *wee1-50/wee1-50 cdc25Δ::ura4-2012::cdc25-GFP::leu1*$^{+}$/ *cdc25Δ::ura4*$^{+}$*::cdc25-GFP::leu1*$^{+}$ *leu1-32/leu1-32 ura4-D18/ura4-D18 ade6-M210/ade6-M216*
	3094	h$^{+/-}$ *wee1-50/wee1-50 cdc25-22/cdc25Δ::ura4*$^{+}$*::cdc25-GFP::leu1*$^{+}$ *leu1-32/leu1-32 ura4-D18/ura4-D18 ade6-M210/ade6-M216*
	3138	h$^{+/-}$ 2x*act1*$^{+}$*::ura4*$^{+}$/2x*act1*$^{+}$*::ura4*$^{+}$ (4x*act1*$^{+}$) *cdc25Δ::ura4-2012::cdc25-GFP::leu1*$^{+}$/ *cdc25Δ::ura4-2012::cdc25-GFP::leu1*$^{+}$ *leu1-32/leu1-32 ura4-D18/ura4-D18 ade6-M210/ade6-M216*
	3167	h$^{+/-}$ 2x*act1*$^{+}$*::ura4*$^{+}$/2x*act1*$^{+}$*::ura4*$^{+}$ (4x*act1*$^{+}$) *cdc25-22/cdc25Δ::ura4-2012::cdc25-GFP::leu1*$^{+}$ *leu1-32/leu1-32 ura4-D18/ura4-D18 ade6-M210/ade6-M216*
	4127	h$^{+/-}$ *wee1-50/wee1-50* 2x*act1*$^{+}$*::ura4*$^{+}$/2x*act1*$^{+}$*::ura4*$^{+}$ (4x*act1*$^{+}$) *cdc25Δ::ura4-2012::cdc25-GFP::leu1*$^{+}$/ *cdc25Δ::ura4-2012::cdc25-GFP::leu1*$^{+}$ *leu1-32/leu1-32 ura4-D18/ura4-D18 ade6-M210/ade6-M216*
Figure 7	1461	h^{-} *cdc25Δ::ura4*$^{+}$*::cdc25-GFP::leu1*$^{+}$ *leu1-32 ura4-D18*
	1557	h^{-} *cps8-188* (*act1-ts*) *cdc25Δ::ura4*$^{+}$*::cdc25-GFP::leu1*$^{+}$ *leu1-32 ura4-D18 ade6-M210*

Figure 7	4708	h$^-$ *adf1-1 cdc25Δ::ura4$^+$::cdc25-GFP::leu1$^+$ leu1-32 ura4-D18*
	1464	h$^-$ *wee1-50 cdc25Δ::ura4$^+$::cdc25-GFP::leu1$^+$ leu1-32 ura4-D18*
	1795	h$^-$ *act1-ts wee1-50 cdc25Δ::ura4$^+$::cdc25-GFP::leu1$^+$ leu1-32 ura4-D18 ade6-M210*
	5739	h$^-$ *adf1-1 wee1-50 cdc25Δ::ura4$^+$::cdc25-GFP::leu1$^+$ leu1-32 ura4-D18 ade6-M210*
	1846	h$^-$ *cdc13-117 cdc25Δ::ura4$^+$::cdc25-GFP::leu1$^+$ leu1-32 ura4-D18 ade6-M210*
	1909	h$^-$ *act1-ts cdc13-117 cdc25Δ::ura4$^+$::cdc25-GFP::leu1$^+$ leu1-32 ura4-D18 ade6-M210*
	4780	h$^-$ *adf1-1 cdc13-117 cdc25Δ::ura4$^+$::cdc25-GFP::leu1$^+$ leu1-32 ura4-D18*
	1587	h$^-$ *cdc25Δ::ura4$^+$::cdc25-NLS-GFP::leu1$^+$ leu1-32 ura4-D18 ade6-M216*
	1870	h$^-$ *wee1-50 cdc25Δ::ura4$^+$::cdc25-NLS-GFP::leu1$^+$ leu1-32 ura4-D18*
	2792	h$^+$ *act1-ts cdc25Δ::ura4$^+$::cdc25-NLS-GFP::leu1$^+$ leu1-32 ura4-D18 ade6-M210*
	4796	h$^-$ *adf1-1 cdc25Δ::ura4$^+$::cdc25-NLS-GFP::leu1$^+$ leu1-32 ura4-D18*
	3614	h$^{-/-}$ *cdc25Δ::ura4$^+$::cdc25-GFP::leu1$^+$/ cdc25Δ::ura4$^+$::cdc25-GFP::leu1$^+$ leu1-32/leu1-32 ura4-D18/ura4-D18 ade6-M210/ade6-M216*
	1740	h$^{+/-}$ *act1-ts/act1-ts cdc25Δ::ura4$^+$::cdc25-GFP::leu1$^+$/ cdc25Δ::ura4$^+$::cdc25-GFP::leu1$^+$ leu1-32/leu1-32 ura4-D18/ura4-D18 ade6-M210/ade6-M216*
	4736	h$^{+/-}$ *adf1-1/adf1-1 cdc25Δ::ura4$^+$::cdc25-GFP::leu1$^+$/ cdc25Δ::ura4$^+$::cdc25-GFP::leu1$^+$ leu1-32/leu1-32 ura4-D18/ura4-D18 ade6-M210/ade6-M216*
	1488	h$^{+/-}$ *wee1-50/wee1-50 cdc25Δ::ura4$^+$::cdc25-GFP::leu1$^+$/ cdc25Δ::ura4$^+$::cdc25-GFP::leu1$^+$ leu1-32/leu1-32 ura4-D18/ura4-D18 ade6-M210/ade6-M216*

Figure 7	1815	h$^{+/-}$ *act1-ts/act1-ts wee1-50/wee1-50 cdc25Δ::ura4^{+}::cdc25-GFP::leu1^{+}/ cdc25Δ::ura4^{+}::cdc25-GFP::leu1^{+} leu1-32/leu1-32 ura4-D18/ura4-D18 ade6-M210/ade6-M216*
	5757	h$^{+/-}$ *adf1-1/+ wee1-50/wee1-50 cdc25Δ::ura4^{+}::cdc25-GFP::leu1^{+}/ cdc25Δ::ura4^{+}::cdc25-GFP::leu1^{+} leu1-32/leu1-32 ura4-D18/ura4-D18 ade6-M210/ade6-M216*
	5761	h$^{+/-}$ *adf1-1/adf1-1 wee1-50/+ cdc25Δ::ura4^{+}::cdc25-GFP::leu1^{+}/ cdc25Δ::ura4^{+}::cdc25-GFP::leu1^{+} leu1-32/leu1-32 ura4-D18/ura4-D18 ade6-M210/ade6-M216*
	5766	h$^{+/-}$ *adf1-1/adf1-1 wee1-50/wee1-50 cdc25Δ::ura4^{+}::cdc25-GFP::leu1^{+}/ cdc25Δ::ura4^{+}::cdc25-GFP::leu1^{+} leu1-32/leu1-32 ura4-D18/ura4-D18 ade6-M210/ade6-M216*
	1861	h$^{+/-}$ *cdc13-117/cdc13-117 cdc25Δ::ura4^{+}::cdc25-GFP::leu1^{+}/ cdc25Δ::ura4^{+}::cdc25-GFP::leu1^{+} leu1-32/leu1-32 ura4-D18/ura4-D18 ade6-M210/ade6-M216*
	1925	h$^{+/-}$ *act1-ts/act1-ts cdc13-117/cdc13-117 cdc25Δ::ura4^{+}::cdc25-GFP::leu1^{+}/ cdc25Δ::ura4^{+}::cdc25-GFP::leu1^{+} leu1-32/leu1-32 ura4-D18/ura4-D18 ade6-M210/ade6-M216*
	4808	h$^{+/-}$ *adf1-1/adf1-1 cdc13-117/cdc13-117 cdc25Δ::ura4^{+}::cdc25-GFP::leu1^{+}/ cdc25Δ::ura4^{+}::cdc25-GFP::leu1^{+} leu1-32/leu1-32 ura4-D18/ura4-D18 ade6-M210/ade6-M216*
	3592	h$^{-/-}$ *wee1Δ::ura4^{+}/+ cdc25Δ::ura4-2012::cdc25-GFP::leu1^{+}/ cdc25Δ::ura4-2012::cdc25-GFP::leu1^{+} leu1-32/leu1-32 ura4-D18/ura4-D18 ade6-M210/ade6-M216*
	2141	h$^{-/-}$ *act1Δ::ura4^{+}/+ cdc25Δ::ura4-2012::cdc25-GFP::leu1^{+}/ cdc25Δ::ura4-2012::cdc25-GFP::leu1^{+} leu1-32/leu1-32 ura4-D18/ura4-D18 ade6-M210/ade6-M216*

Figure 7	3705	h$^{-/-}$ *act1Δ::ura4*$^{+}$*/+ wee1Δ::ura4*$^{+}$*/+ cdc25Δ::ura4-2012::cdc25-GFP::leu1*$^{+}$*/ cdc25Δ::ura4-2012::cdc25-GFP::leu1*$^{+}$ *leu1-32/leu1-32 ura4-D18/ura4-D18 ade6-M210/ade6-M216*
	6134	h$^{+/-}$ *cdc25Δ::ura4*$^{+}$*::cdc25-NLS-GFP::leu1*$^{+}$*/ cdc25Δ::ura4*$^{+}$*::cdc25-NLS-GFP::leu1*$^{+}$ *leu1-32/leu1-32 ura4-D18/ura4-D18 ade6-M210/ade6-M216*
	1886	h$^{+/-}$ *wee1-50/wee1-50 cdc25Δ::ura4*$^{+}$*::cdc25-NLS-GFP::leu1*$^{+}$*/ cdc25Δ::ura4*$^{+}$*::cdc25-NLS-GFP::leu1*$^{+}$ *leu1-32/leu1-32 ura4-D18/ura4-D18 ade6-M210/ade6-M216*
	2797	h$^{+/-}$ *act1-ts/act1-ts cdc25Δ::ura4*$^{+}$*::cdc25-NLS-GFP::leu1*$^{+}$*/ cdc25Δ::ura4*$^{+}$*::cdc25-NLS-GFP::leu1*$^{+}$ *leu1-32/leu1-32 ura4-D18/ura4-D18 ade6-M210/ade6-M216*
	4811	h$^{+/-}$ *adf1-1/adf1-1 cdc25Δ::ura4*$^{+}$*::cdc25-NLS-GFP::leu1*$^{+}$*/ cdc25Δ::ura4*$^{+}$*::cdc25-NLS-GFP::leu1*$^{+}$ *leu1-32/leu1-32 ura4-D18/ura4-D18 ade6-M210/ade6-M216*
	6139	h$^{+/-}$ *wee1Δ::ura4*$^{+}$*/+ cdc25Δ::ura4*$^{+}$*::cdc25-NLS-GFP::leu1*$^{+}$*/ cdc25Δ::ura4*$^{+}$*::cdc25-NLS-GFP::leu1*$^{+}$ *leu1-32/leu1-32 ura4-D18/ura4-D18 ade6-M210/ade6-M216*
Figure 8	1461	h^{-} *cdc25Δ::ura4*$^{+}$*::cdc25-GFP::leu1*$^{+}$ *leu1-32 ura4-D18*
	3614	h$^{-/-}$ *cdc25Δ::ura4*$^{+}$*::cdc25-GFP::leu1*$^{+}$*/ cdc25Δ::ura4*$^{+}$*::cdc25-GFP::leu1*$^{+}$ *leu1-32/leu1-32 ura4-D18/ura4-D18 ade6-M210/ade6-M216*
	3592	h$^{-/-}$ *wee1Δ::ura4*$^{+}$*/+ cdc25Δ::ura4-2012::cdc25-GFP::leu1*$^{+}$*/ cdc25Δ::ura4-2012::cdc25-GFP::leu1*$^{+}$ *leu1-32/leu1-32 ura4-D18/ura4-D18 ade6-M210/ade6-M216*
	6112	h^{-} *cdc25Δ::ura4*$^{+}$*::cdc25-NLS-GFP::leu1*$^{+}$ *leu1-32 ura4-D18*
	6134	h$^{+/-}$ *cdc25Δ::ura4*$^{+}$*::cdc25-NLS-GFP::leu1*$^{+}$*/ cdc25Δ::ura4*$^{+}$*::cdc25-NLS-GFP::leu1*$^{+}$ *leu1-32/leu1-32 ura4-D18/ura4-D18 ade6-M210/ade6-M216*

Figure 8	6139	h$^{+/-}$ *wee1Δ::ura4*$^{+}$/+ *cdc25Δ::ura4*$^{+}$*::cdc25-NLS-GFP::leu1*$^{+}$/ *cdc25Δ::ura4*$^{+}$*::cdc25-NLS-GFP::leu1*$^{+}$ *leu1-32/leu1-32 ura4-D18/ura4-D18 ade6-M210/ade6-M216*
Figure 9	2802	h^{-} wild
	2829	h$^{+/-}$ *ade6-M210/ade6-M216*
	6136	h$^{+/-}$ *nim1Δ::LEU2*/+ *leu1-32/leu1-32 ade6-M210/ade6-M216*
	4445	h$^{+/-}$ *nim1Δ::LEU2*/ *nim1Δ::LEU2 leu1-32/leu1-32 ura4-D18*/+ *ade6-M210/ade6-M216*
	6057	h$^{-/-}$ *pom1Δ::ura4*$^{+}$/+ *leu1-32*/+ *ura4-D18/ura4-D18 ade6-M210/ade6-M216*
	4975	h$^{+/-}$ *pom1Δ::ura4*$^{+}$/*pom1Δ::ura4*$^{+}$ *ura4-D18/ura4-D18 ade6-M210/ade6-M216*
	6114	h$^{+/-}$ *nif1Δ::ura4*$^{+}$/+ *leu1-32*/+ *ura4-D18/ura4-D18 ade6-M210/ade6-M216*
	6117	h$^{+/-}$ *nif1Δ::ura4*$^{+}$/*nif1Δ::ura4*$^{+}$ *leu1-32*/+ *ura4-D18/ura4-D18 ade6-M210/ade6-M216*
	4454	h$^{+/-}$ *nim1Δ::LEU2*/+ *pom1Δ::ura4*$^{+}$/+ *leu1-32/leu1-32 ura4-D18/ura4-D18 ade6-M210/ade6-M216*
	4684	h$^{+/-}$ *wee1Δ::ura4*$^{+}$/+ *leu1-32*/+ *ura4-D18/ura4-D18 ade6-M210/ade6-M216*
	6054	h$^{-/-}$ *wee1Δ::ura4*$^{+}$/+ *nim1Δ::LEU2*/+ *leu1-32/leu1-32 ura4-D18/ura4-D18 ade6-M210/ade6-M216*
	6113	h$^{+/-}$ *wee1Δ::ura4*$^{+}$/+ *pom1Δ::ura4*$^{+}$/+ *leu1-32*/+ *ura4-D18/ura4-D18 ade6-M210/ade6-M216*
	3614	h$^{-/-}$ *cdc25Δ::ura4*$^{+}$*::cdc25-GFP::leu1*$^{+}$/ *cdc25Δ::ura4*$^{+}$*::cdc25-GFP::leu1*$^{+}$ *leu1-32/leu1-32 ura4-D18/ura4-D18 ade6-M210/ade6-M216*
	3390	h$^{+/-}$ *pom1Δ::ura4*$^{+}$/+ *cdc25Δ::ura4-2012::cdc25-GFP::leu1*$^{+}$/ *cdc25Δ::ura4-2012::cdc25-GFP::leu1*$^{+}$ *leu1-32/leu1-32 ura4-D18/ura4-D18 ade6-M210/ade6-M216*
	3592	h$^{-/-}$ *wee1Δ::ura4*$^{+}$/+ *cdc25Δ::ura4-2012::cdc25-GFP::leu1*$^{+}$/ *cdc25Δ::ura4-2012::cdc25-GFP::leu1*$^{+}$ *leu1-32/leu1-32 ura4-D18/ura4-D18 ade6-M210/ade6-M216*

Figure 9	3604	h$^{-/-}$ *pom1Δ::ura4*$^{+}$/+ *wee1Δ::ura4*$^{+}$/+ *cdc25Δ::ura4-2012::cdc25-GFP::leu1*$^{+}$/ *cdc25Δ::ura4-2012::cdc25-GFP::leu1*$^{+}$ *leu1-32/leu1-32 ura4-D18/ura4-D18 ade6-M210/ade6-M216*
	4640	h$^{+/-}$ 2x*act1*$^{+}$*::ura4*$^{+}$/+ (3x*act1*$^{+}$) *leu1-32*/+ *ura4-D18/ura4-D18 ade6-M210/ade6-M216*
	4651	h$^{+/-}$ *nim1Δ::LEU2*/+ 2x*act1*$^{+}$*::ura4*$^{+}$/+ (3x*act1*$^{+}$) *leu1-32*/*leu1-32 ura4-D18/ura4-D18 ade6-M210/ade6-M216*
	4658	h$^{+/-}$ *nim1Δ::LEU2*/*nim1Δ::LEU2* 2x*act1*$^{+}$*::ura4*$^{+}$/+ (3x*act1*$^{+}$) *leu1-32*/*leu1-32 ura4-D18/ura4-D18 ade6-M210/ade6-M216*
	4869	h$^{+/-}$ *pom1Δ::ura4*$^{+}$/+ 2x*act1*$^{+}$*::ura4*$^{+}$/+ (3x*act1*$^{+}$) *leu1-32*/+ *ura4-D18/ura4-D18 ade6-M210/ade6-M216*
	4457	h$^{+/-}$ *nim1Δ::LEU2*/ *nim1Δ::LEU2 pom1Δ::ura4*$^{+}$/+ *leu1-32/leu1-32 ura4-D18*/*ura4-D18 ade6-M210/ade6-M216*
	4962	h$^{+/-}$ *nim1Δ::LEU2*/*nim1Δ::LEU2 pom1Δ::ura4*$^{+}$/*pom1Δ::ura4*$^{+}$ *leu1-32/leu1-32 ura4-D18*/*ura4-D18 ade6-M210/ade6-M216*
	5335	h$^{+/-}$ *nim1Δ::LEU2*/*nim1Δ::LEU2 nif1Δ::ura4*$^{+}$/*nif1Δ::ura4*$^{+}$ *leu1-32/leu1-32 ura4-D18*/*ura4-D18 ade6-M210/ade6-M216*
	4688	h$^{+/-}$ *wee1Δ::ura4*$^{+}$/*wee1Δ::ura4*$^{+}$ *leu1-32*/+ *ura4-D18/ura4-D18 ade6-M210/ade6-M216*
	5469	h$^{+/-}$ *nif1Δ::ura4*$^{+}$/*nif1Δ::ura4*$^{+}$ *wee1Δ::ura4*$^{+}$/*wee1Δ::ura4*$^{+}$ *ura4-D18/ura4-D18 ade6-M210/ade6-M216*
	4693	h$^{+/-}$ *nim1Δ::LEU2/nim1Δ::LEU2 wee1Δ::ura4*$^{+}$/*wee1Δ::ura4*$^{+}$ *leu1-32/leu1-32 ura4-D18/ura4-D18 ade6-M210/ade6-M216*
	5473	h$^{+/-}$ *nif1Δ::ura4*$^{+}$/*nif1Δ::ura4*$^{+}$ *nim1Δ::LEU2/nim1Δ::LEU2 wee1Δ::ura4*$^{+}$/*wee1Δ::ura4*$^{+}$ *leu1-32/leu1-32 ura4-D18/ura4-D18 ade6-M210/ade6-M216*
	5409	h$^{+/-}$ *cdc25-22/cdc25-22 wee1Δ::ura4*$^{+}$/*wee1Δ::ura4*$^{+}$ *ura4-D18/ura4-D18 ade6-M210/ade6-M216*

Figure 9	5388	h$^{+/-}$ *cdc25-22/cdc25-22 wee1Δ::ura4^{+}/wee1Δ::ura4^{+} nim1Δ::LEU2/nim1Δ::LEU2 leu1-32/leu1-32 ura4-D18/ura4-D18 ade6-M210/ade6-M216*
Figure 10	3174	h^{+} *lys1^{+}::GFP-wee1 wee1Δ::ura4^{+} ura4-D18*
	3507	h^{+} *pom1Δ::ura4^{+} lys1^{+}::GFP-wee1 wee1Δ::ura4-3233 ura4-D18*
	4542	h^{+} *nim1Δ::LEU2 lys1^{+}::GFP-wee1 wee1Δ::ura4^{+} leu1-32 ura4-D18 ade6-M210*
	4607	h^{+} *nim1Δ::LEU2 pom1Δ::ura4^{+} lys1^{+}::GFP-wee1 wee1Δ::ura4-3233 leu1-32 ura4-D18 ade6-M216*
	5452	h^{+} *nif1Δ::ura4^{+} lys1^{+}::GFP-wee1 wee1Δ::ura4-3233 ura4-D18 ade6-M210*
	3180	h$^{+/-}$ *lys1^{+}::GFP-wee1/lys1^{+}::GFP-wee1 wee1Δ::ura4^{+}/wee1Δ::ura4^{+} leu1-32/+ ura4-D18/ura4-D18 ade6-M210/ade6-M216*
	3526	h$^{+/-}$ *pom1Δ::ura4^{+}/pom1Δ::ura4^{+} lys1^{+}::GFP-wee1/lys1^{+}::GFP-wee1 wee1Δ::ura4-3233/wee1Δ::ura4-3233 ura4-D18/ura4-D18 ade6-M210/ade6-M216*
	3529	h$^{+/-}$ *pom1Δ::ura4^{+}/+ lys1^{+}::GFP-wee1/lys1^{+}::GFP-wee1 wee1Δ::ura4-3233/wee1Δ::ura4-3233 ura4-D18/ura4-D18 ade6-M210/ade6-M216*
	5277	h$^{+/-}$ 2x*pom1^{+}::ura4^{+}*/2x*pom1^{+}::ura4^{+}* (4x*pom1^{+}*) *lys1^{+}::GFP-wee1/lys1^{+}::GFP-wee1 wee1Δ::ura4-3233/wee1Δ::ura4-3233 ura4-D18/ura4-D18 ade6-M210/ade6-M216*
	3673	h$^{+/-}$ *act1-ts/act1-ts pom1Δ::ura4^{+}/+ lys1^{+}::GFP-wee1/lys1^{+}::GFP-wee1 wee1Δ::ura4-3233/wee1Δ::ura4-3233 ura4-D18/ura4-D18 ade6-M210/ade6-M216*
	4574	h$^{+/-}$ *nim1Δ::LEU2/nim1Δ::LEU2 lys1^{+}::GFP-wee1/lys1^{+}::GFP-wee1 wee1Δ::ura4^{+}/wee1Δ::ura4-3233 leu1-32/leu1-32 ura4-D18/ura4-D18 ade6-M210/ade6-M216*

Figure 10	4880	h$^{+/-}$ *adf1-1/adf1-1 nim1Δ::LEU2/nim1Δ::LEU2 lys1^{+}::GFP-wee1/lys1^{+}::GFP-wee1 wee1Δ::ura4^{+}/wee1Δ::ura4^{+} leu1-32/leu1-32 ura4-D18/ura4-D18 ade6-M210/ade6-M216*
	6126	h$^{+/-}$ *nim1Δ::LEU2/+ lys1^{+}::GFP-wee1/lys1^{+}::GFP-wee1 wee1Δ::ura4^{+}/wee1Δ::ura4-3233 leu1-32/leu1-32 ura4-D18/ura4-D18 ade6-M210/ade6-M216*
	4612	h+/- *nim1Δ::LEU2/nim1Δ::LEU2 pom1Δ::ura4^{+}/+ lys1^{+}::GFP-wee1/lys1^{+}::GFP-wee1 wee1Δ::ura4-3233/wee1Δ::ura4-3233 leu1-32/leu1-32 ura4-D18/ura4-D18 ade6-M210/ade6-M216*
	4554	h$^{+/-}$ *nim1Δ::LEU2/+ pom1Δ::ura4^{+}/+ lys1^{+}::GFP-wee1/lys1^{+}::GFP-wee1 wee1Δ::ura4-3233/wee1Δ::ura4-3233 leu1-32/leu1-32 ura4-D18/ura4-D18 ade6-M210/ade6-M216*
	5233	h$^{+/-}$ 2x*nim1^{+}::ura4^{+}*/2x*nim1^{+}::ura4^{+}* (4x*nim1^{+}*) *lys1^{+}::GFP-wee1/lys1^{+}::GFP-wee1 wee1Δ::ura4-3233/wee1Δ::ura4-3233 ura4-D18/ura4-D18 ade6-M210/ade6-M216*
	5457	h$^{+/-}$ *nif1Δ::ura4^{+}/nif1Δ::ura4^{+} lys1^{+}::GFP-wee1/lys1^{+}::GFP-wee1 wee1Δ::ura4-3233/wee1Δ::ura4-3233 ura4-D18/ura4-D18 ade6-M210/ade6-M216*
	5460	h$^{+/-}$ *nif1Δ::ura4^{+}/+ lys1^{+}::GFP-wee1/lys1^{+}::GFP-wee1 wee1Δ::ura4-3233/wee1Δ::ura4-3233 ura4-D18/ura4-D18 ade6-M210/ade6-M216*
	5502	h$^{+/-}$ *nif1Δ::ura4^{+}/nif1Δ::ura4^{+} nim1Δ::LEU2/nim1Δ::LEU2 lys1^{+}::GFP-wee1/lys1^{+}::GFP-wee1 wee1Δ::ura4-3233/wee1Δ::ura4-3233 leu1-32/leu1-32 ura4-D18/ura4-D18 ade6-M210/ade6-M216*
	4813	h$^{+/-}$ 2x*act1^{+}::ura4^{+}*/+ (3x*act1^{+}*) *lys1^{+}::GFP-wee1/lys1^{+}::GFP-wee1 wee1Δ::ura4-3233/wee1Δ::ura4-3233 ura4-D18/ura4-D18 ade6-M210/ade6-M216*

Figure 10	4816	h$^{+/-}$ 2x*act1^{+}::ura4^{+}*/+ (3x*act1^{+}*) *pom1Δ::ura4^{+}*/+ *lys1^{+}::GFP-wee1/lys1^{+}::GFP-wee1 wee1Δ::ura4-3233/wee1Δ::ura4-3233 ura4-D18/ura4-D18 ade6-M210/ade6-M216*
	4865	h$^{+/-}$ 2x*act1^{+}::ura4^{+}*/+ (3x*act1^{+}*) *nim1Δ::LEU2*/+ *lys1^{+}::GFP-wee1/lys1^{+}::GFP-wee1 wee1Δ::ura4-3233/wee1Δ::ura4-3233 leu1-32/leu1-32 ura4-D18/ura4-D18 ade6-M210/ade6-M216*
	5444	h$^{+/-}$ 2x*act1^{+}::ura4^{+}*/+ (3x*act1^{+}*) 2x*pom1+::ura4^{+}*/2x*pom1^{+}::ura4^{+}* (4x*pom1^{+}*) *lys1^{+}::GFP-wee1/lys1^{+}::GFP-wee1 wee1Δ::ura4-3233/wee1Δ::ura4-3233 ura4-D18/ura4-D18 ade6-M210/ade6-M216*
	5491	h$^{+/-}$ 2x*act1^{+}::ura4^{+}*/+ (3x*act1^{+}*) 2x*nim1^{+}::ura4^{+}*/2x*nim1^{+}::ura4^{+}* (4x*nim1^{+}*) *lys1^{+}::GFP-wee1/lys1^{+}::GFP-wee1 wee1Δ::ura4-3233/wee1Δ::ura4-3233 ura4-D18/ura4-D18 ade6-M210/ade6-M216*
	5567	h$^{+/-}$ 2x*act1^{+}::ura4^{+}*/+ (3x*act1^{+}*) *nif1Δ::ura4^{+}/nif1Δ::ura4^{+} lys1^{+}::GFP-wee1/lys1^{+}::GFP-wee1 wee1Δ::ura4-3233/wee1Δ::ura4-3233 ura4-D18/ura4-D18 ade6-M210/ade6-M216*
	5563	h$^{+/-}$ 2x*act1^{+}::ura4^{+}*/+ (3x*act1^{+}*) *nif1Δ::ura4^{+}*/+ *lys1^{+}::GFP-wee1/lys1^{+}::GFP-wee1 wee1Δ::ura4-3233/wee1Δ::ura4-3233 ura4-D18/ura4-D18 ade6-M210/ade6-M216*
Figure 11	2829	h$^{+/-}$ *ade6-M210/ade6-M216*
	5646	h$^{-/-}$ *cdc25Δ::ura4^{+}*/+ *leu1-32*/+ *ura4-D18/ura4-D18 ade6-M210/ade6-M216*
	6136	h$^{+/-}$ *nim1Δ::LEU2*/+ *leu1-32/leu1-32 ade6-M210/ade6-M216*
	6146	h$^{+/-}$ *cdc25Δ::ura4^{+}*/+ *nim1Δ::LEU2*/+ *leu1-32/leu1-32 ura4-D18*/+ (or -/-) *ade6-M210/ade6-M216*
	6057	h$^{-/-}$ *pom1Δ::ura4^{+}*/+ *leu1-32*/+ *ura4-D18/ura4-D18 ade6-M210/ade6-M216*
	6145	h$^{+/-}$ *cdc25Δ::ura4^{+}*/+ *pom1Δ::ura4^{+}*/+ *leu1-32*/+ (or +/+) *ura4-D18/ura4-D18 ade6-M210/ade6-M216*

Figure 11	3614	h$^{-/-}$ *cdc25Δ::ura4*$^{+}$*::cdc25-GFP::leu1*$^{+}$*/ cdc25Δ::ura4*$^{+}$*::cdc25-GFP::leu1*$^{+}$ *leu1-32/leu1-32 ura4-D18/ura4-D18 ade6-M210/ade6-M216*
	3884	h$^{-/-}$ *cdc25Δ::ura4*$^{+}$*/cdc25Δ::ura4-2012::cdc25-GFP::leu1*$^{+}$ *leu1-32/leu1-32 ura4-D18/ura4-D18 ade6-M210/ade6-M216*
	3733	h$^{-/-}$ *cdc13Δ::ura4*$^{+}$*/+ cdc25Δ::ura4-2012::cdc25-GFP::leu1*$^{+}$*/ cdc25Δ::ura4-2012::cdc25-GFP::leu1*$^{+}$ *leu1-32/leu1-32 ura4-D18/ura4-D18 ade6-M210/ade6-M216*
	3390	h$^{+/-}$ *pom1Δ::ura4*$^{+}$*/+ cdc25Δ::ura4-2012::cdc25-GFP::leu1*$^{+}$*/ cdc25Δ::ura4-2012::cdc25-GFP::leu1*$^{+}$ *leu1-32/leu1-32 ura4-D18/ura4-D18 ade6-M210/ade6-M216*
	4270	h$^{-/-}$ *pom1Δ::ura4*$^{+}$*/+ cdc25Δ::ura4*$^{+}$*/cdc25Δ::ura4-2012::cdc25-GFP::leu1*$^{+}$ *leu1-32/leu1-32 ura4-D18/ura4-D18 ade6-M210/ade6-M216*
	4272	h$^{-/-}$ *pom1Δ::ura4*$^{+}$*/+ cdc13Δ::ura4*$^{+}$*/+ cdc25Δ::ura4-2012::cdc25-GFP::leu1*$^{+}$*/ cdc25Δ::ura4-2012::cdc25-GFP::leu1*$^{+}$ *leu1-32/leu1-32 ura4-D18/ura4-D18 ade6-M210/ade6-M216*
Figure 12	2802	h^{-} wild
	1345	h^{-} *cps8-188* (*act1-ts*)
	3823	h^{-} *cdc25-22*
	1664	h^{-} *act1-ts cdc25-22*
	3967	h^{-} *wee1-50*
	3991	h^{-} *act1-ts wee1-50*
	3760	h^{-} *cdc25-22 wee1-50*
	1689	h^{-} *cdc25-22 wee1-50 act1-ts ade6-M216*
	2829	h$^{+/-}$ *ade6-M210/ade6-M216*
	3660	h$^{+/-}$ *act1-ts*/*act1-ts ade6-M210/ade6-M216*
	3691	h$^{+/-}$ *cdc25-22*/*cdc25-22 ade6-M210/ade6-M216*
	3677	h$^{+/-}$ *act1-ts*/*act1-ts cdc25-22*/*cdc25-22 ade6-M210/ade6-M216*

Figure 12	4031	h$^{+/-}$ *wee1-50/wee1-50 leu1-32/+ ade6-M210/ade6-M216*
	4068	h$^{+/-}$ *act1-ts/act1-ts wee1-50/wee1-50 leu1-32/+ ade6-M210/ade6-M216*
	3797	h$^{+/-}$ *cdc25-22/cdc25-22 wee1-50/wee1-50 ade6-M210/ade6-M216*
	1701	h$^{+/-}$ *act1-ts/act1-ts cdc25-22/cdc25-22 wee1-50/wee1-50 ade6-M210/ade6-M216*
	3872	h$^{+/-}$ *act1-ts/act1-ts cdc25-22/cdc25-22 wee1-50/wee1-50 pom1Δ::ura4^{+}/+ leu1-32/+ ura4-D18/ura4-D18 ade6-M210/ade6-M216*
	5681	h$^{+/-}$ *act1-ts/act1-ts cdc25-22/cdc25-22 wee1-50/wee1-50 pom1Δ::ura4^{+}/+ nim1Δ::LEU2/nim1Δ::LEU2 leu1-32/leu1-32 ura4-D18/ura4-D18 ade6-M210/ade6-M216*
	4684	h$^{+/-}$ *wee1Δ::ura4^{+}/+ leu1-32/+ ura4-D18/ura4-D18 ade6-M210/ade6-M216*
	5669	h$^{-/-}$ *act1Δ::ura4^{+}/+ wee1Δ::ura4^{+}/+ leu1-32/+ ura4-D18/ura4-D18 ade6-M210/ade6-M216*
	6054	h$^{-/-}$ *wee1Δ::ura4^{+}/+ nim1Δ::LEU2/+ leu1-32/leu1-32 ura4-D18/ura4-D18 ade6-M210/ade6-M216*
	6096	h$^{+/-}$ *act1Δ::ura4^{+}/+ wee1Δ::ura4^{+}/+ nim1Δ::LEU2/+ leu1-32/leu1-32 ura4-D18/ura4-D18 ade6-M210/ade6-M216*
Figure 13	1407	h$^{+/-}$ *lys1^{+}::GFP-wee1/lys1^{+}::GFP-wee1 wee1Δ::ura4^{+}/wee1Δ::ura4^{+} leu1-32/leu1-32 ura4-D18/ura4-D18 ade6-M210/ade6-M216*
	1621	h$^{+/-}$ *act1-ts/act1-ts lys1^{+}::GFP-wee1/lys1^{+}::GFP-wee1 wee1Δ::ura4^{+}/wee1Δ::ura4^{+} leu1-32/leu1-32 ura4-D18/ura4-D18 ade6-M210/ade6-M216*
	4734	h$^{+/-}$ *adf1-1/adf1-1 lys1^{+}::GFP-wee1/lys1^{+}::GFP-wee1 wee1Δ::ura4^{+}/wee1Δ::ura4^{+} ura4-D18/ura4-D18 ade6-M210/ade6-M216*
	4854	h$^{+/-}$ *act1-ts/act1-ts adf1-1/adf1-1 lys1^{+}::GFP-wee1/lys1^{+}::GFP-wee1 wee1Δ::ura4^{+}/wee1Δ::ura4^{+} ura4-D18/ura4-D18 ade6-M210/ade6-M216*

Figure 13	2548	h$^{+/-}$ *lys1^{+}::GFP-NESx2-wee1/lys1^{+}::GFP-NESx2-wee1 wee1Δ::ura4^{+}/wee1Δ::ura4^{+} leu1-32/leu1-32 ura4-D18/ura4-D18 ade6-M210/ade6-M216*
	6129	h$^{+/-}$ *act1-ts/act1-ts lys1^{+}::GFP-NESx2-wee1/lys1^{+}::GFP-NESx2-wee1 wee1Δ::ura4^{+}/wee1Δ::ura4^{+} leu1-32/leu1-32 ura4-D18/ura4-D18 ade6-M210/ade6-M216*
	4775	h$^{+/-}$ *adf1-1/adf1-1 lys1^{+}::GFP-NESx2-wee1/lys1^{+}::GFP-NESx2-wee1 wee1Δ::ura4^{+}/wee1Δ::ura4^{+} ura4-D18/ura4-D18 ade6-M210/ade6-M216*
	4944	h$^{+/-}$ *act1-ts/act1-ts adf1-1/adf1-1 lys1^{+}::GFP-NESx2-wee1/lys1^{+}::GFP-NESx2-wee1 wee1Δ::ura4^{+}/wee1Δ::ura4^{+} ura4-D18/ura4-D18 ade6-M210/ade6-M216*
Figure 14	2802	h^{-} wild
	4149	h^{-} 2x*cdc13^{+}::ura4+ ura4-D18*
	4133	h^{-} 2x*cdc25^{+}::ura4^{+} ura4-D18*
	4507	h^{-} 2x*pom1^{+}::ura4^{+} ura4-D18*
	4123	h^{-} 2x*act1^{+}::ura4^{+} ura4-D18*
	3432	h^{-} *lys1^{+}::GFP-wee1*
	3174	h^{+} *lys1^{+}::GFP-wee1 wee1Δ::ura4^{+} ura4-D18*
	4222	h$^{+/-}$ *lys1^{+}::GFP-wee1/lys1-131 wee1Δ::ura4-3233/+ leu1-32/+ ura4-D18/+ ade6-M210/ade6-M216*
	4348	h^{-} 2x*pom1^{+}::ura4^{+} lys1^{+}::GFP-wee1 ura4-D18*
	3471	h^{-} 2x*act1^{+}::ura4^{+} lys1^{+}::GFP-wee1 ura4-D18*
	4405	h^{-} 2x*act1^{+}::ura4^{+} 2x*pom1^{+}::ura4+ lys1^{+}::GFP-wee1 ura4-D18*
	3441	h^{-} *lys1^{+}::GFP-NESx2-wee1*
	4354	h^{-} 2x*pom1^{+}::ura4^{+} lys1^{+}::GFP-NESx2-wee1 ura4-D18*
	3477	h^{-} 2x*act1^{+}::ura4^{+} lys1^{+}::GFP-NESx2-wee1 ura4-D18*
	4410	h^{-} 2x*act1^{+}::ura4^{+} 2x*pom1^{+}::ura4^{+} lys1+::GFP-NESx2-wee1 ura4-D18*
	4742	h^{-} 2x*act1^{+}::ura4^{+} 2x*pom1^{+}::ura4^{+} 2x*cdc13^{+}::ura4^{+} 2x*cdc25^{+}::ura4^{+} lys1^{+}::GFP-wee1 ura4-D18*

Figure 14	4247	h^{-} 2x*act1^{+}::ura4^{+}* 2x*cdc13^{+}::ura4^{+}* 2x*cdc25^{+}::ura4^{+}* *lys1^{+}::GFP-wee1 ura4-D18*
	4750	h^{-} 2x*pom1^{+}::ura4^{+}* 2x*cdc13^{+}::ura4^{+}* 2x*cdc25^{+}::ura4^{+}* *lys1^{+}::GFP-wee1 ura4-D18*
	4467	h^{-} 2x*act1^{+}::ura4^{+}* 2x*pom1^{+}::ura4^{+}* 2x*cdc13^{+}::ura4^{+}* *lys1^{+}::GFP-wee1 ura4-D18*
	4461	h^{-} 2x*act1^{+}::ura4^{+}* 2x*pom1^{+}::ura4^{+}* 2x*cdc25^{+}::ura4^{+}* *lys1^{+}::GFP-wee1 ura4-D18*
	4223	h$^{+/-}$ *lys1^{+}::GFP-NESx2-wee1/lys1-131 wee1Δ::ura4-3233/+ leu1-32/+ ura4-D18/+ ade6-M210/ade6-M216*
	4745	h^{+} 2x*act1^{+}::ura4^{+}* 2x*pom1^{+}::ura4^{+}* 2x*cdc13^{+}::ura4^{+}* 2x*cdc25^{+}::ura4^{+}* *lys1^{+}::GFP-NESx2-wee1 ura4-D18*
	4249	h^{-} 2x*act1^{+}::ura4^{+}* 2x*cdc13^{+}::ura4^{+}* 2x*cdc25^{+}::ura4^{+}* *lys1^{+}::GFP-NESx2-wee1 ura4-D18*
	4754	h^{-} 2x*pom1^{+}::ura4^{+}* 2x*cdc13^{+}::ura4^{+}* 2x*cdc25^{+}::ura4^{+}* *lys1^{+}::GFP-NESx2-wee1 ura4-D18*
	4468	h^{+} 2x*act1^{+}::ura4^{+}* 2x*pom1^{+}::ura4^{+}* 2x*cdc13^{+}::ura4^{+}* *lys1^{+}::GFP-NESx2-wee1 ura4-D18*
	4463	h^{-} 2x*act1^{+}::ura4^{+}* 2x*pom1^{+}::ura4^{+}* 2x*cdc25^{+}::ura4^{+}* *lys1^{+}::GFP-NESx2-wee1 ura4-D18*
Figure 15	4247	h^{-} 2x*act1^{+}::ura4^{+}* 2x*cdc13^{+}::ura4^{+}* 2x*cdc25^{+}::ura4^{+}* *lys1^{+}::GFP-wee1 ura4-D18*
	5215	h^{+} 2x*nim1^{+}::ura4^{+}* 2x*act1^{+}::ura4^{+}* 2x*cdc13^{+}::ura4^{+}* 2x*cdc25^{+}::ura4^{+}* *lys1^{+}::GFP-wee1 ura4-D18*
	5168	h^{-} 2x*nim1^{+}::ura4^{+}* 2x*pom1^{+}::ura4^{+}* 2x*act1^{+}::ura4^{+}* 2x*cdc13^{+}::ura4^{+}* 2x*cdc25^{+}::ura4^{+}* *lys1^{+}::GFP-wee1 ura4-D18*
	4249	h^{-} 2x*act1^{+}::ura4^{+}* 2x*cdc13^{+}::ura4^{+}* 2x*cdc25^{+}::ura4^{+}* *lys1^{+}::GFP-NESx2-wee1 ura4-D18*
	5184	h^{-} 2x*nim1^{+}::ura4^{+}* 2x*act1^{+}::ura4^{+}* 2x*cdc13^{+}::ura4^{+}* 2x*cdc25^{+}::ura4^{+}* *lys1^{+}::GFP-NESx2-wee1 ura4-D18*
	4217	h^{-} 2x*cdc13^{+}::ura4^{+}* 2x*cdc25^{+}::ura4^{+}* *lys1^{+}::GFP-wee1 ura4-D18*
	5126	h^{-} 2x*nim1^{+}::ura4^{+}* 2x*cdc13^{+}::ura4^{+}* 2x*cdc25^{+}::ura4^{+}* *lys1^{+}::GFP-wee1 ura4-D18*

Figure 15	4213	h^{-} 2x*act1^{+}::ura4^{+}* 2x*cdc13^{+}::ura4^{+} lys1^{+}::GFP-wee1 ura4-D18*
	5115	h^{-} 2x*nim1^{+}::ura4^{+}* 2x*act1^{+}::ura4^{+}* 2x*cdc13^{+}::ura4^{+} lys1^{+}::GFP-wee1 ura4-D18*
	4208	h^{-} 2x*act1^{+}::ura4^{+}* 2x*cdc25^{+}::ura4^{+} lys1^{+}::GFP-wee1 ura4-D18*
	5112	h^{-} 2x*nim1^{+}::ura4^{+}* 2x*act1^{+}::ura4^{+}* 2x*cdc25^{+}::ura4^{+} lys1^{+}::GFP-wee1 ura4-D18*
Figure S1	1579	h^{+} *cdc25Δ::ura4^{+}::cdc25-GFP::leu1^{+} leu1-32 ura4-D18*
	1286	h^{-} *cdc25-22 leu1-32 ura4-D18 ade6-M216*
	1845	h^{+} *cdc13-l17 cdc25Δ::ura4^{+}::cdc25-GFP::leu1^{+} leu1-32 ura4-D18 ade6-M210*
	1289	h^{-} *wee1-50 leu1-32 ura4-D18*
	2266	h^{-} 2x*act1^{+}::ura4^{+} leu1-32 ura4-D18 ade6-M210*
	3351	h$^{-/-}$ *cdc25Δ::ura4^{+}::cdc25-GFP::leu1^{+}/ cdc25Δ::ura4^{+}::cdc25-GFP::leu1^{+} leu1-32/leu1-32 ura4-D18/ura4-D18*
	2148	h$^{+/-}$ *act1Δ::ura4^{+}/+ cdc25Δ::ura4-2012::cdc25-GFP::leu1^{+}/ cdc25Δ::ura4-2012::cdc25-GFP::leu1^{+} leu1-32/leu1-32 ura4-D18/ura4-D18 ade6-M210/ade6-M216*
Figure S2	3174	h^{+} *lys1^{+}::GFP-wee1 wee1Δ::ura4^{+} ura4-D18*
	3180	h$^{+/-}$ *lys1^{+}::GFP-wee1/lys1^{+}::GFP-wee1 wee1Δ::ura4^{+}/wee1Δ::ura4^{+} leu1-32/+ ura4-D18/ura4-D18 ade6-M210/ade6-M216*
Figure S3	1461	h^{-} *cdc25Δ::ura4^{+}::cdc25-GFP::leu1^{+} leu1-32 ura4-D18*
	3614	h$^{-/-}$ *cdc25Δ::ura4^{+}::cdc25-GFP::leu1^{+}/ cdc25Δ::ura4^{+}::cdc25-GFP::leu1^{+} leu1-32/leu1-32 ura4-D18/ura4-D18 ade6-M210/ade6-M216*

Figure 1

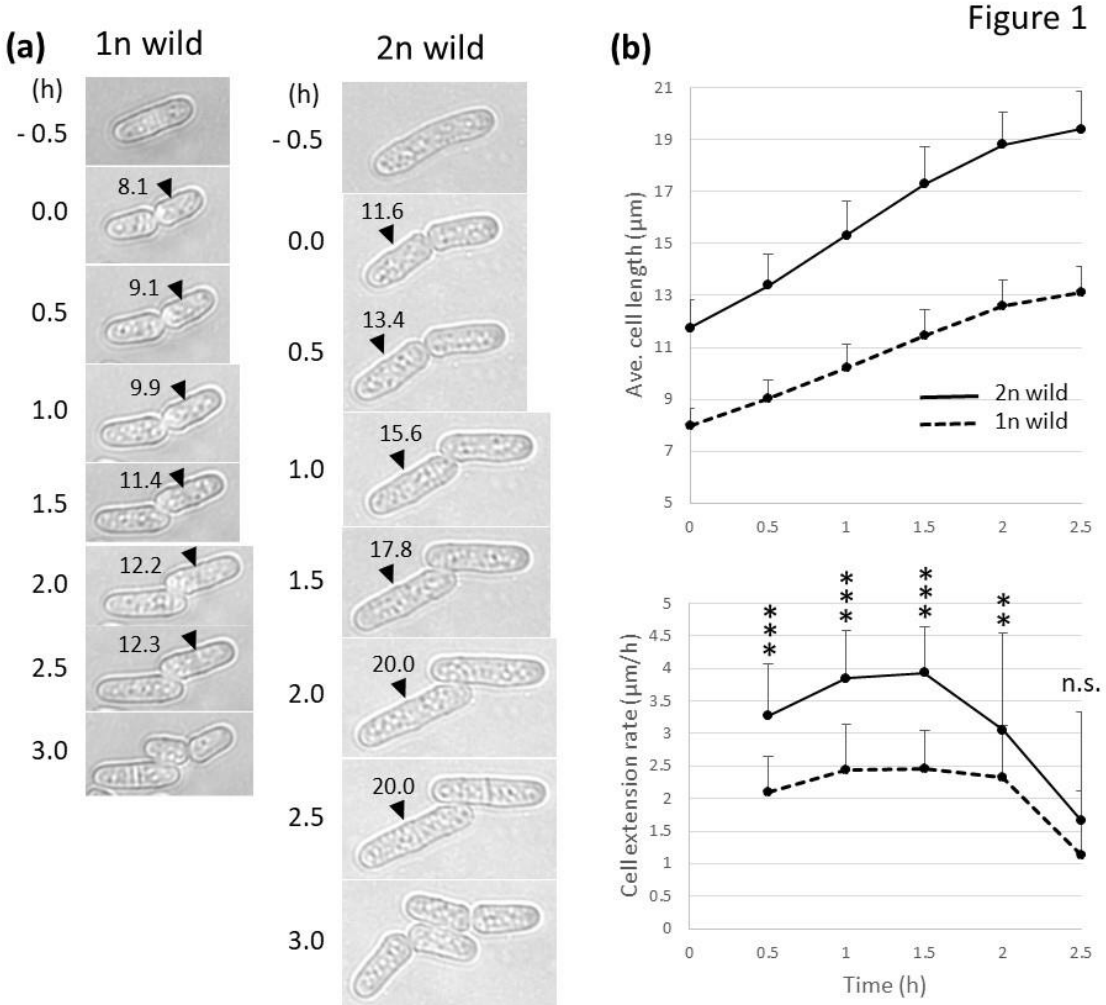
(a)
1n wild
2n wild
(h)
- 0.5
0.0
0.5
1.0
1.5
2.0
2.5
3.0
8.1
9.1
9.9
11.4
12.2
12.3
11.6
13.4
15.6
17.8
20.0
20.0
(b)
Ave. cell length (μm)
2n wild
1n wild
Cell extension rate (μm/h)
***
***
***
**
n.s.
Time (h)

Figure 2

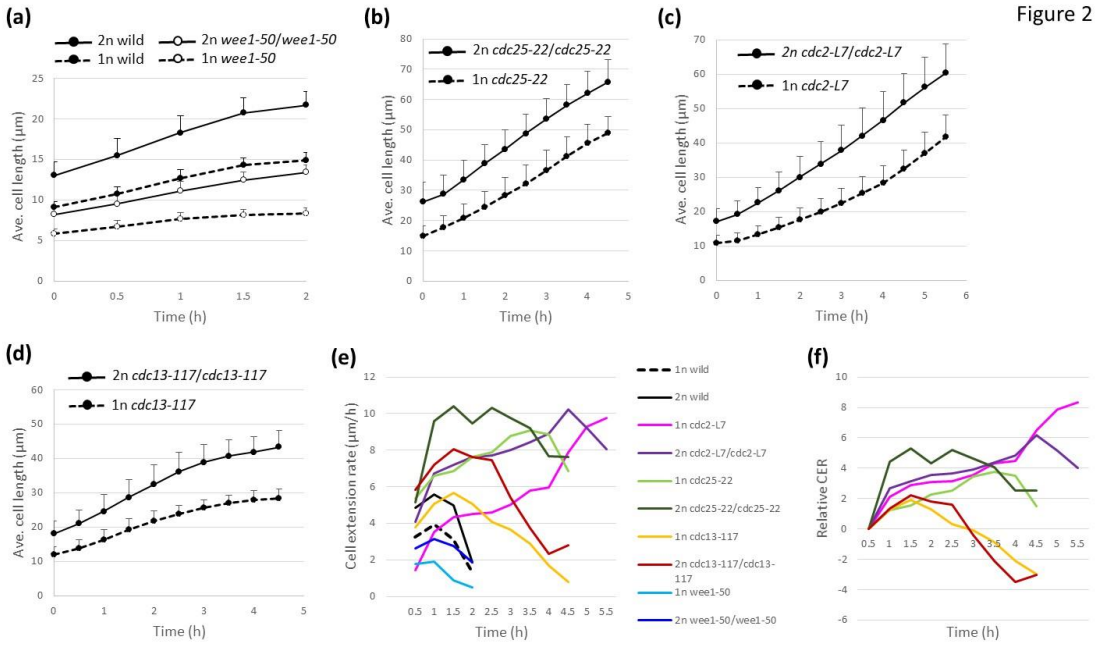
(a)
2n wild
2n wee1-50/wee1-50
1n wild
1n wee1-50
Ave. cell length (μm)
Time (h)
(b)
2n cdc25-22/cdc25-22
1n cdc25-22
Ave. cell length (μm)
Time (h)
(c)
2n cdc2-L7/cdc2-L7
1n cdc2-L7
Ave. cell length (μm)
Time (h)
(d)
2n cdc13-117/cdc13-117
1n cdc13-117
Ave. cell length (μm)
Time (h)
(e)
Cell extension rate (μm/h)
Time (h)
1n wild
2n wild
1n cdc2-L7
2n cdc2-L7/cdc2-L7
1n cdc25-22
2n cdc25-22/cdc25-22
1n cdc13-117
2n cdc13-117/cdc13-117
1n wee1-50
2n wee1-50/wee1-50
(f)
Relative CER
Time (h)

Figure 3

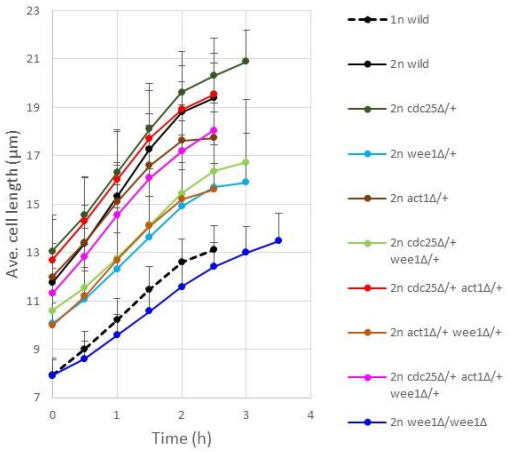

Genotype	CER (max)	P value			
2n wild	3.94±0.71	—			
2n *cdc25Δ/+*	3.57±0.95	*	—		
2n *wee1Δ/+*	2.66±0.66	***		—	(n.s.)
2n *act1Δ/+*	3.33±0.84	***			—
2n *cdc25Δ/+ wee1Δ/+*	2.75±0.87	*** (—)	***	n.s.	
2n *cdc25Δ/+ act1Δ/+*	3.47±1.0	*	n.s. (—)		n.s.
2n *act1Δ/+ wee1Δ/+*	2.98±0.81	***		* (—)	*
2n *cdc25Δ/+ act1Δ/+ wee1Δ/+*	3.43±0.81	** (***)	(n.s.)	(*)	
2n *wee1Δ/wee1Δ*	2.08±0.58	***			(*)
1n wild	2.47±0.59	***			(—)

Figure 4

(a)

Ploidy	Genotype
1n	wild
1n	*cdc2-3w*
1n	*cdc2-L7*
1n	*cdc25-22*
1n	*cdc13-117*
1n	2x*act1+*
1n	2x*act1+ cdc13-117*
1n	*act1-ts*
1n	*act1-ts cdc13-117*
1n	*adf1-1*
1n	*cdc2-3w adf1-1*
2n	wild
2n	*cdc2-3w/cdc2-3w*
2n	*cdc2-L7/cdc2-L7*
2n	*cdc25-22/cdc25-22*
2n	*cdc13-117/cdc13-117*
2n	*cdc25Δ/+*
2n	*cdc13Δ/+*
2n	*act1Δ/+*
2n	3x*act1+*
2n	3x*act1+ cdc13-117/cdc13-117*
2n	3x*act1+ cdc25Δ/+*
2n	3x*act1+ cdc13Δ/+*
2n	*act1-ts/act1-ts*
2n	*act1-ts/act1-ts cdc13-117/cdc13-117*
2n	*adf1-1/adf1-1*
2n	*act1-ts/act1-ts adf1-1/adf1-1*
2n	*cdc2-3w/cdc2-3w adf1-1/adf1-1*

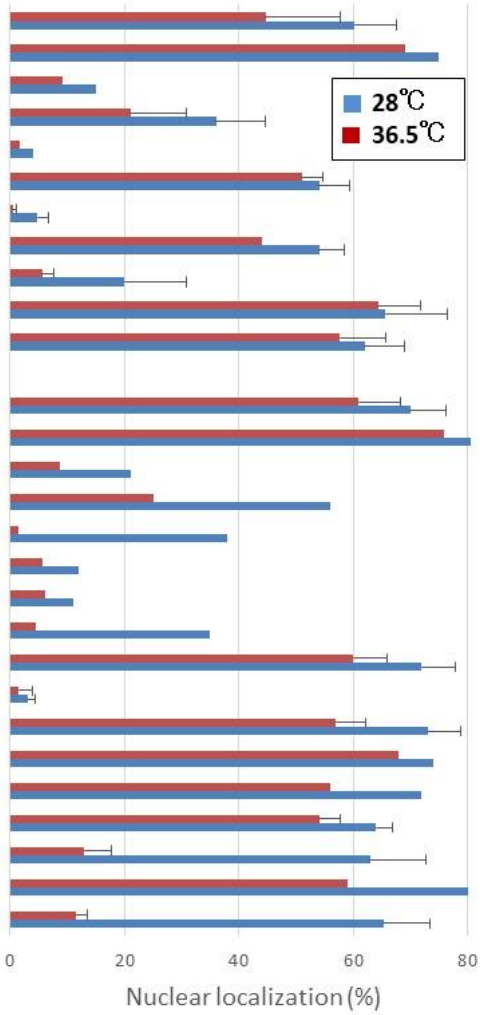

Figure 4

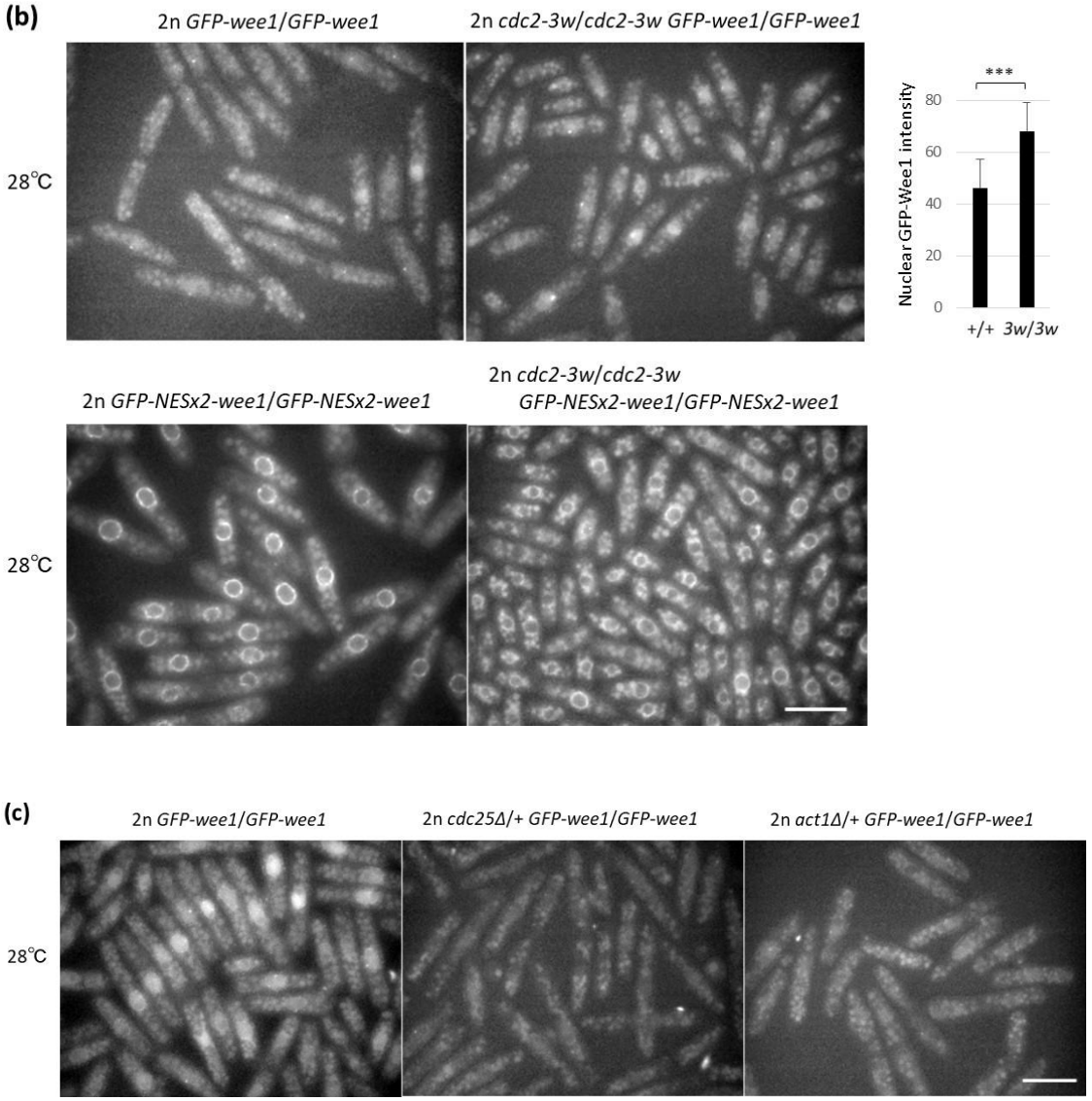
(b)
2n GFP-wee1/GFP-wee1
2n cdc2-3w/cdc2-3w GFP-wee1/GFP-wee1
28℃
***
Nuclear GFP-Wee1 intensity
80
60
40
20
0
+/+
3w/3w
2n GFP-NESx2-wee1/GFP-NESx2-wee1
2n cdc2-3w/cdc2-3w
GFP-NESx2-wee1/GFP-NESx2-wee1
28℃
(c)
2n GFP-wee1/GFP-wee1
2n cdc25Δ/+ GFP-wee1/GFP-wee1
2n act1Δ/+ GFP-wee1/GFP-wee1
28℃

Figure 4

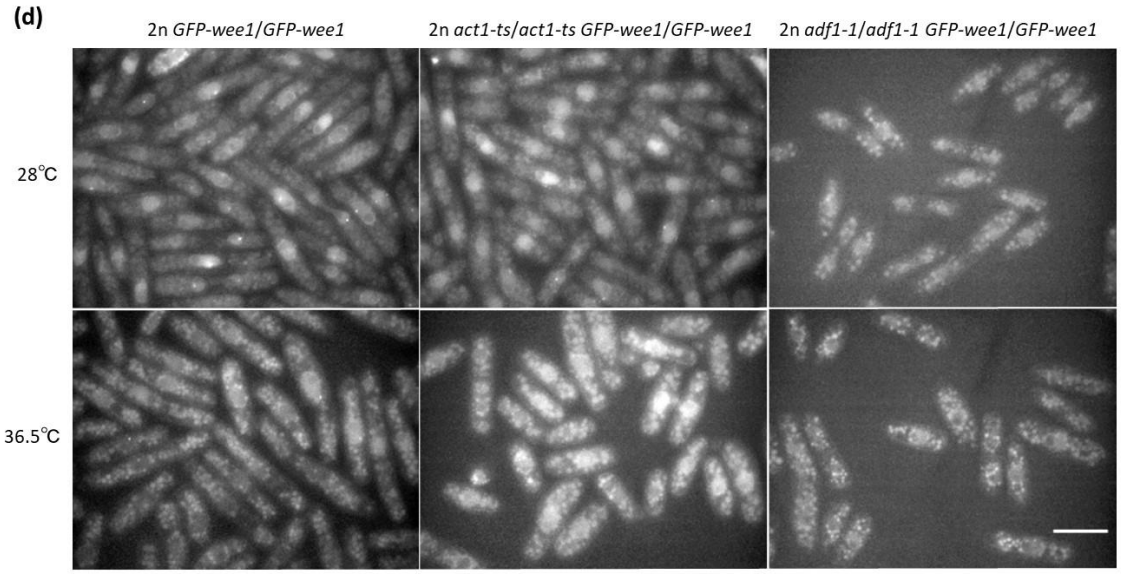
(d)
2n GFP-wee1/GFP-wee1
2n act1-ts/act1-ts GFP-wee1/GFP-wee1
2n adf1-1/adf1-1 GFP-wee1/GFP-wee1
28℃
36.5℃

Figure 5

(a)

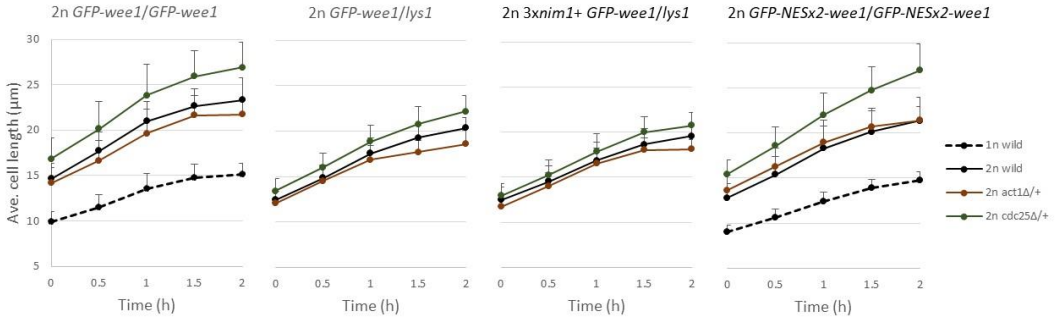

Genotype	CER (max)	P value	CER (max)	P value	CER (max)	P value	CER (max)	P value
2n wild	6.53±1.60	—	5.40±1.25	—	4.59±1.30	—	5.80±1.44	—
2n *act1Δ/+*	5.91±1.88	*	4.94±1.62	n.s.	4.99±1.07	n.s.	5.37±1.85	n.s.
2n *cdc25Δ/+*	7.33±2.27	*	5.67±1.24	n.s.	5.20±1.14	*	6.83±1.59	**
1n wild	4.02±1.01	***					3.66±0.78	***

(b)

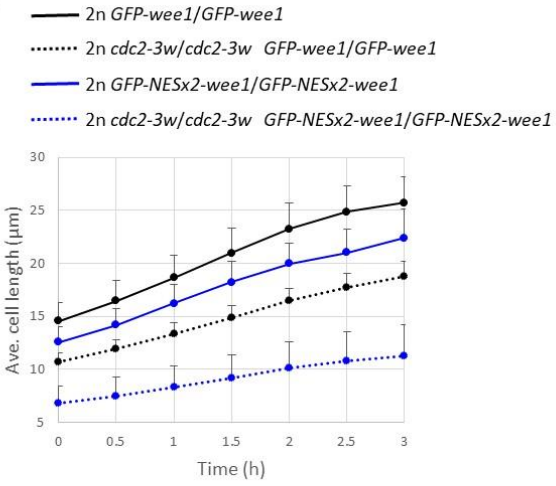

Genotype	CER (max)	P value
2n *GFP-wee1/GFP-wee1*	5.49±0.72	—
2n *cdc2-3w/cdc2-3w GFP-wee1/GFP-wee1*	3.93±0.57	***
2n *GFP-NESx2-wee1/GFP-NESx2-wee1*	4.84±0.90	(—)
2n *cdc2-3w/cdc2-3w GFP-NESx2-wee1/GFP-NESx2-wee1*	2.46±0.71	(***)

Figure 6

(a)

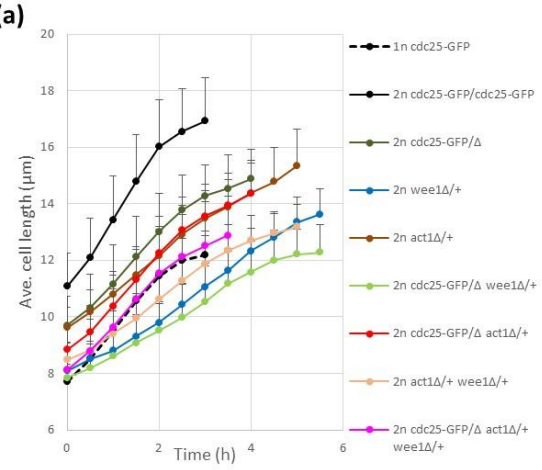

Genotype	CER (max)	P value			
2n *cdc25-GFP/ cdc25-GFP*	2.71±0.76	—			
2n *cdc25-GFP/Δ*	1.91±0.56	***	—		
2n *wee1Δ/+*	1.38±0.83	***		—	
2n *act1Δ/+*	1.51±0.53	***			—
2n *cdc25-GFP/Δ wee1Δ/+*	1.37±0.86	(—)	**	n.s.	(***)
2n *cdc25-GFP/Δ act1Δ/+*	1.91±0.50		n.s. (—)		*** (n.s.)
2n *act1Δ/+ wee1Δ/+*	1.39±0.61			n.s. (—)	n.s. (***)
2n *cdc25-GFP/Δ act1Δ/+ wee1Δ/+*	1.98±0.67	(***)	(n.s.)	(***)	(n.s.)
1n *cdc25-GFP*	2.02±0.67	***			(—)

(b)

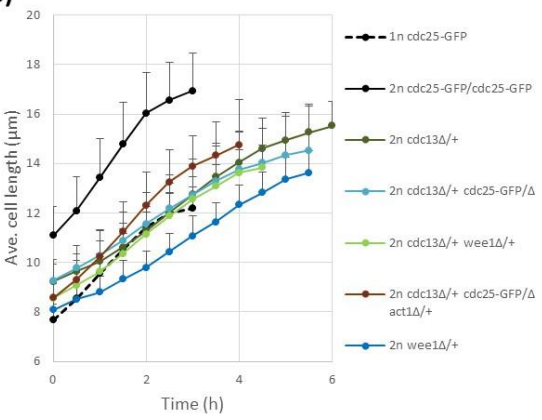

Genotype	CER (max)	P value			
2n *cdc25-GFP/ cdc25-GFP*	2.71±0.76	—			
2n *cdc13Δ/+*	1.51±0.70	***	—		
2n *wee1Δ/+*	1.38±0.83	***		—	
2n *act1Δ/+*	1.51±0.53	***			—
2n *cdc13Δ/+ cdc25-GFP/Δ*	1.33±0.62	(—)	n.s.		
2n *cdc13Δ/+ wee1Δ/+*	1.60±0.59		n.s.	n.s.	
2n *cdc25-GFP/Δ act1Δ/+*	1.91±0.50		(—)		
2n *cdc13Δ/+ cdc25-GFP/Δ act1Δ/+*	2.15±0.70	(***)	(*)		***

Figure 6

(c)

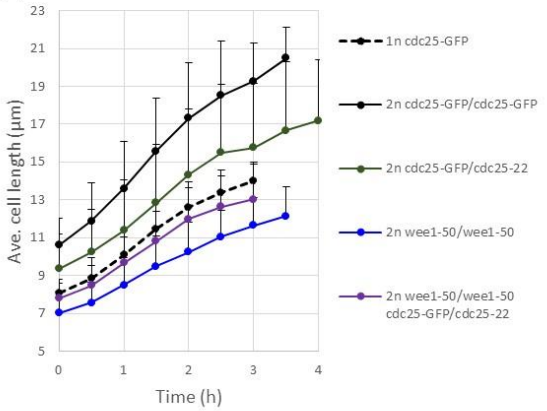

Genotype	CER (max)	P value	
2n *cdc25-GFP/ cdc25-GFP*	3.95±1.16	—	
2n *cdc25-GFP/-*	3.04±1.07	***	
2n *wee1-50/-*	1.93±1.04		—
2n *wee1-50/- cdc25-GFP/-*	2.38±1.03		*
1n *cdc25-GFP*	2.67±0.71	***	

(d)

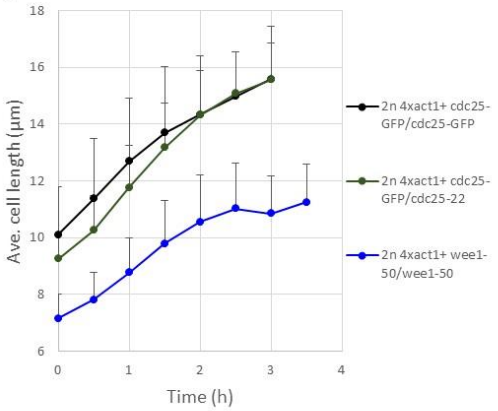

Genotype	CER (max)	P value
2n 4xact1+ *cdc25-GFP/ cdc25-GFP*	2.66±1.31	—
2n 4xact1+ *cdc25-GFP/-*	3.02±1.02	n.s.
2n 4xact1+ *wee1-50/-*	2.03±1.15	*

(a)

Ploidy	*cdc25-GFP*	*act1*	*adf1*	*wee1*	*cdc13*
1n	+	+	+	+	+
1n	+	-	+	+	+
1n	+	+	-	+	+
1n	+	+	+	-	+
1n	+	-	+	-	+
1n	+	+	-	-	+
1n	+	+	+	+	-
1n	+	-	+	+	-
1n	+	+	-	+	-
1n	*NLS*	+	+	+	+
1n	*NLS*	+	+	-	+
1n	*NLS*	-	+	+	+
1n	*NLS*	+	-	+	+

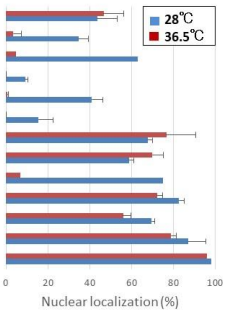

Ploidy	*cdc25-GFP*	*act1*	*adf1*	*wee1*	*cdc13*
2n	+/+	+/+	+/+	+/+	+/+
2n	+/+	-/-	+/+	+/+	+/+
2n	+/+	+/+	-/-	+/+	+/+
2n	+/+	+/+	+/+	-/-	+/+
2n	+/+	-/-	+/+	-/-	+/+
2n	+/+	+/+	+/-	-/-	+/+
2n	+/+	+/+	-/-	+/-	+/+
2n	+/+	+/+	-/-	-/-	+/+
2n	+/+	+/+	+/+	+/+	-/-
2n	+/+	-/-	+/+	+/+	-/-
2n	+/+	+/+	-/-	+/+	-/-
2n	+/+	+/+	+/+	+/Δ	+/+
2n	+/+	+/Δ	+/+	+/+	+/+
2n	+/+	+/Δ	+/+	+/Δ	+/+
2n	*NLS/NLS*	+/+	+/+	+/+	+/+
2n	*NLS/NLS*	+/+	+/+	-/-	+/+
2n	*NLS/NLS*	-/-	+/+	+/+	+/+
2n	*NLS/NLS*	+/+	-/-	+/+	+/+
2n	*NLS/NLS*	+/+	+/+	+/Δ	+/+

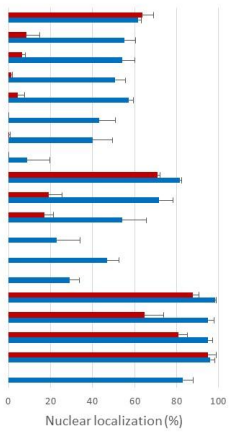

(b)

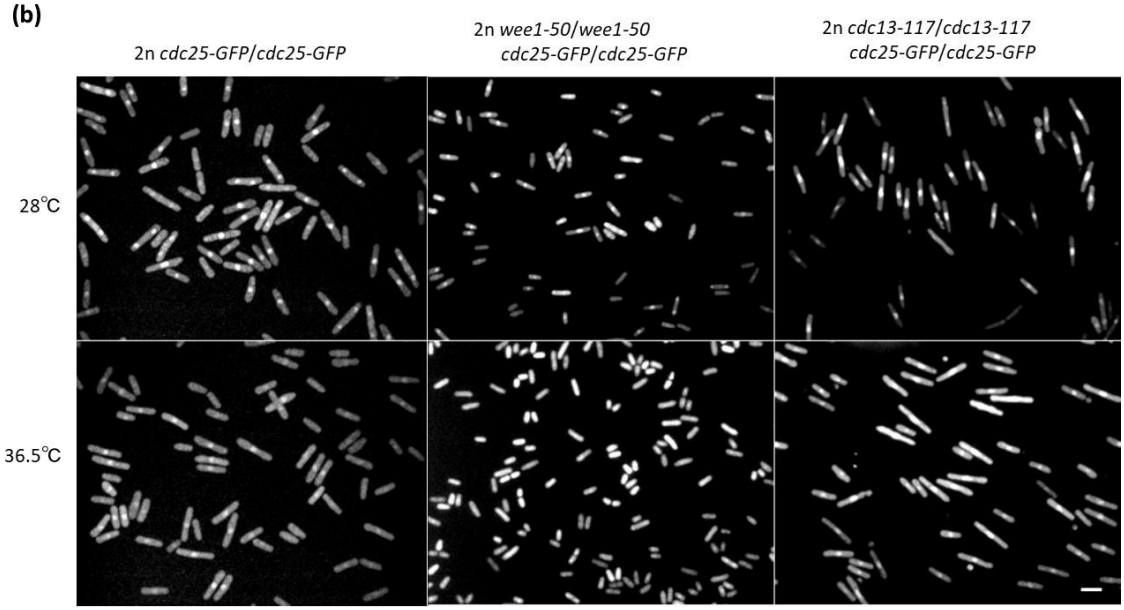

Figure 7

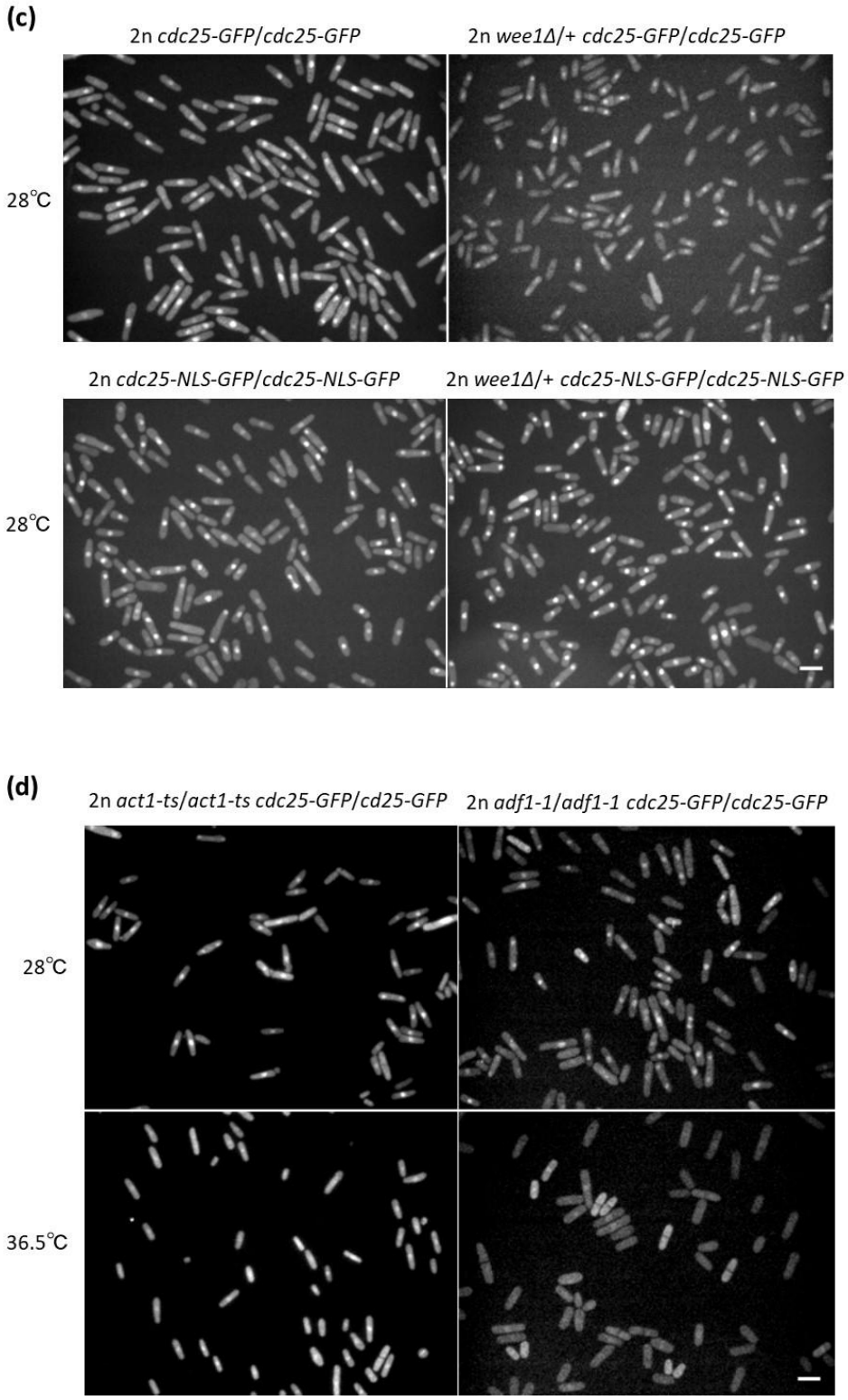
(c)
2n cdc25-GFP/cdc25-GFP
2n wee1Δ/+ cdc25-GFP/cdc25-GFP
28°C
2n cdc25-NLS-GFP/cdc25-NLS-GFP
2n wee1Δ/+ cdc25-NLS-GFP/cdc25-NLS-GFP
28°C
(d)
2n act1-ts/act1-ts cdc25-GFP/cd25-GFP
2n adf1-1/adf1-1 cdc25-GFP/cdc25-GFP
28°C
36.5°C

Figure 8

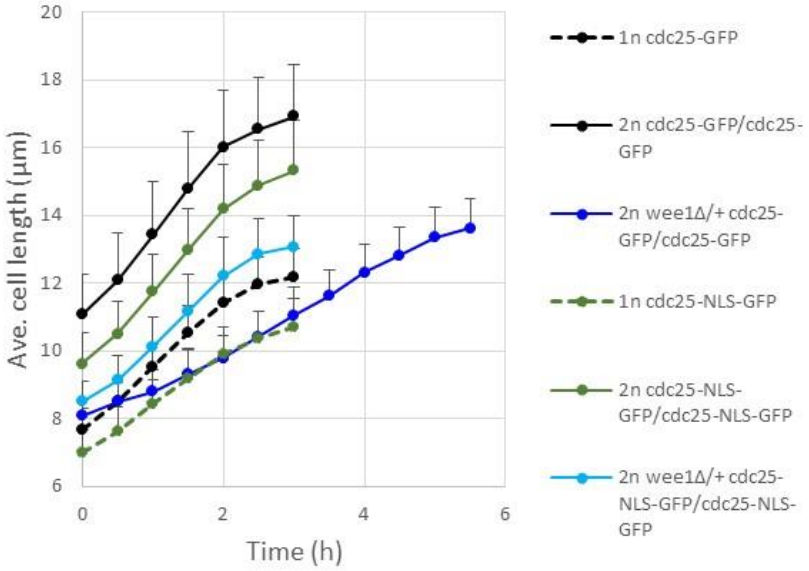

Genotype	CER (max)	P value	
2n *cdc25-GFP/cdc25-GFP*	2.71±0.76	—	
2n *wee1Δ/+ cdc25-GFP/cdc25-GFP*	1.38±0.83	***	(—)
1n *cdc25-GFP*	2.02±0.67	***	
2n *cdc25-NLS/cdc25-NLS*	2.50±0.74		—
2n *wee1Δ/+ cdc25-NLS/cdc25-NLS*	2.09±0.63		* (***)
1n *cdc25-NLS*	1.57±0.47		***

Figure 9

(a)

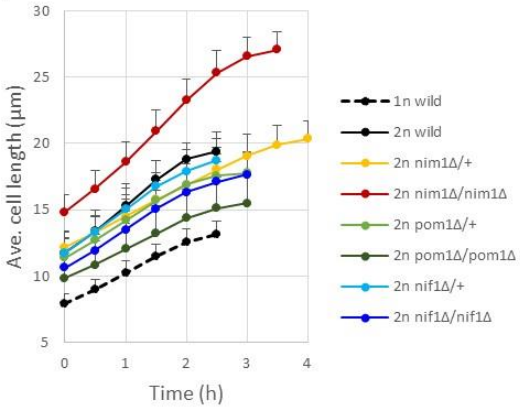

Genotype	CER (max)	P value
2n wild	3.94±0.71	—
2n *nim1Δ*/+	2.54±0.87	*** (n.s.)
2n *nim1Δ*/*nim1Δ*	4.62±0.80	***
2n *pom1Δ*/+	3.02±0.86	***
2n *pom1Δ*/*pom1Δ*	2.38±0.89	***
2n *nif1Δ*/+	3.49±0.92	*
2n *nif1Δ*/*nif1Δ*	3.16±0.79	***
1n wild	2.47±0.59	*** (—)

(b)

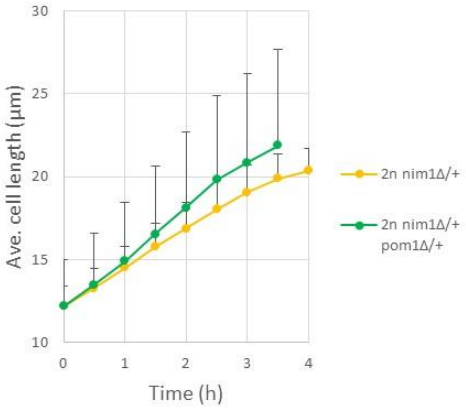

Genotype	CER (max)	P value
2n *nim1Δ*/+	2.54±0.87	—
2n *nim1Δ*/+ *pom1Δ*/+	3.36±1.38	**

(c)

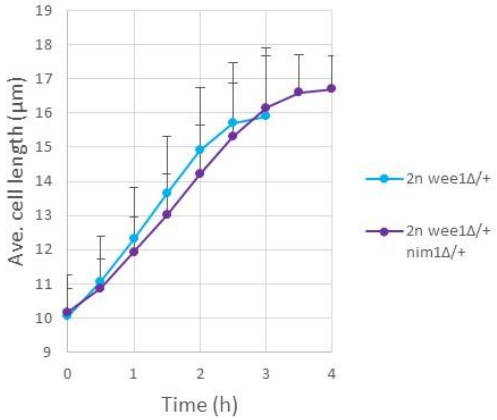

Genotype	CER (max)	P value
2n *wee1Δ*/+	2.66±0.66	—
2n *wee1Δ*/+ *nim1Δ*/+	2.42±0.73	n.s.

(d)

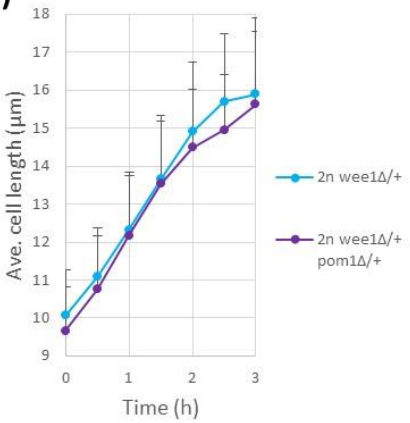

Genotype	CER (max)	P value
2n *wee1Δ*/+	2.66±0.66	—
2n *wee1Δ*/+ *pom1Δ*/+	2.82±0.81	n.s.

Figure 9

(e)

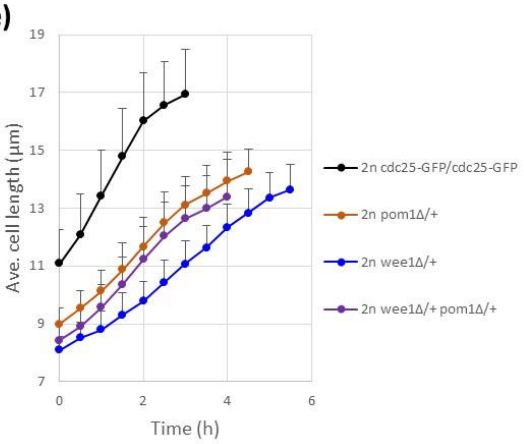

Genotype	CER (max)	P value	
2n *cdc25-GFP/ cdc25-GFP*	2.71±0.76	—	
2n *pom1Δ/+*	1.64±0.70	***	
2n *wee1Δ/+*	1.38±0.83	***	—
2n *wee1Δ/+ pom1Δ/+*	1.72±0.73		*

(f)

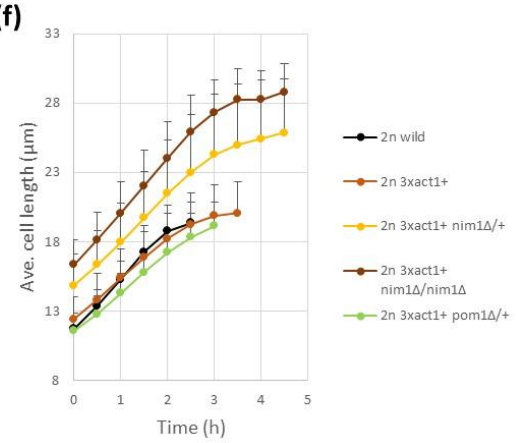

Genotype	CER (max)	P value
2n 3x*act1+*	3.17±0.80	—
2n 3x*act1+ nim1Δ/+*	3.54±1.39	n.s.
2n 3x*act1+ nim1Δ/nim1Δ*	3.95±1.02	***
2n 3x*act1+ pom1Δ/+*	3.04±0.83	n.s.
2n wild	3.94±0.71	***

(g)

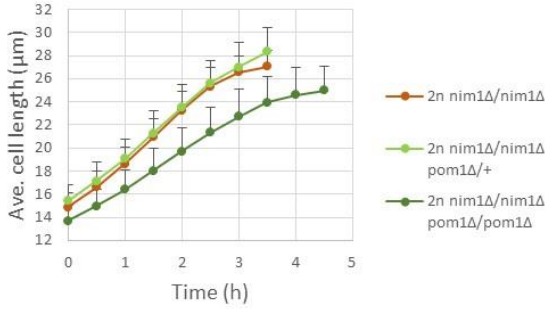

Genotype	CER (max)	P value
2n *nim1Δ/nim1Δ*	4.62±0.80	—
2n *nim1Δ/nim1Δ pom1Δ/+*	4.51±1.19	n.s.
2n *nim1Δ/nim1Δ pom1Δ/pom1Δ*	3.37±0.82	***

(h)

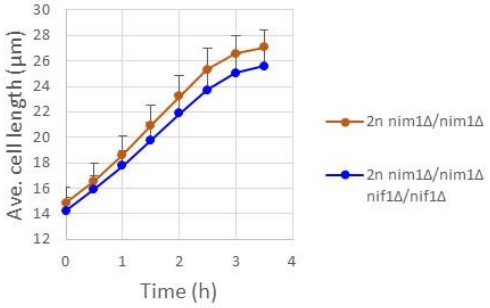

Genotype	CER (max)	P value
2n *nim1Δ/nim1Δ*	4.62±0.80	—
2n *nim1Δ/nim1Δ nif1Δ/nif1Δ*	4.18±0.87	*

Figure 9

(i)

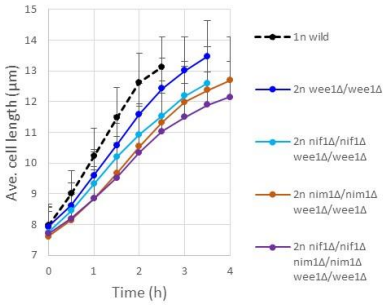

Genotype	CER (max)	P value
2n *wee1Δ/wee1Δ*	2.08±0.58	—
2n *wee1Δ/wee1Δ nif1Δ/nif1Δ*	1.77±0.50	*
2n *wee1Δ/wee1Δ nim1Δ/nim1Δ*	1.76±0.81	*
2n *wee1Δ/wee1Δ nif1Δ/nif1Δ nim1Δ/nim1Δ*	1.63±0.69	**
1n wild	2.47±0.59	*

(j)

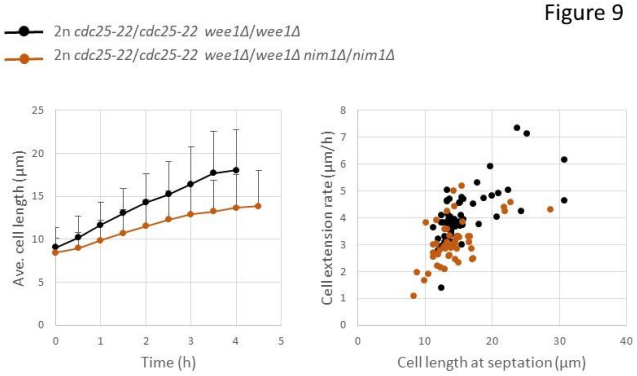

Genotype	CER (max)	P value
2n *cdc25-22/cdc25-22 wee1Δ/wee1Δ*	2.92±1.14	—
2n *cdc25-22/cdc25-22 wee1Δ/wee1Δ nim1Δ/nim1Δ*	1.78±1.37	***

Figure 10

(a)

Ploidy	Genotype
1n	wild
1n	*pom1Δ*
1n	*nim1Δ*
1n	*pom1Δ nim1Δ*
1n	*nif1Δ*
2n	wild
2n	*pom1Δ/pom1Δ*
2n	*pom1Δ/+*
2n	4x*pom1+*
2n	*act1-ts/act1-ts pom1Δ/+*
2n	*nim1Δ/nim1Δ*
2n	*adf1-1/adf1-1 nim1Δ/nim1Δ*
2n	*nim1Δ/+*
2n	*pom1Δ/+ nim1Δ/nim1Δ*
2n	*pom1Δ/+ nim1Δ/+*
2n	4x*nim1+*
2n	*nif1Δ/nif1Δ*
2n	*nif1Δ/+*
2n	*nif1Δ/nif1Δ nim1Δ/nim1Δ*
2n	3x*act1+*
2n	3x*act1+ pom1Δ/+*
2n	3x*act1+ nim1Δ/+*
2n	3x*act1+* 4x*pom1+*
2n	3x*act1+* 4x*nim1+*
2n	3x*act1+ nif1Δ/nif1Δ*
2n	3x*act1+ nif1Δ/+*

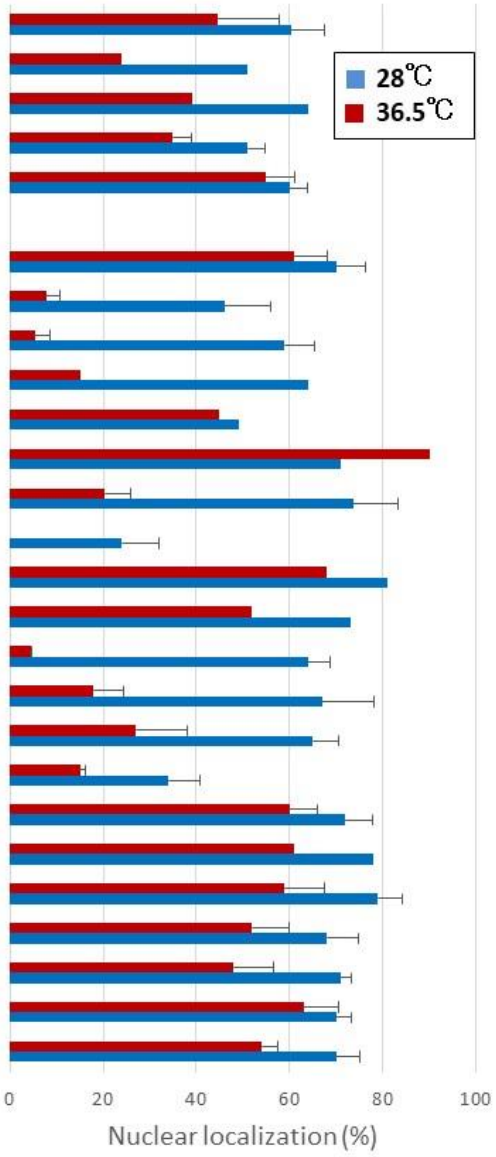

Figure 10

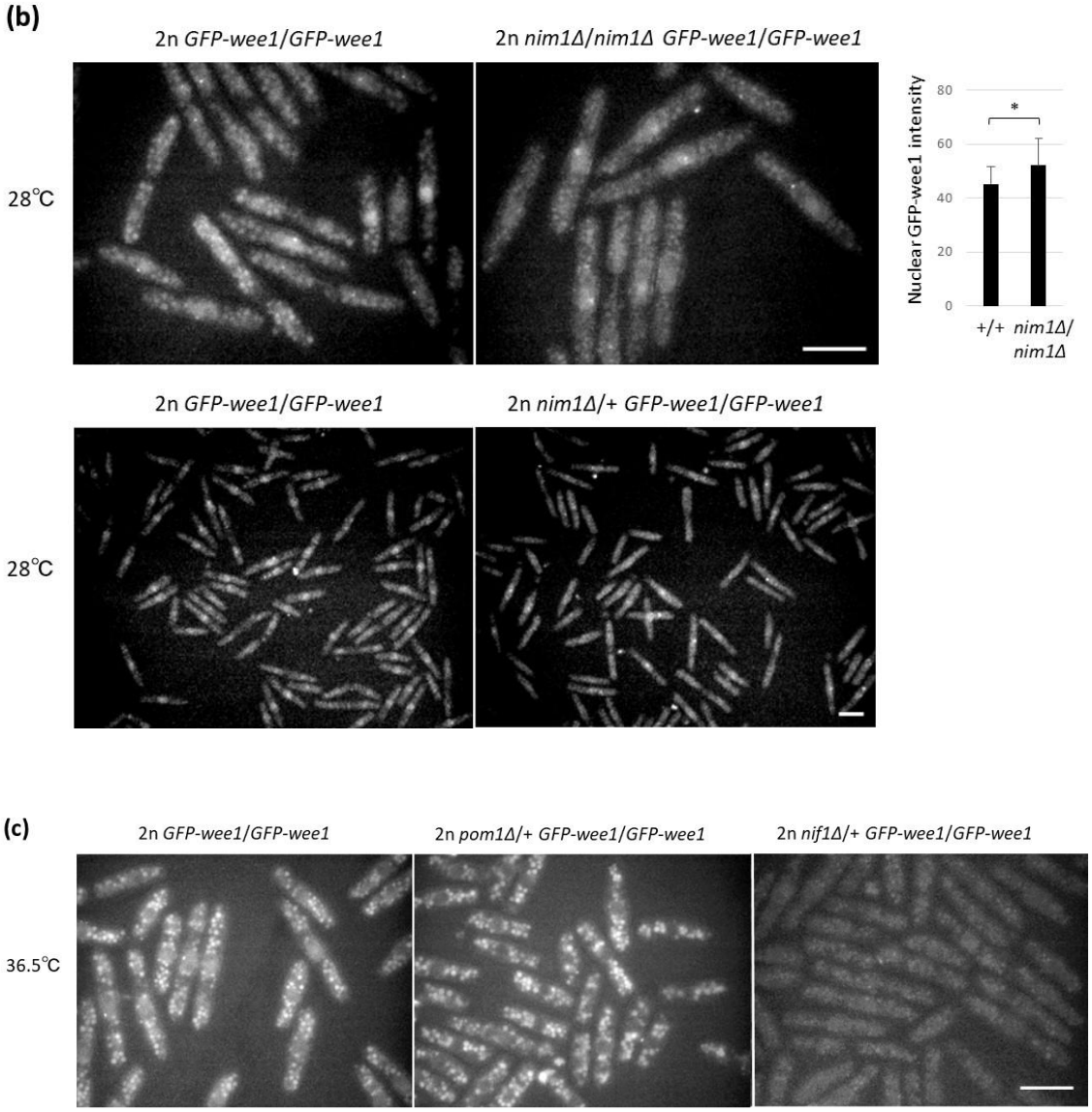
(b)
2n GFP-wee1/GFP-wee1
2n nim1Δ/nim1Δ GFP-wee1/GFP-wee1
28℃
Nuclear GFP-wee1 intensity
80
60
40
20
0
*
+/+
nim1Δ/ nim1Δ
2n GFP-wee1/GFP-wee1
2n nim1Δ/+ GFP-wee1/GFP-wee1
28℃
(c)
2n GFP-wee1/GFP-wee1
2n pom1Δ/+ GFP-wee1/GFP-wee1
2n nif1Δ/+ GFP-wee1/GFP-wee1
36.5℃

Figure 11

(a)

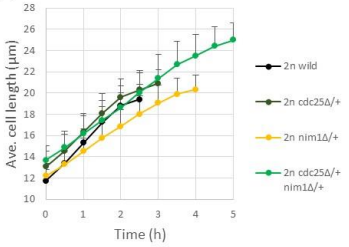

Genotype	CER (max)	P value	
2n *cdc25Δ/+*	3.57±0.95	—	
2n *nim1Δ/+*	2.54±0.87		—
2n *cdc25Δ/+ nim1Δ/+*	2.78±0.89	***	n.s.
2n wild	3.94±0.71	*	***

(b)

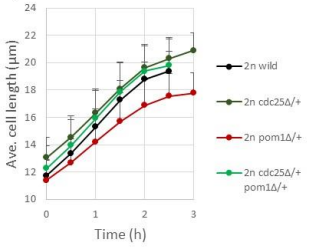

Genotype	CER (max)	P value	
2n *cdc25Δ/+*	3.57±0.95	—	
2n *pom1Δ/+*	3.02±0.86		—
2n *cdc25Δ/+ pom1Δ/+*	3.89±0.98	n.s.	***
2n wild	3.94±0.71	*	***

(c)

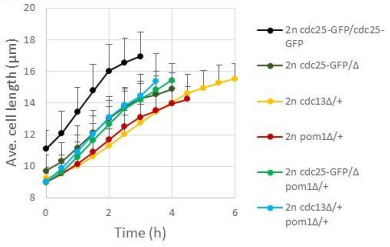

Genotype	CER (max)	P value	
2n *cdc25-GFP/Δ*	1.91±0.56	n.s.	
2n *cdc13Δ/+*	1.51±0.70		***
2n *pom1Δ/+*	1.64±0.70	**	***
2n *cdc25=GFP/Δ pom1Δ/+*	2.12±0.55	—	
2n *cdc13Δ/+ pom1Δ/+*	2.22±0.58		—

Figure 12

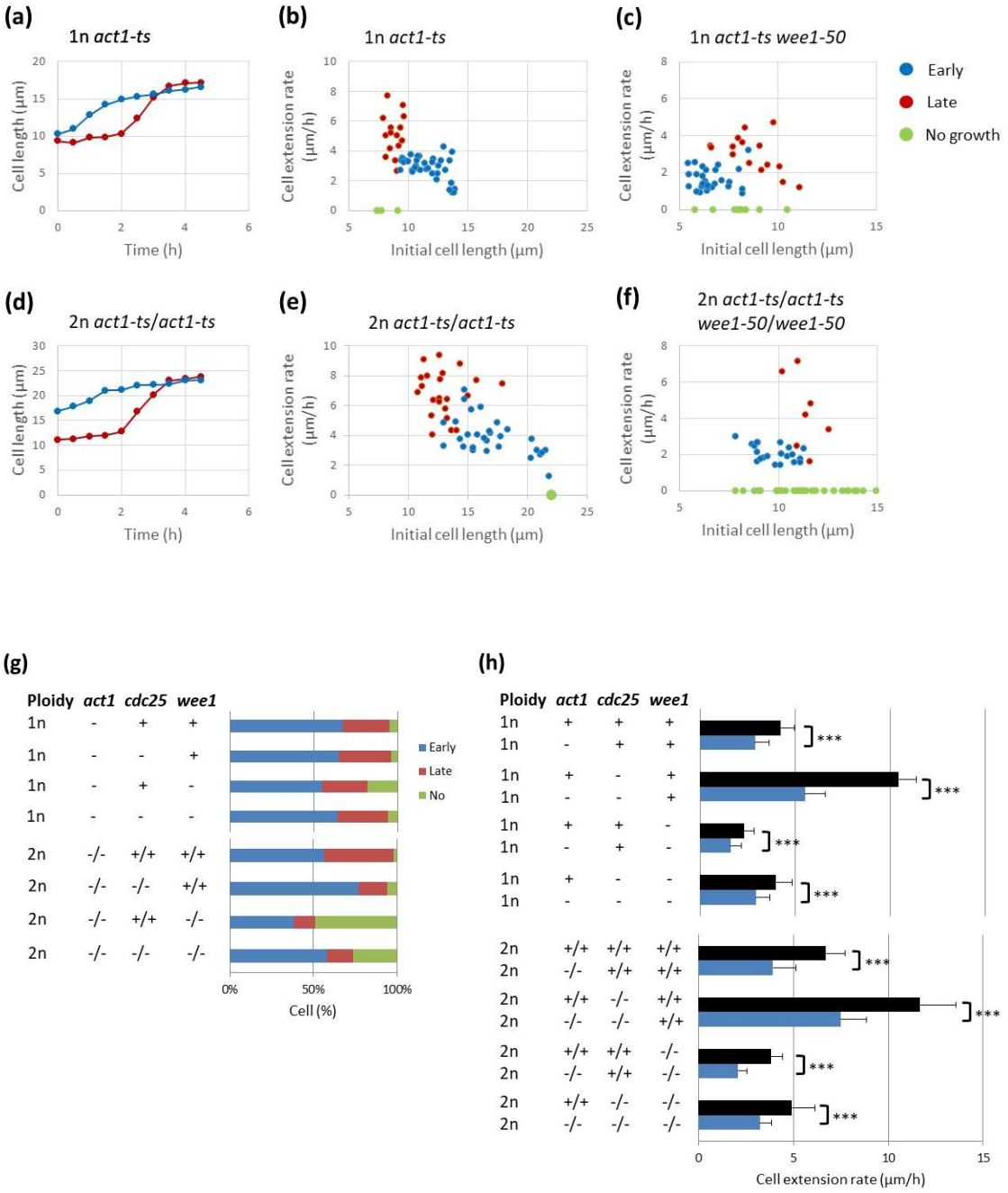
(a)
1n act1-ts
Cell length (µm)
Time (h)
(b)
1n act1-ts
Cell extension rate (µm/h)
Initial cell length (µm)
(c)
1n act1-ts wee1-50
Cell extension rate (µm/h)
Initial cell length (µm)
Early
Late
No growth
(d)
2n act1-ts/act1-ts
Cell length (µm)
Time (h)
(e)
2n act1-ts/act1-ts
Cell extension rate (µm/h)
Initial cell length (µm)
(f)
2n act1-ts/act1-ts wee1-50/wee1-50
Cell extension rate (µm/h)
Initial cell length (µm)
(g)
Ploidy act1 cdc25 wee1
1n - + +
1n - - +
1n - + -
1n - - -
2n -/- +/+ +/+
2n -/- -/- +/+
2n -/- +/+ -/-
2n -/- -/- -/-
Early
Late
No
0%
50%
100%
Cell (%)
(h)
Ploidy act1 cdc25 wee1
1n + + +
1n - + +
1n + - +
1n - - +
1n + + -
1n - + -
1n + - -
1n - - -
2n +/+ +/+ +/+
2n -/- +/+ +/+
2n +/+ -/- +/+
2n -/- -/- +/+
2n +/+ +/+ -/-
2n -/- +/+ -/-
2n +/+ -/- -/-
2n -/- -/- -/-
***
Cell extension rate (µm/h)

Figure 12

(i)

Ploidy	*cdc25*	*wee1*	*act1*	*pom1*	*nim1*
2n	-/-	-/-	+/+	+/+	+/+
2n	-/-	-/-	-/-	+/+	+/+
2n	-/-	-/-	-/-	+/Δ	+/+
2n	-/-	-/-	-/-	+/Δ	Δ/Δ

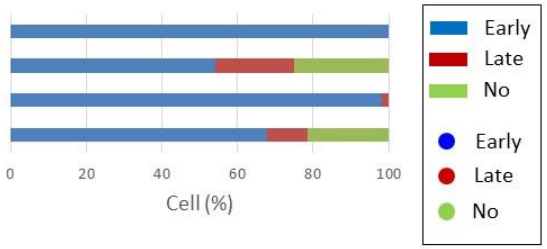

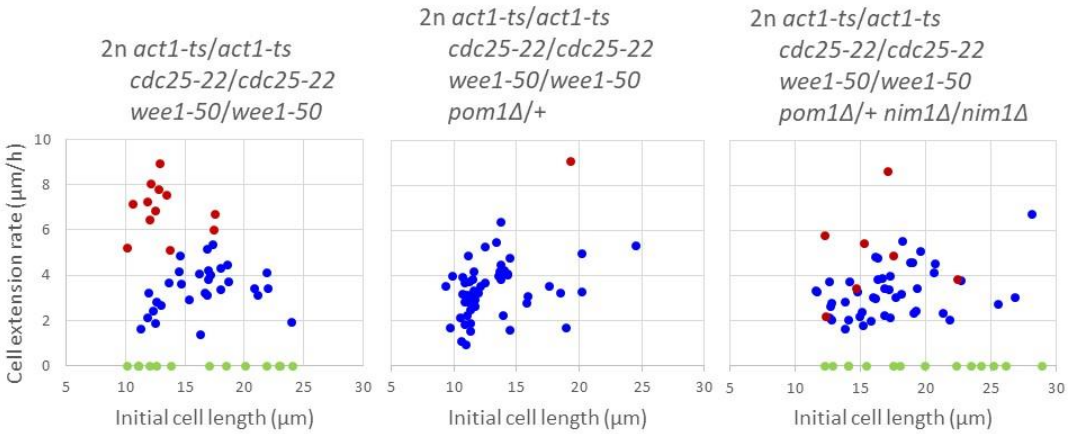

(j)

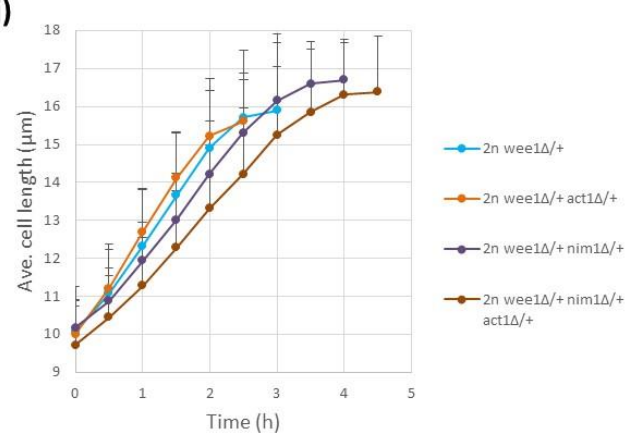

Genotype	CER (max)	P value	
2n *wee1Δ/+*	2.66±0.66	—	
2n *wee1Δ/+ act1Δ/+*	2.98±0.81	*	***
2n *wee1Δ/+ nim1Δ/+*	2.42±0.73	n.s.	*
2n *wee1Δ/+ nim1Δ/+ act1Δ/+*	2.08±0.80		—

Figure 13

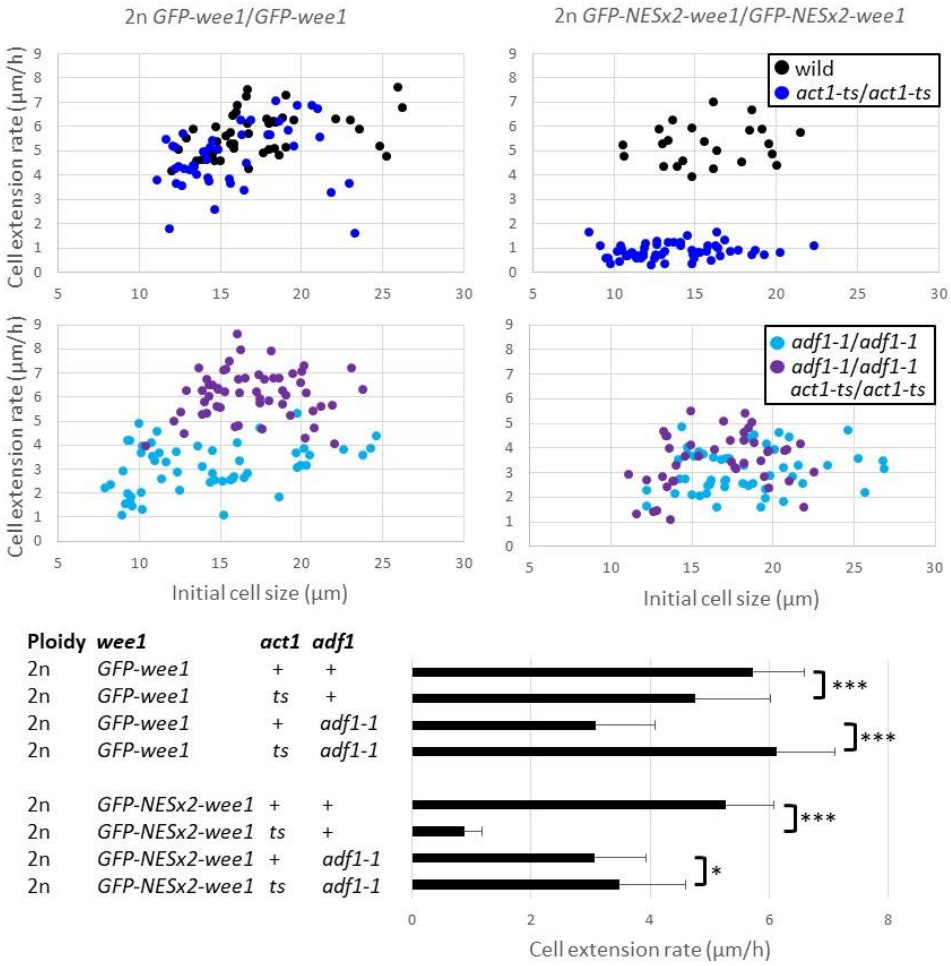
2n GFP-wee1/GFP-wee1
2n GFP-NESx2-wee1/GFP-NESx2-wee1
Cell extension rate (µm/h)
wild
act1-ts/act1-ts
adf1-1/adf1-1
adf1-1/adf1-1 act1-ts/act1-ts
Initial cell size (µm)
Ploidy wee1 act1 adf1
2n GFP-wee1 + +
2n GFP-wee1 ts +
2n GFP-wee1 + adf1-1
2n GFP-wee1 ts adf1-1
2n GFP-NESx2-wee1 + +
2n GFP-NESx2-wee1 ts +
2n GFP-NESx2-wee1 + adf1-1
2n GFP-NESx2-wee1 ts adf1-1
***
***
***
*
Cell extension rate (µm/h)

Figure 14

(a)

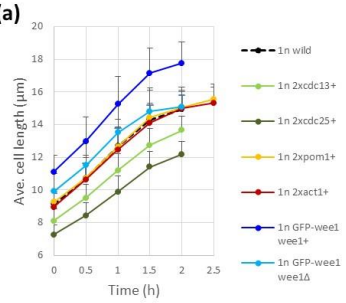

Genotype	CER (max)	P value
1n wild	3.95±0.77	—
1n 2x*cdc13+*	3.39±0.72	***
1n 2x*cdc25+*	3.05±0.88	***
1n 2x*pom1+*	3.85±0.92	n.s.
1n 2x*act1+*	3.63±0.77	*
1n *GFP-wee1 wee1+*	4.57±0.90	** (*)
1n *GFP-wee1 wee1Δ*	4.02±1.01	n.s. (—)

(b)

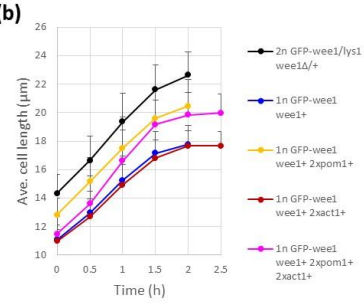

Genotype	CER (max)	P value
1n *GFP-wee1 wee1+*	4.57±0.90	—
1n *GFP-wee1 wee1+* 2x*pom1+*	4.71±1.59	n.s. (***)
1n *GFP-wee1 wee1+* 2x*act1+*	4.44±0.91	n.s. (***)
1n *GFP-wee1 wee1+* 2x*pom1+* 2x*act1+*	6.03±1.17	*** (—)
2n *GFP-wee1/lys1 wee1Δ/+*	5.43±1.49	(*)

(c)

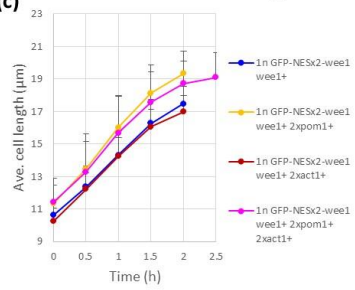

Genotype	CER (max)	P value
1n *GFP-NESx2-wee1 wee1+*	3.90±0.83	—
1n *GFP-NESx2-wee1 wee1+* 2x*pom1+*	5.09±1.11	*** (n.s.)
1n *GFP-NESx2-wee1 wee1+* 2x*act1+*	4.05±0.75	n.s. (**)
1n *GFP-NESx2-wee1 wee1+* 2x*pom1+* 2x*act1+*	4.82±1.49	(—)

(d)

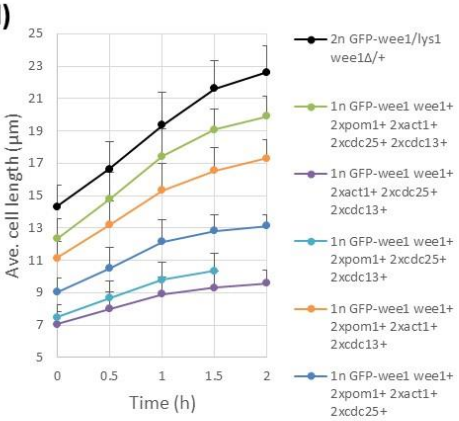

Genotype	CER (max)	P value
1n *GFP-wee1 wee1+* 2x*pom1+* 2x*act1+* 2x*cdc25+* 2x*cdc13+*	5.30±1.06	—
1n *GFP-wee1 wee1+* 2x*act1+* 2x*cdc25+* 2x*cdc13+*	1.85±0.96	***
1n *GFP-wee1 wee1+* 2x*pom1+* 2x*cdc25+* 2x*cdc13+*	2.40±0.99	***
1n *GFP-wee1 wee1+* 2x*pom1+* 2x*act1+* 2x*cdc13+*	4.29±1.48	***
1n *GFP-wee1 wee1+* 2x*pom1+* 2x*act1+* 2x*cdc25+*	3.27±1.20	***
2n *GFP-wee1/lys1 wee1Δ/+*	5.43±1.49	n.s.

(e)

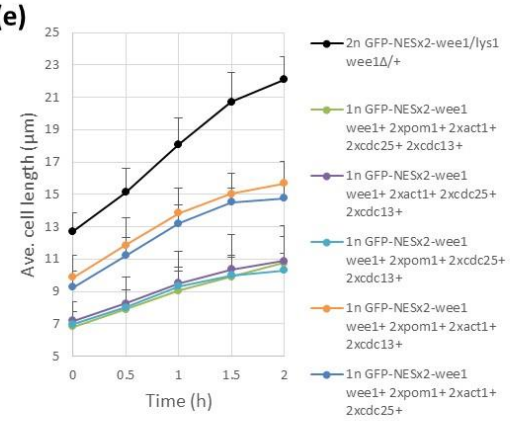

Genotype	CER (max)	P value
1n *GFP-NESx2-wee1 wee1+* 2x*pom1+* 2x*act1+* 2x*cdc25+* 2x*cdc13+*	2.34±0.90	—
1n *GFP-NESx2-wee1 wee1+* 2x*act1+* 2x*cdc25+* 2x*cdc13+*	2.50±1.06	n.s.
1n *GFP-NESx2-wee1 wee1+* 2x*pom1+* 2x*cdc25+* 2x*cdc13+*	2.59±0.79	n.s.
1n *GFP-NESx2-wee1 wee1+* 2x*pom1+* 2x*act1+* 2x*cdc13+*	3.97±1.15	***
1n *GFP-NESx2-wee1 wee1+* 2x*pom1+* 2x*act1+* 2x*cdc25+*	3.93±0.84	***
2n *GFP-NESx2-wee1/lys1 wee1Δ/+*	5.89±1.19	***

Figure 14

(f)

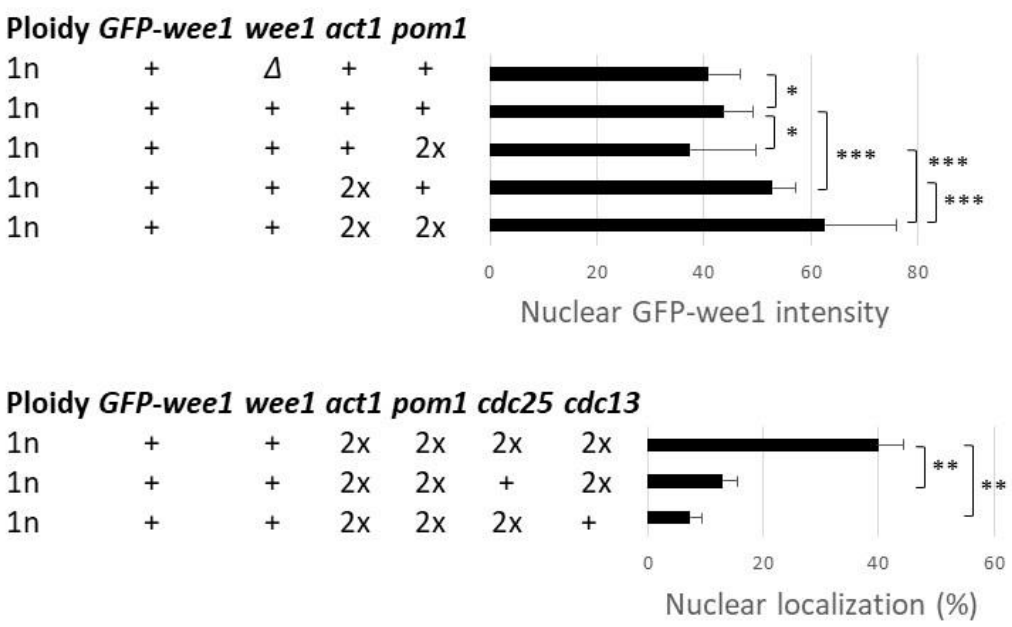
Ploidy GFP-wee1 wee1 act1 pom1
1n + Δ + +
1n + + + +
1n + + + 2x
1n + + 2x +
1n + + 2x 2x
*
*
***
***
***
0
20
40
60
80
Nuclear GFP-wee1 intensity
Ploidy GFP-wee1 wee1 act1 pom1 cdc25 cdc13
1n + + 2x 2x 2x 2x
1n + + 2x 2x + 2x
1n + + 2x 2x 2x +
**
**
0
20
40
60
Nuclear localization (%)

Figure 15

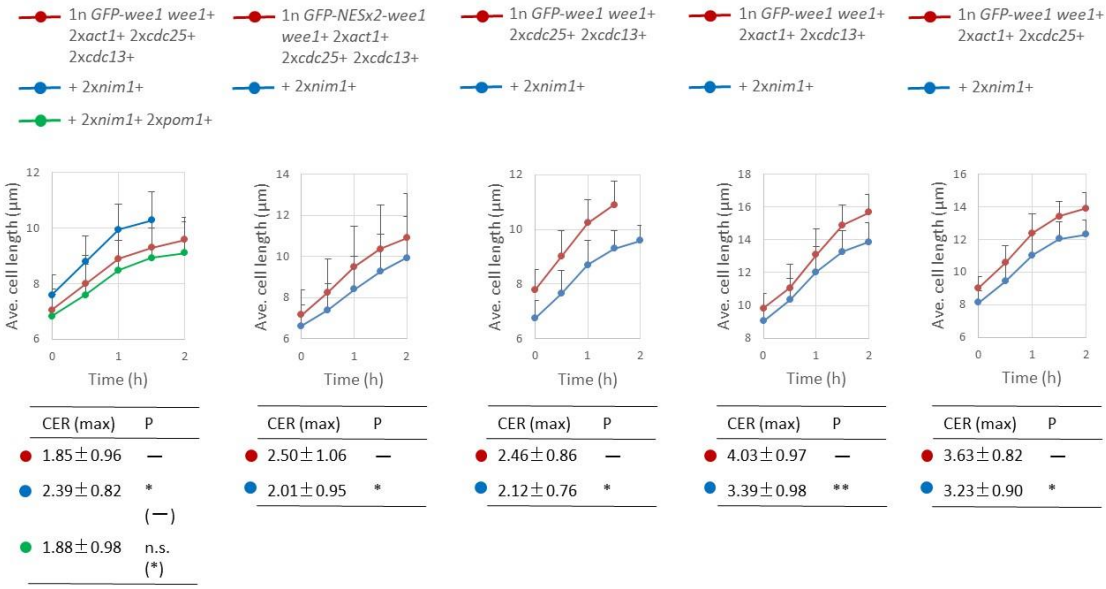

CER (max)	P
1.85±0.96	—
2.39±0.82	* (—)
1.88±0.98	n.s. (*)

CER (max)	P
2.50±1.06	—
2.01±0.95	*

CER (max)	P
2.46±0.86	—
2.12±0.76	*

CER (max)	P
4.03±0.97	—
3.39±0.98	**

CER (max)	P
3.63±0.82	—
3.23±0.90	*

Figure 16

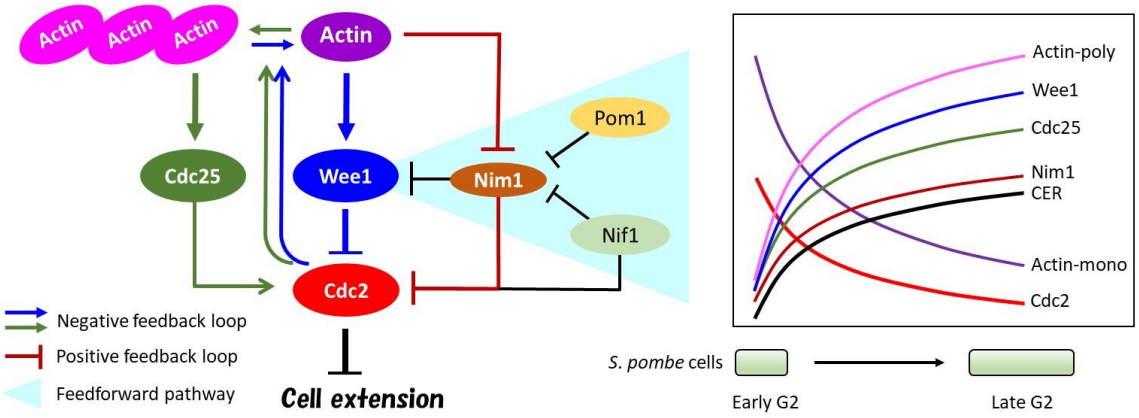
Actin
Actin
Actin
Actin
Cdc25
Wee1
Nim1
Pom1
Nif1
Cdc2
Negative feedback loop
Positive feedback loop
Feedforward pathway
Cell extension
Actin-poly
Wee1
Cdc25
Nim1
CER
Actin-mono
Cdc2
S. pombe cells
Early G2
Late G2

Figure S1

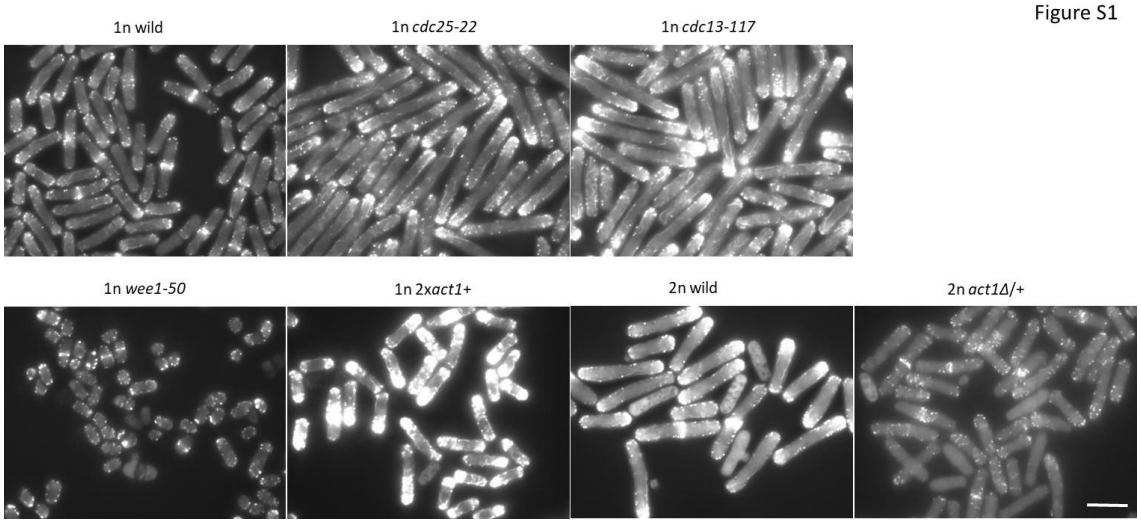
1n wild
1n *cdc25-22*
1n *cdc13-117*
1n *wee1-50*
1n 2x*act1+*
2n wild
2n *act1Δ/+*

Figure S2

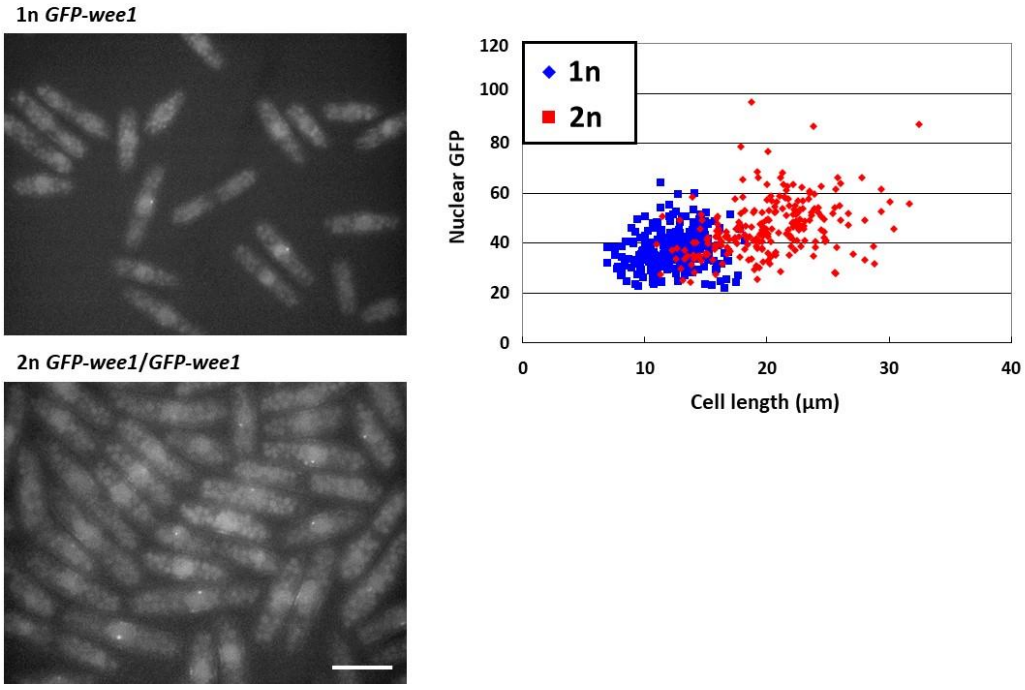
1n *GFP-wee1*
2n *GFP-wee1/GFP-wee1*
1n
2n
Nuclear GFP
Cell length (μm)
0
20
40
60
80
100
120
0
10
20
30
40

Figure S3

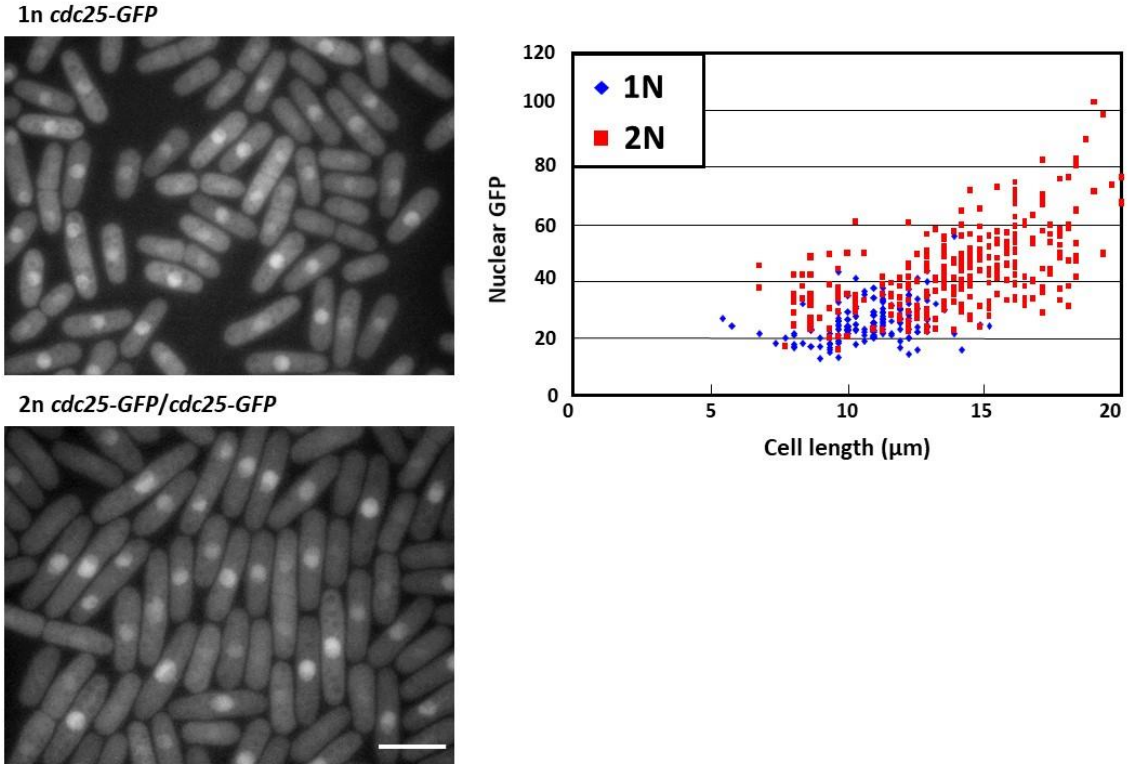
1n cdc25-GFP
2n cdc25-GFP/cdc25-GFP
1N
2N
Nuclear GFP
Cell length (µm)
0
20
40
60
80
100
120
0
5
10
15
20